IN VITRO SCREENING SYSTEM FOR MACROSTEATOSIS REVERSAL IN LIVER CELLS

by

NIR ISRAEL NATIV

A dissertation submitted to the

Graduate School-New Brunswick

Rutgers, The state University of New Jersey

and

The Graduate School of Biomedical Sciences

University of Medicine and Dentistry of New Jersey

In partial fulfillment of the requirements

For the degree of

Doctor of Philosophy

Graduate program in Biomedical Engineering

Written under the direction of

Professor Martin L. Yarmush

And approved by

New Brunswick, New Jersey

May, 2014

ABSTRACT OF THE DISSERTATION

IN VITRO SCREENING SYSTEM FOR MACROSTEATOSIS REVERSAL IN LIVER CELLS

by

NIR ISRAEL NATIV

Dissertation Director:

Professor Martin L. Yarmush

Orthotopic liver transplantation is the only therapeutic option for end-stage liver disease, but it is limited by the scarcity of suitable grafts. Macrosteatotic livers exhibit elevated triglyceride (TG) levels in the form of large lipid droplets (LDs), elevated reactive oxygen species (ROS) and reduced adenosine triphosphate (ATP) levels in the liver's hepatocytes. These abnormalities increase sensitivity of hepatocytes to ischemia and reperfusion (I/R) stress during transplantation and to increased hepatocyte death and graft failure following transplantation. Macrosteatosis reversal several weeks prior to live-donor liver transplantation reduces graft I/R sensitivity and enables successful transplantation. However, to apply this concept to livers from deceased donors, the defatting process must be accelerated using ex-vivo perfusion with defatting agents. To explore macrosteatosis defatting phenomena and to identify potent defatting agents prior to whole liver studies, an in-vitro system simulating macrosteatosis was developed.

Primary rat hepatocyte cultures incubated for several days with elevated free fatty acid (FFA) levels exhibited characteristics of clinical macrosteatosis based on LD morphology, elevated TG levels and elevated sensitivity to hypoxia and reoxygenation (H/R) induced stress, simulating I/R. This novel system was used to explore the ability of selected defatting cocktails to

reverse macrosteatosis and reduce H/R sensitivity as measured by hepatocyte viability and function.

We found that pretreatment of macrosteatotic cultures with an L-carnitine supplemented defatting cocktail under hyperoxic conditions for 48h prior to H/R induction led to a ~82% reduction in the number of macrosteatotic LDs and to a ~57% reduction in intrahepatic TG by promoting β-oxidation of FFAs. Furthermore, this treatment reduced ROS stress by ~32%, elevated the ATP levels to that of lean controls and fully abolished H/R associated hepatic death. Treated cultures maintained ~83% viability and exhibited superior functionality compared to untreated macrosteatotic cultures as assessed by urea secretion and bile canalicular transport 48h post H/R stress.

The developed system is suitable for exploring additional defatting cocktails that may reverse macrosteatosis and elevated H/R sensitivity. The developed in-vitro defatting routine can now be scaled-up for whole organ perfusion systems to recover macrosteatotic livers in order to mitigate the persistent shortage of suitable livers for transplantation.

ACKNOWLEDGMENTS AND DEDICATIONS

This dissertation summarizes the work I have performed over the last 4 years in the laboratories of my advisor Dr. Martin L. Yarmush and my co-advisor, Dr. Francoise Berthiaume. I am very grateful to Dr. Yarmush for believing in my abilities to perform the scientific work to his uncompromised standards and to develop as a scientist. I would like to thank Dr. Berthiaume for sharing his immense knowledge in the field of liver metabolism with me and for teaching me invaluable scientific skills. I would like to especially thank Dr. Rene Schloss for mentoring me from day one and provided me with unlimited support to be successful in my Ph.D. In addition, I would like to acknowledge my committee members and collaborators: Dr. Tim Maguire, Dr. James V. Guarrera, Dr. Scot Henry, Dr. Dawn Brasaemle and Dr. Ken Klein for their vast support and valuable knowledge which propelled my dissertation project forward.

I am very appreciative for all the members of Drs. Yarmush, Berthiaume, Guarrera and Brasaemle laboratories who assisted me along the way and would like to give a special thanks to: Gabe Yarmush for his significant contribution to the project; Alvin Chen for his invaluable image analysis skills; Ashely So for her great help as an undergraduate researcher and Dr. Jeff Barminko for his scientific collaboration, as well as being a good friend and confidante.

I would also like to thank my parents, Shmulik and Sara, my brother, Guy, and grandparents. They have always supported and encouraged me with their best wishes. I am grateful for my in laws, Ivan and Eva Horak, who consistently do everything to help me and my family be successful and happy. Without their support in all aspects of live, I would not have been able to pursue this degree. Lastly, I am dedicating this dissertation to my loving wife, Simona, and my children, Eitan, Talya and Yonatan. You believed in me from day one. Your happiness is my great motivation to excel.

TABLE OF CONTENTS

LIST OF TABLES

LIST OF FIGURES

LIST OF ABBREVIATIONS

Triglyceride (TG), lipid droplet (LD), adenosine triphosphate (ATP), reactive oxygen species (ROS), ischemia reperfusion (I/R), free fatty acid (FFA), lactate dehydrogenase (LDH), hypoxia reoxygenation (H/R), organ procurement and transplantation network (OPTN), nonalcoholic fatty liver disease (NAFLD), body mass index (BMI), tumor necrosis factor-alpha (TNF-alpha), glutathione (GSH), choline- and methionine-deficient diet (CMDD), intercellular adhesion molecule-1 (ICAM-1), nitric oxide (NO), heat shock protein (HSP), heme oxygenase-1 (HO-1), carnitine palmitoyltransferase-1(CPT-1), hematoxylin and eosin (H&E), magnetic resonance imaging (MRI), cross sectional surface area (CSSA), active contour models (ACM), aspartate aminotransferase (AST), alanine transaminase (ALT), phosphate buffered saline (PBS), no steatosis reduction supplements (NSRS), steatosis reduction supplements (SRS), ethidium homodimer-1 (EthD-1), 5-(and-6)-carboxy-2',7'-dichlorofluorescein diacetate (carboxy-DCFDA), calcein acetoxymethylester (calcein-AM), hypoxia and reoxygenation (H/R), ratio of oxidized to reduced glutathione (GSSG/GSH).

INTRODUCTION

Orthotopic liver transplantation is the only therapeutic option for patients with end-stage liver disease, but is limited by the number of suitable grafts available for transplantation [1-6]. Based on the Organ Procurement and Transplantation Network (OPTN), during the last decade about 15,000 patients have been waiting for a liver graft in the U.S alone, while the donor pool has enabled transplantation of only about 7,000 livers per year. This liver graft shortage leads to about 2,000 annual deaths of patients on the transplantation waiting list. An additional 2,000 patients experience deterioration in physical condition which leads to their removal from the list and ultimately to their death.

It is estimated that about 1,000 harvested macrosteatotic liver grafts are being discarded from the transplantation pool annually [4]. Macrosteatotic livers exhibit abnormally high levels of TG in the liver parenchymal cells, the hepatocytes, which appear in the form of lipid droplets large enough to displace the nucleus to the hepatocyte's periphery [2, 4, 6-8]. Lean or microsteatotic livers, which contain only small lipid droplets in the hepatocyte cytoplasm, can be transplanted successfully even at high levels of microsteatosis. However, macrosteatotic LDs in more than 30% of the liver hepatocytes is associated with increased rate of graft primary non-function, morbidity and mortality shortly after transplantation due to hypersensitivity to I/R stress inherent to the transplantation process as described in greater detail in chapter 1 of this dissertation [2, 4, 6-8] . As a result, livers that are assessed as macrosteatotic above 30% based on the pathologist's "naked eye" evaluation of H&E stained liver sections are discarded and no longer available for transplantation [7-9]. Furthermore, macrosteatotic livers are expected to increase their proportion in the liver donor pool in years to come since fatty livers such as macrosteatotic livers are strongly associated with non-alcoholic fatty liver disease (NAFLD) as part of the obesity epidemic [1, 4, 10, 11].

Therefore, in an effort to alleviate the persisting liver graft shortage by enabling optimal utilization of macrosteatotic livers for transplantation, two approaches will be explored in this dissertation, with the ultimate goal to save the lives of an additional 1,000 patients annually in the U.S alone. The first approach involves the utilization of the current liver graft pool to its fullest by ensuring that the discarded macrosteatotic livers are indeed above the 30% macrosteatotic cut-off. The current gold standard method of macrosteatotic percentage assessment is heavily reliant on the biased "naked eye" assessment of H&E stained liver histology slide or its digital image by a trained pathologist. In some transplantation centers where a pathologist is not available the decision is made by the surgeon alone [7-9, 12, 13]. Due to the inconsistencies among centers and the limitation in accurate quantification of an image by an individual, computer based image analysis methods have been developed to quantify macrosteatosis percentage from H&E stained liver slides [7, 14-17]. These methods were deficient in distinguishing between microsteatotic LD and the clinically relevant macrosteatotic LDs and therefore exhibited limited success in correlating macrosteatosis percentage assessments with that of trained pathologists [7]. While pathologists define macrosteatotic LDs based on LD size and its ability to displace the hepatocyte nucleus to the periphery of the hepatocyte, all the current computer-based methods available used only LD size as the defining criterion [7, 14-17].

Herein, it was hypothesized that including the nucleus displacement by LDs as a determining feature in an image analysis algorithm can improve separation between microsteatotic and macrosteatotic LD and ultimately the clinically relevant macrosteatotic percentage estimation. Based on this hypothesis, the development of an image analysis based method to quantify macrosteatosis percentage in H&E stained liver slides using both LD size and nuclear displacement was explored, as described in chapter 2 of this dissertation. Such a non-biased and automated macrosteatosis assessment can be incorporated together with additional

transplantation related variables such as donor age, warm and cold ischemic time, etc. to assist clinicians in ensuring optimal utilization of the current liver pool.

In most cases, following harvesting the graft is transported to its recipient in a different center. During the time period between graft harvesting and transplantation, which may last up to 12h, the grafts must be preserved. The current gold standard for preservation of all liver grafts is storage over ice with a preservation solution. The concept beyond this preservation method is to slow-down liver metabolism and oxygen consumption to diminish the development of I/R hypersensitivity by metabolic dependent mechanisms such as ATP depletion and ROS generation [3, 18-20]. While this preservation method is efficient for lean and microsteatotic livers for up to ~12h, it is not suitable for transplantation of macrosteatotic livers, which exhibit elevated sensitivity to I/R stress compared to lean or microsteatotic livers [3, 4, 6, 21, 22]. Therefore, the second approach explored in this dissertation to alleviate the liver graft shortage is the development of metabolic preconditioning method for macrosteatotic livers prior to their transplantation in order to ameliorate their hypersensitivity to I/R stress.

In order to metabolically precondition such livers, the origin for hypersensitivity to I/R stress leading to rapid graft failure post transplantation needs to be better understood. As described in great detail in chapter 1 of this dissertation, the cause of I/R hypersensitivity in macrosteatotic livers is a combination of several mechanisms at the cellular, organ and systemic levels which leads to elevated hepatic cell death levels. At the hepatocyte level, the hypersensitivity is a result of alterations in hepatocyte metabolism such as ATP depletion, increased ROS stress, increased TG, etc. [4, 6, 18, 21-27]. At the organ level, the hypersensitivity results from sinusoidal space narrowing leading to impaired blood flow during reperfusion. The intrahepatic content released to the blood stream due to necrotic cell death activates the liver immune cells, Kupffer cells. In addition, neutrophils from the blood stream penetrate the liver tissue as part of a systemic innate immune response following reperfusion [4, 6, 18, 21-28].

Based on these mechanisms, several methods have been developed to reduce hypersensitivity of macrosteatotic livers using preconditioning with pharmacological agents prior to transplantation to reduce ROS stress or to elevate ATP levels, for example [27, 29]. Other methods involve stress preconditioning approaches such as short I/R or heat-sock treatments prior to transplantation [27, 28, 30]. These methods were not translated to clinical success and target only a few of the underlying mechanisms involved in I/R hypersensitivity while ignoring the macrosteatotic state of the liver, which one would likely consider the root cause of these underlying mechanisms [4].

Interestingly, dieting and exercise for several days to weeks prior to transplantation in human live donor transplantation and animal models of orthotopic liver transplantation reversed macrosteatosis, reduced hypersensitivity to I/R, and enabled successful transplantation [23, 31, 32]. Following these studies, the idea of preconditioning macrosteatotic grafts from deceased donors by means of reversing the macrosteatosis emerged. The main challenge, however, is that these macrosteatotic liver grafts must be defatted following their harvest and within a clinically relevant time frame of a few hours prior to orthotopic transplantation. Since macrosteatotic reversal is a metabolically dependent process, it is expected to be most efficient when performed at physiological temperature of 37^{o}C and not 0-4^{o}C as is currently used to preserve livers prior to transplantation. Livers maintained under a physiological temperature for ~12h must be connected to an ex-vivo normothermic perfusion machine that supplies essential oxygen and nutrients [33]. It was recently reported that two lean livers were successfully transplanted following a 10h normothermic perfusion using an OrganOx® ex-vivo perfusion device [34]. In addition, normothermic ex-vivo perfusion of steatotic livers has been reported in animal models [14, 35]. Based on these studies, it is likely that whole macrosteatotic livers can be defatted as part of an ex-vivo normothermic machine perfusion. [4, 14, 33, 35]. However, various aspects of this

method should be explored in order to translate this idea to successful clinical application as described in chapter 1.

More specifically, the effect of macrosteatosis on hepatocyte metabolism and fat metabolism, the composition of the metabolic active defatting agents and their potency in reversing macrosteatotic and I/R hypersensitivity need to be explored. Performing such studies using whole livers in animal models or whole discarded human livers is not practical due to low throughput and high cost. In addition, the use of whole livers in such studies does not allow differentiation between I/R hypersensitivity on the hepatocytes or organ levels. The use of an in-vitro hepatocyte system that simulates macrosteatotic livers "on a dish" may enable higher throughput defatting studies at the hepatocyte level prior to animal or human studies. Current in-vitro systems aimed at simulating steatotic livers exhibit only microsteatotic hepatocyte features, but not macrosteatotic features [23, 35, 36]. For such a system to be clinically relevant, it must exhibit the following characteristics seen in whole macrosteatotic livers:

a. Macrosteatotic LDs of large size that displace the hepatocyte nucleus.

b. Biochemical similarities such as elevated TG levels.

c. Hypersensitivity to H/R stress used to simulate I/R stress in static cultures.

d. I/R hypersensitivity underlying mechanisms such as ATP and ROS stress levels.

e. Macrosteatotic reversibility by metabolically active agents for screening purposes.

Chapter 3 in this dissertation describes the development of such an in-vitro primary rat hepatocyte system induced for macrosteatosis and its utilization to explore the defatting effects of a previously developed metabolically active defatting cocktail. A combination of the following steatosis reduction supplements (SRS): 10uM forskolin, 1uM GW7647, 10uM scoparone (Sigma-Aldrich), 1uM GW501516, 10uM hypericin (Enzo, Farmingdale, NY), 0.4ng/ml visfatin

(Biovision, Mountain view, CA) and amino acids (Invitrogen) at final concentrations described in supplementary table 1 of chapter 4 was previously developed in a microsteatotic in-vitro system and is explored for the first time in the developed macrosteatotic in-vitro system [35]. Chapter 4 of this dissertation describes the effects of defatting with SRS on the ability of macrosteatotic hepatocyte to resist H/R induced death. Furthermore, addition of agents to the SRS cocktail has been explored to promote the desired hepatocytes resistance to H/R induced death.

The studies described in this dissertation were designed to address the following questions in the field of macrosteatotic liver preconditioning research:

a. What agents can be used to reverse macrosteatosis? Can this process be accelerated? What are the suggested intrahepatic pathways governing defatting?

b. What is the effect of accelerated macrosteatotic reversal on hepatocyte viability and function?
c. What is the time scale for such a process in a static in-vitro culture system?
d. How much defatting is required? Is breaking down macrosteatotic LDs alone or further catabolism of liberated TG and FFA is required to abolish H/R hypersensitivity?
e. What is the effect of such defatting on hepatocyte viability and function post H/R induced stress?

The answers to these questions may further develop the concept of macrosteatosis preconditioning prior to transplantation. The knowledge gained in this dissertation, can be then applied to preconditioning studies performed in whole macrosteatotic livers in animal models and in discarded human livers. If successful, this approach can develop into a clinical therapy that will add about 1,000 livers to the donor pool and save the lives of a similar number of patients annually in the U.S alone.

CHAPTER 1:

Current State of the Art in Macrosteatotic Liver Preconditioning

The materials, images and text used in this chapter have been previously published, at least in part, in the American Journal of Transplantation as a Mini-review as can be found in the appendix (Nativ NI, Maguire TJ, Yarmush G, Brasaemle DL, Henry SD, Guarrera JV, Berthiaume F, Yarmush ML. "Liver defatting: an alternative approach to enable steatotic liver transplantation", American Journal of Transplantation, 12: 3176-83. December 2012) .This publication represent the original work of Nir Israel Nativ as a first author as part of collaborative effort with several co-authors as customary to this field of research. Nir Israel Nativ has significantly contributed the following to this publication: Literature search, understanding the current state of art in macrosteatotic liver preconditioning, writing and/ or editing the text in all sections of the review, creating the relevant figures, addressing reviewers' comments and submission of review.

A. Abstract

Macrovesicular steatosis in greater than 30% of hepatocytes is a significant risk factor for primary graft non-function due to increased sensitivity to I/R injury. The growing prevalence of hepatic steatosis due to the obesity epidemic, in conjunction with an aging population, may negatively impact the availability of suitable deceased liver donors. Some have suggested that metabolic interventions could decrease the fat content of liver grafts prior to transplantation. This concept has been successfully tested through nutritional supplementation in a few living donors. Utilization of deceased donor livers, however, requires defatting of explanted organs. Animal studies suggest that this can be accomplished by ex-vivo warm perfusion in a time scale of a few hours. We estimate that this approach could significantly boost the size of the donor pool by increasing the utilization of steatotic livers. This chapter reviews the current knowledge on the mechanisms whereby excessive lipid storage and macrosteatosis exacerbate hepatic I/R injury,

and possible approaches to address this problem, including ex-vivo perfusion methods as well as metabolically induced defatting. We also discuss the challenges ahead that need to be addressed for clinical implementation.

B. The Prevalence of Hepatic Steatosis in the Donor Pool

Liver steatosis (fatty liver) is an early and mild stage abnormality within a broad spectrum of conditions that fall under the umbrella of NAFLD [1]. It is a very common chronic liver-related abnormality in North America and is estimated to occur in more than 65% of individuals who are obese (defined as body mass index, BMI > 30) [11]. Morphologically, steatosis is the accumulation of lipid droplets within hepatocytes. Microvesicular steatosis is defined as an accumulation of relatively small lipid droplets that do not displace the hepatocyte nuclei. Microsteatotic livers can be successfully transplanted even at high steatosis percentages [2, 3, 5, 8]. In contrast, macrovesicular steatosis, which is characterized by large lipid droplets that displace the nucleus to the cell periphery, is a significant risk factor for primary non-function post transplantation in humans and is associated with increased morbidity and secondary injury such as renal failure [2, 3, 5, 8]. A recent large-scale analysis suggests that macrovesicular steatosis in more than 30% of hepatocytes decreases 1-year survival post-transplant [8]. Therefore, transplantation centers typically shy away from using procured livers exhibiting > 30% macrovesicular steatosis for orthotopic liver transplantation. Macrosteatotic livers below this cutoff may be used, however, if transplantation can be performed after a static cold storage period not exceeding 6 hours [2, 3, 5, 8]. On the other hand, in the presence of additional risk factors, such as increasing donor age, macrosteatotic livers are more likely to be discarded [8]. Given that obesity in the U.S has surged from 19.8 to 27.2% in the last decade [37], it is expected that the proportion of macrosteatotic livers in the donor pool will increase. Another daunting trend is the increasing age of the general population, which will superpose on the effects of the obesity

epidemic. As a result, without measures to salvage more macrosteatotic livers, we are facing a likely decrease in the number of eligible donors in the coming years.

C. Elevated Sensitivity of Steatotic Livers to I/R Injury

Evidence suggests that steatosis increases sensitivity of the liver to the stresses that are inherent to the liver transplantation procedure, more specifically cold ischemia and I/R-related events. In-vivo and in-vitro studies using animal models suggest that liver injury due to I/R is largely initiated within the liver parenchymal cells [21-23]. Furthermore, there is evidence that the presence of excess lipids within hepatocytes exacerbates I/R response. For example, one study has shown that microsteatotic hepatocytes in culture are more sensitive to I/R-mediated injury compared to their lean counterparts. The level of injury, measured by hepatic intracellular enzyme release as a cellular death marker, was correlated with the level of intracellular TG content [23]. Furthermore, by comparing mouse models of microsteatosis and macrosteatosis, Selzner et al. showed that macrosteatotic livers are more susceptible to I/R-mediated injury than microsteatotic livers with a similar TG content, clearly suggesting that besides the amount of TG stored, the presence of macrodroplets also exacerbates I/R sensitivity [21]. We must also be cognizant of the fact that in human livers, the presence of steatosis is a well-described response to hepatocyte injury and could also be a marker of one or several predisposing conditions that may contribute to the increased sensitivity to I/R. Nonetheless, as discussed further below, I/R sensitivity of steatotic hepatocytes can be reversed by reducing stored fat [23], consistent with the notion that excess lipid storage is independently a major cause of I/R hypersensitivity.

D. Mechanisms of Elevated Sensitivity of Steatotic Livers to I/R Injury

Several mechanisms have been proposed to explain the exacerbating effect of steatosis on I/R injury, although it should be pointed out that these studies do not generally attempt to distinguish between microsteatotic and macrosteatotic livers. Human as well as animal studies suggest that

post I/R, steatotic livers are subject to more lipid peroxidation [19, 23, 27, 38] and more exuberant pro-inflammatory responses, including increased release of pro-inflammatory mediators such as tumor necrosis factor-alpha (TNF-α) [6, 38], and increased neutrophil infiltration [39]. In addition, animal models have shown that the increased cellular volume of steatotic hepatocytes leads to narrowed and tortuous microvessels in steatotic livers, consistent with reduced hepatic and sinusoidal blood flow post injury compared to lean livers [19, 21, 28, 39].The impaired sinusoidal blood flow is also consistent with reported hepatocyte mitochondrial dysfunction and decreased intrahepatic energy as indicated by reduced ATP levels in steatotic livers [19, 23, 28]. Interestingly, an in-vivo Zucker rat model of I/R suggests that livers containing micro and macrosteatosis exhibit hepatocellular necrosis as the predominant form of cell death while lean livers mainly exhibit apoptosis [26]. It is possible that reduced ATP levels in steatotic livers favored necrosis vs. apoptosis because the latter is an ATP-requiring pathway. It was reported that inhibiting apoptosis pathways in lean livers undergoing I/R is effective in reducing the extent of injury, but not effective in the case of steatotic livers due to the difference in cell death mechanisms [26].

E. Experimental Approaches To Target I/R Injury Mechanisms in Fatty Livers

A variety of techniques have been tested to address one or more of the putative mechanisms that predispose steatotic livers to I/R injury in experimental animals. These approaches generally consist of using pharmacological agents or pre-conditioning methods to turn on protective pathways before subjecting the liver to I/R stress.

Pharmacological approaches

While many pharmacological agents have been tested in the context of liver transplantation, only few have been used on macrosteatotic livers [3]. Some of these agents have been added to the cold storage preservation solution, and found to reduce I/R injury-related markers in reperfused

Zucker rat steatotic livers [19]. For example, carvedilol, a beta- and alpha-adrenergic blocker to treat ischemic heart, reduced hepatic death markers, vascular resistance, and reactive oxygen species, as well as increased bile production and hepatic ATP levels post reperfusion [19]. In a separate study aimed at reducing the increased levels of peroxidation observed in steatotic livers, obese Zucker rat livers containing micro and macrosteatosis were intravenously administered the anti-oxidant glutathione (GSH)-ester shortly prior to reperfusion in a surgically-induced hepatic ischemia model. The treatment elevated intracellular levels of GSH and significantly reduced lipid peroxidation, I/R injury markers and hepatic death [27]. In a similar animal model, Laurens et al. successfully reduced liver injury markers and enhanced the 15-day survival rate from 40 to 70% by increasing hepatic ATP content via intravenous administration of Tacrolimus 24 h prior to surgically induced I/R injury [29]. In a hypothermic I/R model where hepatic micro and macrosteatosis were induced by feeding the rats a choline- and methionine-deficient diet (CMDD), administration of the GSH precursor N-acetylcysteine 15 minutes before liver harvesting normalized GSH levels, reduced hepatic death markers and microcirculatory injury [39]. In the same study, it was also shown that pretreatment with an antibody to intercellular adhesion molecule-1 (ICAM-1) prior to subjecting the graft to 60 minutes of warm ischemia inhibited neutrophil infiltration and reduced hepatic death markers [39]. In sum, although a significant reduction several I/R injury markers was generally reported in these studies, in most cases the level of injury remained high above that of steatotic livers which did not undergo I/R injury, or lean livers [19, 27, 29]. It is worth noting that none of these studies investigated the possibility of combining several pharmacological agents at once, therefore it is possible that doing so would lead to more dramatic decrease in sensitivity to I/R injury.

Ischemic pre-conditioning approach

A surgical method whereby the major blood vessels to the liver are clamped momentarily, known as ”ischemic pre-conditioning”, has been shown to reduce lipid peroxidation, hepatic

microcirculation failure, and neutrophil accumulation after subsequent I/R injury, when applied to microsteatotic and macrosteatotic livers [21]. This treatment restored microcirculatory parameters to those observed in lean livers for both micro and macrosteatotic livers, but had a more mitigated benefit on cell death markers. While cell death markers in microsteatotic livers returned to levels found in lean livers, macrosteatotic livers remained above baseline [21]. The protective mechanism appears to involve nitric oxide (NO) [21, 27]. Ischemic preconditioning has been shown to protect human livers against a subsequent period of ischemia in patients undergoing hemihepatectomy. The analysis of a subgroup of patients with mild to moderate steatosis presented reduced serum levels of liver damage markers (aspartate/alanine aminotransferases) when preconditioned [40].

Heat shock pre-conditioning approach

Another experimental approach to alleviate I/R injury is heat shock pre-conditioning, which has been shown to preserve microcirculatory parameters (sinusoidal perfusion rate, sinusoidal diameter, minimal leukocyte-endothelial adhesion) and prevent microvascular perfusion failure after surgically induced I/R in livers from obese Zucker rats containing micro and microsteatosis [30]. This study reported decreased oxidative stress (as measured by the oxidized /reduced glutathione ratio) and liver damage markers such as hepatic intracellular enzyme release [30]. Similarly, in a CMDD rat liver transplantation model containing micro and macrosteatosis, heat shock preconditioning dramatically improved the recipient 1 week post-transplant survival rate to that of lean liver recipients [41]. Interestingly, there was a time window of efficacy ranging from 6 to 24 hours post heat shock, which correlated with the dynamics of heat shock protein (HSP) expression in liver, in particular HSP72 and heme oxygenase-1 (HO-1) [30, 41]. The protective mechanisms of heat shock pre-conditioning are not fully understood, but the utility of this approach warrants further studies that would enable a rational design of heat shock preconditioning regimens to improve effectiveness and practicality.

F. Defatting as an Alternative Way to Recondition Steatotic Livers

The methods described above focus on reducing one or more of the I/R injury related events that are elevated in macrosteatotic livers. If excessive lipid storage is indeed a primary initiating event in the exacerbated response of macrosteatotic livers to I/R, a conceptually different approach would be to more directly address the initiating cause of I/R hypersensitivity in steatotic livers by "defatting" livers prior to subjecting the grafts to I/R. The concept has been tested in humans, where a combination of a protein-rich (1000 kcal/day) diet, exercise (600 kcal/day) and fibrate drugs (bezafibrate 400mg/day) for 2–8 weeks led to a 3 fold reduction in macrosteatosis [31, 32]. In a separate study, the consumption of omega-3 fatty acids for one month was used to decrease macrosteatosis in three candidates for living donor transplantation who had biopsy-proven hepatic macrosteatosis >30% prior to donation [31, 32]. In both studies, the "defatting" process led to decreased hepatic macrosteatosis, normalized donor liver tests, and successful transplantation [31, 32]. It should be pointed out that alterations in diet and exercise could have wider effects on the donor metabolic state; therefore, we cannot exclude the possibility that besides decreased steatosis, additional indirect effects may impacted the performance of the donor livers.

Animal studies in which diet was used to modulate liver fat content, and studies in cultured hepatocytes incubated with different medium compositions, have clearly shown that when fatty hepatocytes or livers are cleared of intracellular lipids, they recover the normal response to I/R similar to that of their lean counterparts [23, 42]. For example, in a rat model of CMDD-induced macrosteatosis, pre-treating the donors with a diet to reduce the intrahepatic TG content for 3 days or more prior to transplantation increased recipient viability from 0% to greater than 75% [23]. Another study reported that 48 hours of treatment of ob/ob mice with the fatty acid synthase inhibitor cerulenin resulted in a shift from macro to microsteatosis and improved survival after I/R injury [42]. In addition, treatment with cerulenin for 2, 4 or 7 days before liver procurement and transplantation increased recipient survival proportionally with treatment

duration. Notably, cerulenin treatment increased liver ATP and downregulated the endogenous mitochondrial uncoupling protein 2, which may have also contributed to its beneficial effects [42]. Taken together, these studies demonstrate the principle that the higher sensitivity of macrosteatotic livers to I/R injury can be reversed by defatting.

G. Ex-Vivo Machine Perfusion to Defat Steatotic Livers

The studies mentioned above describe defatting strategies that are effective if implemented over a period of several days and may be relevant in the case of living donor liver transplantation. For the defatting approach to be useful on procured liver grafts, however, the kinetics of defatting will need to be accelerated to a time scale of hours, so that defatting can fit into the existing logistics of liver transplantation that typically involve procurement to transplantation within a maximum of 12 hours [20, 43]. Although pretreatment of deceased donors prior to organ procurement is theoretically possible, there is likely more flexibility in the types and doses of agents that could be used during machine perfusion on procured macrosteatotic livers [33]. There is encouraging evidence that defatting is possible within a few hours via ex-vivo normothermic machine perfusion of procured steatotic livers from Zucker rats [35].

Besides being a potential delivery platform for defatting agents, machine perfusion of livers has been shown to be superior to static cold storage in restoring graft viability prior to transplantation when carried out on lean, ischemic, or macrosteatotic explanted rat livers [33, 38, 44]. For example, during one hour normothermic perfusion of macrosteatotic livers procured from CMDD rats, cell death markers were reduced while liver function markers, including bile production, ammonia clearance, urea production, and ATP levels, were significantly higher, compared to livers that underwent static cold storage [18]. While normothermic machine perfusion has yet to be studied on human livers, a recently completed human phase 1 clinical trial at Columbia University reported several beneficial effects of hypothermic machine perfusion on

procured human livers. Hypothermic machine perfusion for up to 7 hours resulted in reduced early allograft dysfunction, biliary complications, vascular complications, and decreased hospital stay length compared to static cold storage [20]. Follow-up studies showed that machine perfusion reduced pro-inflammatory markers while icreasing hepatic ATP in the recipient [43]. However, machine perfusion of human macrosteatotic livers has not been reported.

So far, three animal experimental studies have reported macrosteatotic liver defatting using ex-vivo perfusion [14, 35, 38]. In a preliminary study using porcine livers, ex-vivo normothermic perfusion for 48 hours led to 50% reduction in lipid droplet size in perivenous hepatocytes to reach the size found in control lean livers [14]. During a 60 hour perfusion defatting process, liver function markers such as bile, urea, and albumin production maintained levels similar to that in control lean livers [14]. Similar techniques (6 hours at 20°C or less) applied to micro and macrosteatotic livers procured from obese Zucker rats showed significantly improved preservation compared to static cold storage as indicated by reduced cell death markers and elevated liver functionality such as bile production [38]. While perfusion at 4 and 8°C improved steatotic liver preservation compared to static cold storage, perfusion at the highest temperature examined, 20°C, was superior to that of lower temperatures [38]. It is worth noting that histological examination of the perfused livers revealed a decrease in steatosis at 20°C, but not at 4 or 8°C, which may have contributed to the superior graft preservation [38].

In a separate study aimed at accelerating the defatting kinetics to be within the clinically relevant time scale of several hours, livers obtained from obese Zucker rats were normothermic perfused ex-vivo with a cocktail of agents which proved their defatting potency in a microsteatotic hepatocyte culture model [35]. After only 3 hours of perfusion, a 50% reduction in intracellular triglyceride content as well as reduction in lipid droplet size was observed [35]. The rapid rate of defatting in perfused livers is surprising, since the same agents required several days to defat cultured microsteatotic hepatocytes [35]. One fundamental difference is that the culture

systems consist of hepatocytes only and are devoid of nonparenchymal cells present in liver, although the role of the latter in defatting is elusive [22, 23]. Another plausible explanation is that organ perfusion provides efficient transport of nutrients and other factors to cells, as well as effective removal of waste and secreted products, thus speeding up the defatting process in comparison to static cell culture systems [35].

H. Strategies to Further Enhance Defatting

Normothermic machine perfusion

Clinical implementation of defatting via normothermic perfusion of steatotic liver grafts, even if successful in laboratory animal experiments, will have to overcome several logistical obstacles. Although the concept of machine perfusion is gaining clinical acceptance, all systems used to date have been with hypothermic rather than normothermic conditions [20, 45]. The data suggest that hypothermic machine perfusion was beneficial to non-steatotic livers compared to simple cold storage [20, 43]. Because the processes of lipid oxidation and export are likely to be significantly slower at lower temperatures, decreasing temperature may not be desirable for defatting, although this question has not been investigated experimentally [24, 44]. On the other hand, it may be interesting to evaluate supraphysiological temperatures, as it may be possible to trigger heat shock preconditioning, which has been shown to be protective against I/R stress, as discussed previously [41]. Nevertheless, once more evidence is available to support the use of hypothermic perfusion; it is likely that clinician-investigators will be inclined to move forward into the realm of normothermic perfusion.

Normothermic perfusion systems will need to be further developed into portable perfusion devices that are equipped to handle the rigors of clinical use and transportation by ground and air, a challenging endeavor given their complexity. The reliability of a normothermic perfusion system will require a much higher threshold, since any flow stoppage due to machine

failure - either unrecognized or not acted upon - would cause rapidly damaging warm ischemia. In contrast, the same problem in hypothermic perfusion would not be as damaging since such systems have a "backup" static hypothermic mode, in which case, the result would be similar to simple cold storage, which is the current standard used for transplantation [20, 33, 43].

Normothermic perfusion may however provide major advantages that could mitigate these concerns. During normothermic perfusion, the liver is in a metabolically active state, which enables thorough evaluation of its function and thus suitability for transplantation well beyond what is possible when livers are stored using simple cold storage or cold perfusion. The benefits of normothermic perfusion as a tool to deliver novel resuscitative interventions will likely result in researchers continuing to push the envelope in developing normothermic techniques applicable to clinical setting [33].

Optimizing the perfusion solution

Ultimately, the goal of liver defatting is to rapidly decrease the proportion of macrosteatotic hepatocytes, while maintaining high viability and functionality. Steatosis is the result of an imbalance between TG synthesis and breakdown processes in hepatocytes [1, 11, 23, 35]. Therefore, to achieve significant defatting, the protocol of choice should shift this balance towards more efficient TG breakdown (lipolysis) and excretion of related byproducts, as well as minimizing TG synthesis [14, 23, 35, 46]. The pathways responsible for lipid metabolism are well known; however, there is much work to be done on how best to modulate this metabolism using cocktails of agents in order to achieve rapid defatting without adversely affecting viability and other critical liver functions.

There is a considerable body of literature on transcription factors that regulate lipid metabolism in liver; however, transcriptional regulation typically has a response lag time of greater than 6 hours. Thus, compounds that target such pathways will be minimally effective over

the time scale of ex-vivo perfusion. Rather, agents that mediate their effects via post-translational mechanisms, including signaling effectors, metabolic substrates and co-factors, should be considered for this approach. The major pathways that control TG storage, as well as defatting agents which have been tested to decrease TG storage in a short timeframe are summarized in Figure 2 and briefly discussed here.

The control of lipolysis requires cooperation between perilipins, which are proteins associated with the surfaces of lipid droplets where TG is stored, and lipases, which cleave TGs into diacylglycerol, monoacylglycerol, FFAs and glycerol [35, 46-48]. Indirect activation of protein kinase A by compounds such as forskolin increases phosphorylation of perilipin 5 on the surfaces of lipid droplets and promotes lipolysis [35, 48, 49]. The lipolysis products will readily reform TG unless they are further metabolized and/or excreted from the hepatocytes. This is achieved, in part, by re-esterification of lipolysis products into TG to be packaged in VLDL particles, which are then secreted from the hepatocytes [46]. The addition of amino acids and choline has been shown to promote the synthesis of apolipoprotein B and phospholipids, respectively, both critical for VLDL assembly and to reduce steatosis [35, 50]. Another approach to promote defatting is to increase the transport of FFAs to mitochondria where they undergo β-oxidation to generate ATP and CO_2, as well as ketone bodies that are excreted from the liver [35, 51]. A rate-limiting step in β-oxidation is the transport of FFAs from the cytoplasm into the mitochondria, which requires the conjugation of acyl-coA with L-carnitine by carnitine palmitoyltransferase-1(CPT-1) located on the outer mitochondrial membrane [52]. In-vivo and in-vitro studies have shown that supplementation of L-carnitine in the diet or cell culture medium promotes β-oxidation and a reduction in hepatic TG [52].

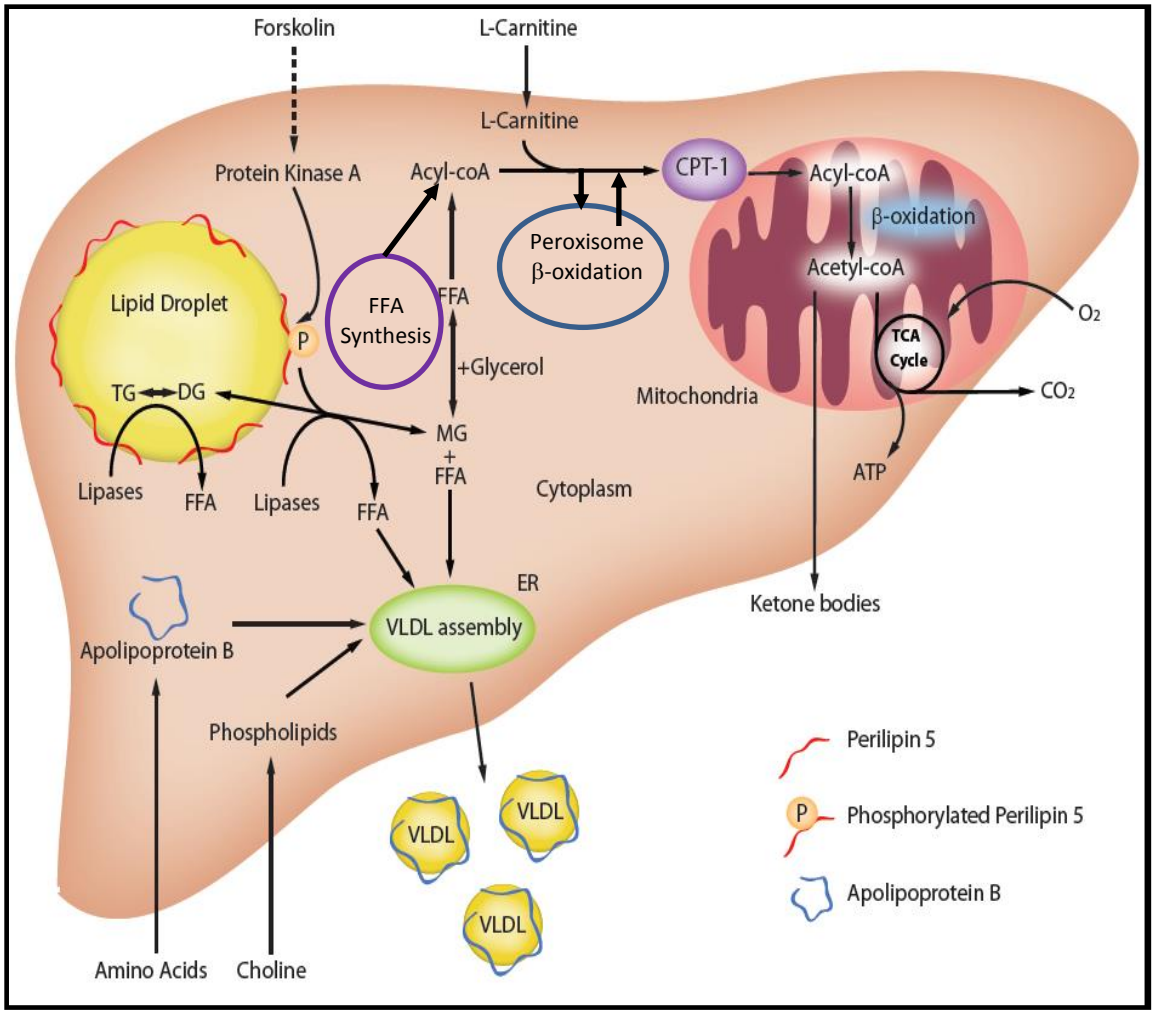

Chapter 1, Figure 1: TG metabolism in steatotic hepatocytes.

Lipids are primarily stored in the form of TG inside lipid droplets which are coated with perilipins. Perilipins control access of the stored TG to cytosolic lipases, which liberate free fatty acids (FFA). FFAs can then undergo oxidation through mitochondrial β-oxidation. FFA and MG translocate to the ER, where they can be reesterified to TG and packaged into VLDL, which is then secreted out of the cells. Major lipid metabolic pathways, including those involved in the removal of TG from steatotic hepatocytes are illustrated. Addition of potential defatting agents that target some of these pathways, such as forskolin, L-carnitine, amino acids and choline, to the perfusate are shown here and discussed further in the text. The dashed arrow represents indirect activation of protein kinase A by forskolin. TG: Triglyceride; FFA: Free fatty acid; DG: Diacylglycerol; MG: Monoacylglycerol; VLDL: Very low density lipoprotein; CPT-1: Carnitine palmitoyltransferase-1; ER: Endoplasmic reticulum; ATP: Adenosine triphosphate.

Targeting multiple routes simultaneously, as illustrated in Figure 2, may provide the most effective approach, but rational design of defatting protocols will require a better understanding of the potential interactions among the relevant metabolic pathways in macrosteatotic hepatocytes. This would be greatly facilitated if a suitable cell culture model of hepatic macrosteatosis were available to perform both screening and mechanistic studies in an efficient manner, prior to testing in actual livers. Although some steatotic hepatocyte culture systems have been described in the literature, they all exhibited microsteatotic, and not macrosteatotic, features [23, 35].

Ultimately, surgeons will require proof that defatted livers are indeed similar to normal lean livers before this approach will gain wide acceptance. It will therefore be important to assess the short and long term functionality of steatotic livers for which TG content has been dramatically reduced by rapid normothermic ex-vivo perfusion defatting in a relatively short period of time. While many challenges need to be overcome, liver defatting is a potentially promising approach to reduce the sensitivity of macrosteatotic livers to I/R injury, and a new modality that may enable the successful recovery of a large number of livers that would otherwise be discarded.

CHAPTER 2:

Image Analysis Methods to Quantify Steatotic Droplets in Human H&E Stained Liver Histology Slides

The materials, images and text used in this chapter have been previously published, at least in part, in Liver transplantation as an original manuscript as can be found in the appendix (Nir I. Nativ, Alvin I. Chen, Gabriel Yarmush, Scot D. Henry, Jay H. Lefkowitch, Kenneth M. Klein, Timothy J. Maguire, Rene Schloss, James V. Guarrera, Francois Berthiaume, Martin L. Yarmush, "Automated image analysis method to detect and quantify macrovesicular steatosis in human liver hematoxylin and eosin-stained histology images", Liver Transplantation, 20: 228-36. February 2014). This publication represent the original work of Nir Israel Nativ as a first author as part of collaborative effort with several co-authors as customary to this field of research. Nir Israel Nativ has significantly contributed the following to this publication: Literature search, understanding the current state of art in macrosteatotic image analysis based quantification, obtaining the histology slides from Columbia University, designing the approach of nucleus proximity to lipid droplet as a macrosteatosis biomarker, writing and/ or editing the text in all sections of the review, creating the relevant figures and tables, addressing reviewers' comments and submission of the original manuscript.

A. Abstract:

Macrovesicular steatosis in over 30% of the liver graft hepatocytes is a major risk factor in liver transplantation. An accurate assessment of macrovesicular steatosis percentage is crucial to determine liver graft transplantability. The gold standard relies on pathologists' evaluations of hematoxylin and eosin (H&E) stained liver histology slides, with the predominant criteria being the LDs relative size and their propensity to displace the hepatocyte's nucleus to the cell periphery. Current automated image analysis systems aimed at objectively quantifying

macrovesicular steatosis do not accurately differentiate macrovesicular LDs from their smaller microvesicular counterparts and do not take into account the effect of the LD on nuclear displacement, leading to poor correlation with pathologists' assessment. Here we present an improved image analysis method that incorporates nuclear displacement as a key image feature to segment and classify macrovesicular LDs from H&E stained liver histology slides. More than 52,000 LDs in 54 digital images from 9 patients were analyzed, and the performance of the proposed method was compared against that of current image analysis methods and the macrovesicular steatosis percentage evaluations of two trained pathologists from different centers. We show that combining nuclear displacement and LD size information significantly improves the separation between micro and macrovesicular LDs (specificity=94%, sensitivity=99%) and the correlation with the pathologists' macrovesicular steatotic percentage assessment (R^2=0.97). This performance vastly exceeds that of other automated image analyzers, which typically underestimate or overestimate the pathologists' macrovesicular steatosis score. This work demonstrates the potential of automated macrovesicular steatosis analysis to be utilized in real-time to ensure the graft transplantability by monitoring the steatotic state of livers and will help standardize macrovesicular steatosis scores among centers.

B. Introduction:

Orthotopic liver transplantation is a highly successful therapy for the treatment of both acute and chronic liver failure but is limited by donor scarcity [2, 8, 43, 53]. Excessive intrahepatic TG accumulation in the form of large LDs that displace the nucleus to the cell periphery, known as macrovesicular steatosis, in more than 30% of the hepatocytes is one of the most common causes of liver graft removal from the donor pool [2, 8]. Such livers are more sensitive to I/R injury inherent to liver procurement, storage, and transplantation, leading to increased rates of primary non-function, as well as increased morbidity and mortality [2, 8]. Macrovesicular steatosis assessment is currently performed by pathologists who rely entirely on H&E stained frozen or

paraffin embedded liver histology slides or images [2, 8]. While the pathologist's quantification of macrovesicular steatosis (in terms of the percentage of hepatocytes which contain macrovesicular steatotic LDs) has been shown to correlate with transplantation outcome [2, 8], it is also a rather subjective analysis and reports indicate significant discrepancies in scoring results among different pathologists [7]. There have been attempts to use other steatosis detection methods such as magnetic resonance imaging (MRI), and they have been shown to correlate with a pathologist's semi quantitative steatosis assessment, however, these methods are limited to detection of total steatosis without the ability to differentiate between small (microvesicular steatotic) and the clinically relevant macrovesicular steatotic LDs [54, 55]. These methods prevent the correct macrovesicular steatosis percentage assessment, which is crucial for the determination of liver graft eligibility for transplantation.

This has motivated several groups to develop an un-biased steatosis assessment of H&E stained liver slides based on image analysis algorithms [7, 14-17]. El-Badry et al. and Li et al. both reported, in separate studies, that these "first generation" algorithms, which quantify steatosis based on the ratio of the total cross sectional surface area (CSSA) of all LDs (micro as well as macrovesicular) to that of the entire tissue area under consideration, underestimates the pathologist's steatosis quantification [7, 16]. This discrepancy likely results from the lack of information on the size distribution of the LDs, as well as the distribution of the LDs among the individual cells, which are features employed by pathologists to generate a macrovesicular steatosis percentage [2, 8, 16]. Other studies followed up with analyses which differentiate micro and macrovesicular steatosis using a predetermined LD CSSA cutoff size [15, 17, 56]. Boyles et al. found good agreement between one such image analysis algorithm and a pathologist's semi quantitative metric of 4 steatosis grades in biopsy specimens obtained from chronic hepatitis C patients [15]. However, the semi quantitative grade used in this study is not an established metric to evaluate liver graft suitability for transplantation, which is usually based on a 30% cutoff in the

percentage of hepatocytes that are macrovesicular steatotic [2, 8]. Marsman et al. found that that automated image-based quantification of macrovesicular steatosis poorly correlated to pathologists' quantification of macrovesicular steatosis percentage in cadaveric liver grafts [17]. In both studies, the distinction between micro and macrovesicular steatosis was based on a universal predetermined cutoff in LD CSSA. Currently, no rigorous optimization of the LD size cutoff has been performed, and none of the existing algorithms take into account a key feature used by pathologists to identify macrovesicular steatotic LDs, namely their ability to push the nucleus towards the edge of the cytoplasm [2, 8].

Herein, we show that using the single criterion of LD size tends to either underestimate or overestimate (depending on the cutoff between micro and macrovesicular steatotic LDs) macrovesicular steatosis percentage compared with trained pathologists' assessment. We also demonstrate that incorporating a criterion of LD-induced nuclear dislocation to the cell periphery dramatically improves the ability to separate the micro and macrovesicular steatotic LDs and the correlation between pathologists' based and automated image analysis-based evaluation of macrovesicular steatosis percentage.

C. Methods:

Human Liver Histology

Human liver tissue samples were collected by core needle biopsy, paraffin embedded, serially sectioned to 5μm,mounted on adhesive slides and eventually stained with H&E stain as described elsewhere [43]. Digital Images were obtained using the Micromaster II (Fisher, Pittsburgh, PA) benchtop phase contrast digital video microscope using Micron 2.0 software (Westover Scientific, Mill Creek, WA) [43].

Segmentation of liver cellular and tissue structures

The H&E stained liver histology image is characterized by multiple types of tissue structures, including steatotic LDs, hepatocyte nuclei and cytoplasm, non-parenchymal cells and sinusoidal spaces. In order to accurately quantify macrovesicular steatosis, cell nuclei and hepatic LDs must be accurately distinguished from the remaining tissue. This requires segmentation that is optimized to have strong edges at the boundaries, circular morphologies with smooth contours, and homogeneous internal features. Model-based segmentation methods such as active contours model (ACM) have been extensively used for such applications [57-59]. However, in order to accurately segment complex images such as those presented in H&E stained liver histology slides, algorithms that employ ACM must overcome several potential limitations. First, a method must be introduced to accurately initialize seeds in the proximity of each image object [60]; this is a difficult task for histology images with thousands of LDs. Second, a stochastic or other factor must be included to prevent convergence at suboptimal local minima [58] and thereby produce segmentations that do not correspond to the outline of the actual object. Third, initial parameters and boundary conditions must be carefully established to prevent numerical instabilities that lead to degenerative segmentations; however, given the high variability between LD sizes, it is challenging to identify a set of initial conditions suitable across all cases. Region based segmentation algorithms are another well-established class of algorithms which enables construction of high quality seed points that can be used in the ACM.

In order to objectively quantify hepatic macrovesicular steatosis from liver histology images, a method that combines the advantages of the ACM and region-growing methodologies have been developed as indicated in Figure 1. Edge function was first discerned from the color gradient of the H&E stained liver histology digital image [61, 62], which notably produces significantly stronger edges than the traditional grayscale gradient [63] (Figure 1B). Next, seed-points for potential steatotic droplets and nuclei were automatically initialized based on light and dark intensity contrast from the color image (Figure 1C) [57-59]. At that point, the ACM is

utilized to refine the optimal surface area boundary by fitting each object to a model of LD or nucleus based on the following characteristics: strong edges at the boundaries, circular morphologies, smooth contours and homogeneous internal features (Figure 1D). The candidate object's score is compared to its score at the previous iteration, and the object's segmentation with the highest score is stored (Figure 1E). Based on trained pathologist assessment, an object's final score cutoff was established to distinguish segmented LDs from segmented sinusoidal spaces and segmented hepatocyte nuclei from nonparenchymal cells.

Quantifying nucleus displacement based on LD- nucleus Adjacency

Macrovesicular steatotic LDs are defined to be intrahepatic LDs large enough to displace the nucleus from the center of the cytoplasm and therefore are typically observed to be adjacent to the nucleus (Supplementary Figure 1A). To quantify this phenomenon using image analysis methods, the LD-nucleus adjacency parameter was generated. The LD radii of 52,000 LDs from 24 liver histology digital images of 6 patients were quantified. In addition, the shortest distance between each LD's perimeter and the perimeter of its nearest nucleus was quantified and LD-nucleus adjacency was calculated as follows: LD-nucleus adjacency = Radius of LD/ (Radius of LD + Distance between LD and nucleus perimeters) (Supplementary Figure 2). Adjacency values approaching 1 indicate that the LD is adjacent to the nearest nucleus.

Exploring the relationship between LD-nucleus adjacency and LD CSSA

The relationship between LD-nuclei adjacency of 52,000 LDs from 54 liver histology digital images of 9 patients and the LD CSSA was explored. The LDs were grouped in 7 clusters based on CSSA, and the percentage of LD-nucleus adjacency > 0.9 in each group was quantified and plotted vs. the average CSSA in each group (Supplementary Figure 1B).

Discriminating micro and macrovesicular steatosis by unsupervised cluster analysis

K-means unsupervised clustering of 52,000 LDs from 54 histology images of 9 patients was employed to investigate whether distinct, homogeneous groupings could be found that suggest separation between micro and macrovesicular steatotic LDs. Six parameters of the image feature space were included in the analysis, namely LDs' radius, mean color intensity, circularity, convexity, aspect ratio, LD-nucleus adjacency, as well as their combinations. Two population distributions (corresponding to micro and macrovesicular steatotic LDs) were assumed for the cluster analysis. Cluster strength was determined using the mean silhouette score s, where s values approaching 1 reflect high inter-cluster distance and low intra-cluster distance, thus indicating improved separation between the two groups [64].

Decision tree learning from unsupervised cluster analysis

Based on the K-means unsupervised clustering of 52,000 LDs from 54 histology images of 9 patients described above, a decision tree classifier was established to provide a set of interpretable (un-factored) rules that delineate micro and macrovesicular steatotic LDs. The size and accuracy of the decision tree was optimized using n-fold cross-validation with n set to 10, as is common with such methods; the final number of nodes selected for the tree was selected to minimize cross-validation error [65] .

Macrovesicular steatosis sensitivity and specificity analysis

LDs in 8 H&E stained liver histology images from 5 different patients were assessed for micro or macrovesicular steatosis by a trained pathologist. LDs in those images were segmented for micro or macrovesicular steatosis using 3 different macrovesicular steatosis distinguishing methods: 1) 176μm^2 CSSA cutoff; 2) 350μm^2 CSSA cutoff, and 3) a two-level decision tree-based criteria. Sensitivity was determined for each image as the ratio of true positives (number of LDs marked as macrovesicular steatotic by both the algorithm and the pathologist) to the true positives and false negatives (number of LDs marked as macrovesicular steatotic by the pathologist but missed

by the algorithm). Specificity was determined for each image as the ratio of true negatives (LDs that were not marked as macrovesicular steatotic by neither the software nor the pathologist) to the true negatives and false positives (LDs that were not marked as macrovesicular steatotic by the pathologist but determined to be macrovesicular steatotic by the algorithm). The percentage values obtained for each image were averaged to yield the mean algorithm sensitivity and specificity values for each method.

Comparing macrovesicular steatosis percentage determined by image analysis methods to pathologists assessments

Macrovesicular steatosis percentage for each H&E stained liver histology image was estimated using 5 classification methods: 1) relative image CSSA occupied by total LDs (micro and macrovesicular steatotic) normalized to image CSSA; 2) relative number of total LDs (micro and macrovesicular steatotic) normalized to the cell number as assessed by nucleus count; 3) relative number of macrovesicular steatotic LDs determined based on a CSSA cutoff of 176μm^2 and normalized to cell number; 4) relative number of macrovesicular steatotic LDs determined based on a CSSA cutoff of 350μm^2 and normalized to cell number, and 5) relative number of macrovesicular steatotic LDs determined based on decision tree classification and normalized to cell number. For each method, the percent macrovesicular steatosis values attained from 3-6 images were averaged to represent the image analysis-based percent macrovesicular steatosis for each patient.

The obtained values were compared to the trained pathologists' estimations based on the values of Log_2-fold difference, fractional deviation, and R^2 of linear regression to assess the accuracy of each method. Log_2-fold difference was calculated as Log_2-(%Macrovesicular steatotic by algorithm/% Macrovesicular steatotic by pathologist). Log_2-fold difference measures the multiplicative deviation of the algorithm's estimate from the pathologists' estimation. A small

Log_2-fold difference indicates higher accuracy. Fractional deviation was calculated as (%Macrovesicular steatotic by algorithm - %Macrovesicular steatotic by pathologist)/ %Macrovesicular steatotic by pathologist. Fractional deviation measures the additive deviation of the algorithm's estimate from the pathologists' estimation. A small fractional deviation indicates higher accuracy. The linear regression coefficient of determination, R^2, it is the squared correlation between the algorithm estimated macrovesicular steatosis percentage and the pathologists' estimation. A R^2 value approaching 1 indicates better fit to a linear model.

Statistical analysis

Results shown in text and figures are means ±1 standard error. One way ANOVA followed by Fisher's LSD post-hoc test was performed using KaleidaGraph (Synergy Software, Reading, PA). Values of $p<0.05$ indicate statistical significance.

D. Results:

By applying a novel image analysis algorithm to H&E stained liver histology images, steatotic relevant morphological features, such as LD size, number, and shape were obtained in an automated and therefore objective manner (Figure 1). Figure 2 demonstrates that an image analysis method aimed at quantifying macrovesicular steatosis percentage solely based on the relative CSSA occupied by all the LDs (micro and macrovesicular steatotic) in the tissue underestimates the pathologists' assessment of macrovesicular steatosis percentage, which is consistent with previous reports [7, 16]. Conversely, determining macrovesicular steatosis percentage using an image analysis method which quantifies the total number of LDs (micro and macrovesicular steatotic) present in the tissue overestimates the pathologists' assessment (Figure 2), which is expected since pathologists account for macrovesicular steatotic LDs only [2, 4, 8].

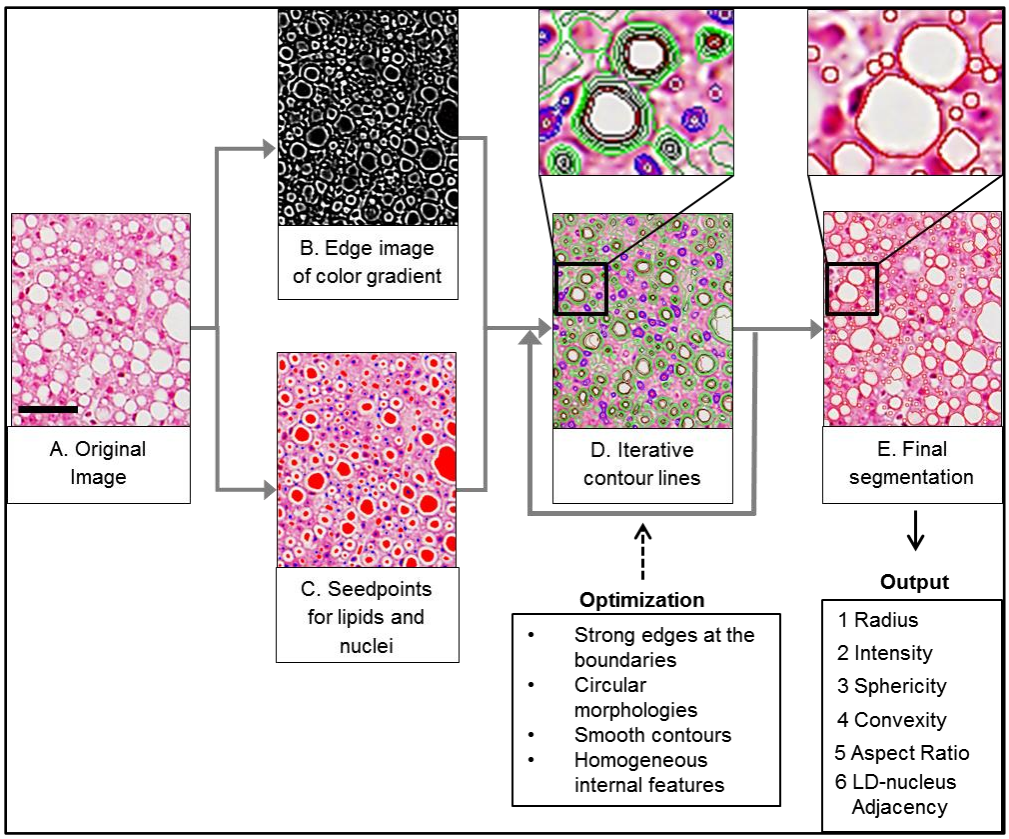

Chapter 2, figure 1: Segmentation scheme of liver tissue and cellular structures in H&E stained liver histology images.

A. H&E stained liver histology image. Bar= 50µm^2.

B. Edge function of color gradient applied to the original image.

C. Seed-points for potential steatotic droplets and nuclei were automatically initialized based on light and dark intensity contrast from the smoothed color image. These seed-points were used in the ACM.

D. ACM is utilized to refine the optimal surface area boundary by fitting each object to a model of LD or nucleus based on the following characteristics: strong edges at the boundaries, circular morphologies, smooth contours and homogeneous internal features.

E. Final segmented image indicates LDs, cell nuclei and morphological features obtained from the image.

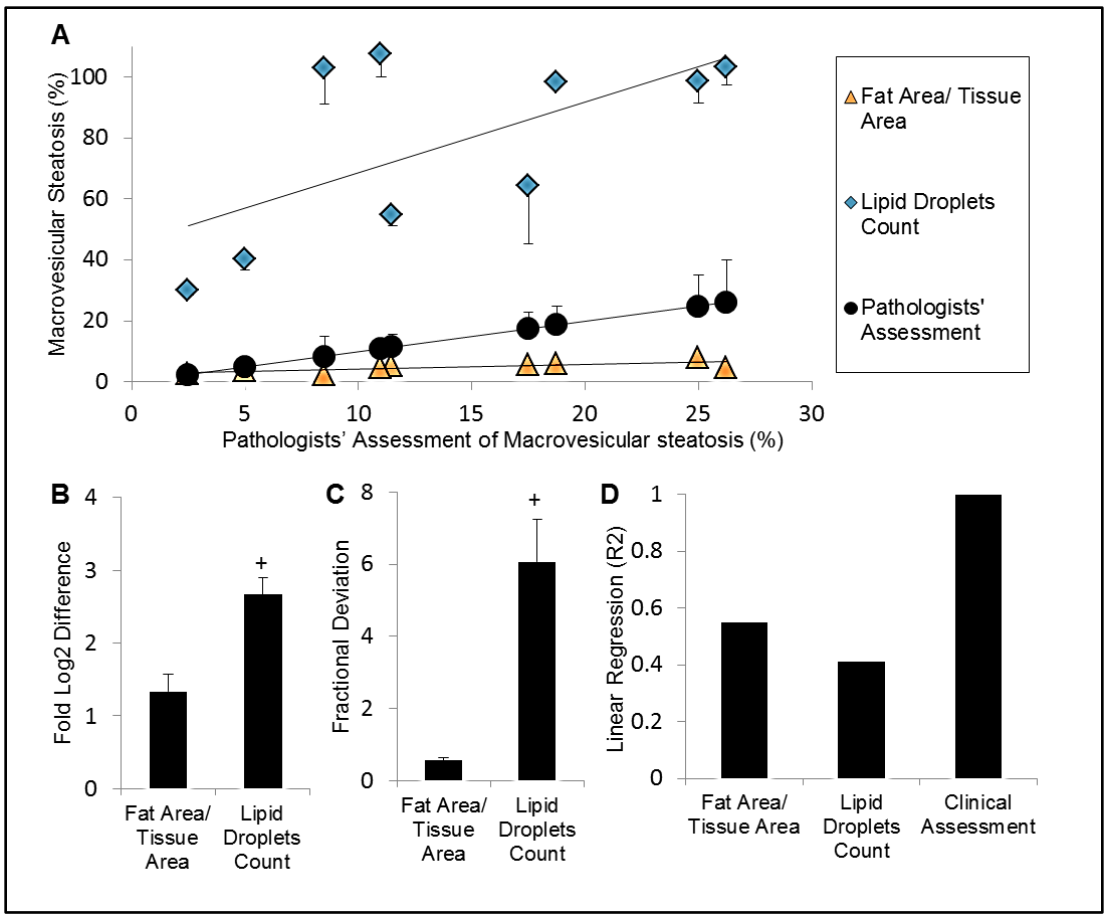

Chapter 2, figure 2: Comparison of image analysis methods reporting steatosis score based on total number of LDs with the pathologists' macrovesicular steatosis percentage score.

A. **Steatosis percentage, as estimated by image analysis methods not separating microvesicular steatotic from macrovesicular steatotic LDs, compared with the average macrovesicular steatosis percentage reported by two trained pathologists from two different centers for 9 patients (N=6 images per patient were analyzed; standard error is shown).**

B. **Log_2 fold difference from pathologists' assessment for each method. Smaller value indicates less multiplicative deviation from the pathologists' assessment. N=9 patients; standard error is shown.**

C. **Fractional deviation for each method. Smaller fractional deviation indicates less additive deviation from the pathologists' assessment. N=9 patients; standard error is shown.**

D. **Linear regression fit (R^2) of each method relative to pathologist's macrovesicular steatosis percentage estimate. N=9 patients.**

The two criteria used by pathologists to define LDs as macrovesicular steatotic are size, as determined by CSSA, together with ability to displace the hepatocyte's nucleus to the cell periphery. Previous reports have sought to differentiate between micro and macrovesicular steatotic LDs solely based on a predetermined LD CSSA cutoff, but with limited success [17, 56]. Here we explored the impact of five shape-dependent features of the LDs – namely LD's mean color intensity, circularity, convexity, aspect ratio, and CSSA – and then added the sixth criterion of LD-nucleus adjacency as an indicator of nucleus displacement (Figure 1 and Supplementary Figure 2). Two-group k-means unsupervised cluster analysis of these six features revealed their relative importance in differentiating the macrovesicular steatotic LDs from the microvesicular steatotic ones within an H&E-stained liver histology digital image (Table 1).

Morphological Features	S Value*
Intensity, Sphericity, Convexity and Aspect ratio	0.33
Radius	0.56
Radius, Intensity, Sphericity, Convexity and Aspect ratio	0.63
LD-nucleus Adjacency	0.59
Radius and LD-nucleus Adjacency	0.74
Radius, Intensity, Sphericity, Convexity, Aspect ratio and LD-nucleus Adjacency	0.78

Chapter 2, Table 1: K-means clustering of macrovesicular steatotic relevant image features
The following morphological features: 1. radius, 2. intensity, 3. sphericity, 4. convexity, 5. aspect ratio, 6. LD-nucleus adjacency, as well as their combinations were evaluated using mean silhouette score *s* for their ability to classify microvesicular steatotic and macrovesicular steatotic LD into two distinct groups. The silhouette score is a measure of cluster strength, where *s* values approaching 1 reflect high inter-cluster distance and low intra-cluster distance; thus indicate improved separation between the two groups.

Clusters resulting from the incorporation of LD mean intensity, circularity, convexity, and aspect ratio yielded a silhouette separation score lower than the separation score for CSSA alone (s=0.33 vs. s = 0.56, Table 1) or when combined (s = 0.63, Table 1). Next, we examined if

the addition of LD-nucleus adjacency to the previously explored features contributes to the ability to distinguish between micro and macrovesicular steatosis. LD-nucleus adjacency alone was observed to yield the highest separation for any single feature (s = 0.59, Table 1), slightly higher than that of CSSA (s = 0.56, Table 1). The combination of the two latter features (incidentally the main ones used by pathologists to differentiate between micro and macrovesicular steatotic LDs), namely LD-nucleus adjacency and LD CSSA, improved separation (s=0.74, Table 1) to levels nearly similar to that obtained by a combination of all 6 features (s = 0.78, Table 1), suggesting that LD-nucleus adjacency and LD CSSA are clearly the main determining features and that other features have little impact on the determination.

These results motivated the inclusion of LD-nucleus adjacency as part of the algorithm which determine if a LD should be defined as macrovesicular steatosis. Analysis of 52,000 LDs from 24 liver histology images of 9 patients has indicated that the as the LD CSSA increases, the percentage of LDs with adjacent nucleus increases (Supplementary Figure 1 A, B). Pathologist examination of these LDs confirmed that the large LDs are adjacent to the nucleus due to nuclear displacement. Furthermore, this analysis revealed that more than 95% of LDs with CSSA equal or higher than 350μm^2 were characterized by LD-nuclei adjacency (Supplementary Figure 1B). This CSSA cutoff is ~2 fold higher than a 176μm^2 cutoff previously described [17, 56] (Supplementary Figure 1B). At the 176μm^2 cutoff, only ~70% of the LDs exhibit LD-nucleus adjacency (Supplementary Figure 1B).

The two LD CSSA cutoffs mentioned above (176μm^2 CSSA cutoff and the LD-nucleus adjacency-dependent 350μm^2 CSSA cutoff) were compared in terms of their ability to generate a macrovesicular steatosis percentage assessment consistent with that of trained pathologists. This comparison revealed that the utilization of any of these two methods have improved ability to determine the gold standard assessment of macrovesicular steatosis compared to methods that does not separate between micro and macrovesicular steatotic LDs (Figures 2 and 3).

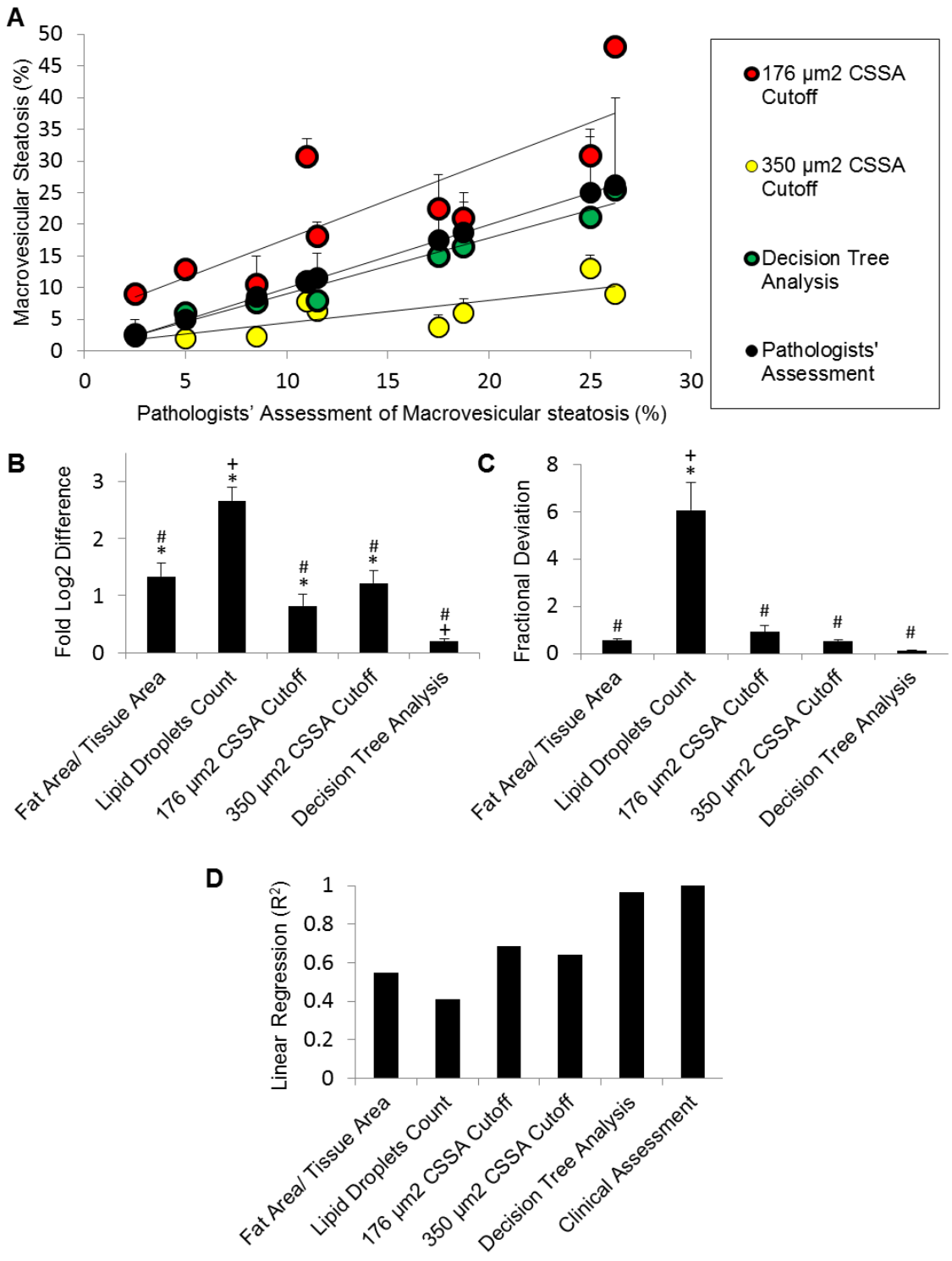
A
Macrovesicular Steatosis (%)
Pathologists' Assessment of Macrovesicular steatosis (%)
176 µm2 CSSA Cutoff
350 µm2 CSSA Cutoff
Decision Tree Analysis
Pathologists' Assessment
B
Fold Log2 Difference
C
Fractional Deviation
Fat Area/ Tissue Area
Lipid Droplets Count
176 µm2 CSSA Cutoff
350 µm2 CSSA Cutoff
Decision Tree Analysis
D
Linear Regression (R2)
Clinical Assessment

Chapter 2, Figure 3: Comparison of image analysis methods reporting macrovesicular steatosis score based on total number of macrovesicular steatotic LDs with the pathologists' macrovesicular steatosis percentage score.

A. **Macrovesicular steatosis percentage, as estimated by image analysis methods separating macrovesicular steatotic from microvesicular steatotic LDs, compared with the average macrovesicular steatosis percentage reported by two trained pathologists from two different centers for 9 patients (N=6 images per patient were analyzed; standard error is shown).**
B. **Log_2 fold difference for each method. Smaller value indicates less multiplicative deviation from the pathologists' assessment. N=9 patients; standard error is shown.**
C. **Fractional deviation for each method. Smaller fractional deviation indicates less additive deviation from the pathologists' assessment.**
D. **Linear regression fit (R^2) of each method to pathologist's macrovesicular steatosis percentage estimate.**

In addition, the LD-nucleus adjacency based cutoff of 350μm^2 yields improved prediction over the previously reported 176μm^2 cutoff (Figure 3). While the macrovesicular steatosis percentage assessment derived from the previously cited cutoff of 176μm^2 overestimates the pathologists' assessment, the 350μm^2 cutoff underestimates it (Figure 3). To explore the reasons for these discrepancies, macrovesicular steatosis assessment sensitivity and specificity analysis using either criteria was performed on individual LDs in 8 H&E stained liver histology images from 5 different patients. Utilizing the previously reported 176μm^2 CSSA cutoff led to ~97% sensitivity, but only ~60% specificity, which may explain the macrovesicular steatosis percentage overestimation (Figure 4A). This relatively low specificity was improved by ~39% to reach ~99% by using a 350μm^2 cutoff ($P<0.001$) (Figure 4A); however, this higher cutoff led to ~30% reduction in sensitivity ($P<0.02$) (Figure 4A). This reduction in sensitivity may be resulted by LDs that displace their adjacent nucleus and would be defined to be macrovesicular steatotic by pathologists, but were slightly below the 350μm^2 CSSA cutoff, and as a result were not counted as macrovesicular steatotic, which may explain the macrovesicular steatosis percentage underestimation (Figure 4B).

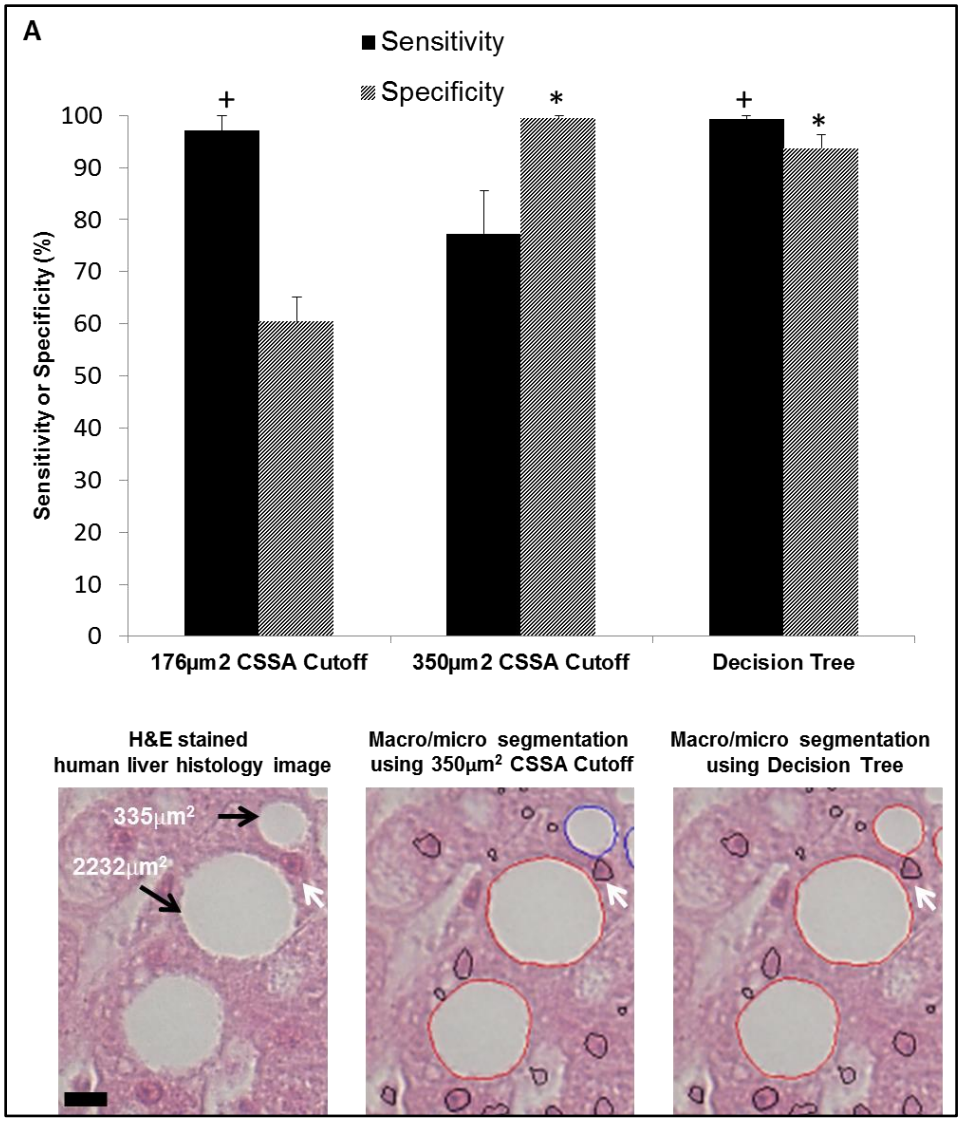

Chapter 2, Figure 4: Sensitivity and specificity of three image analysis methods to detect macrovesicular steatotic LDs in H&E stained human liver tissue sections.

A. Macrovesicular steatotic LDs' sensitivity and specificity percentage of three image analysis methods: 1. 176um^2 CSSA cutoff, 2. 350 um^2 CSSA cutoff and 3. Two-level decision tree. LDs in 8 H&E stained liver histology images from 5 different patients were analyzed. Standard error is shown.

B. Three versions of the same H&E stained human liver histology image: 1. without segmentation, 2. with LD segmentation based on the 350um^2 CSSA cutoff for macrovesicular steatosis, and 3. with LD segmentation based on the decision tree method. Bar=20um^2. Black arrows point to macrovesicular steatotic LDs where their CSSA is indicated as well. White arrows indicates

nuclei. Red and blue border segmentations indicate macrovesicular steatotic and microvesicular steatotic LDs, respectively.

In contrast to the classifiers based on droplet size alone, sensitivity and specificity analysis of a decision tree revealed classifications that were much more comparable to the pathologists' assessment. A 4-node decision tree, pruned to minimize cross-validation error, yielded a sensitivity of ~99% and specificity of ~94% (Figure 4A). The optimized 4-node tree (Supplementary Figure 3) set a low end CSSA cutoff of 174.9 μm^2, under which all droplets were classified as microvesicular steatotic. A high end CSSA cutoff of 347.7 um^2 was set, above which all droplets were classified as macrovesicular steatotic. LDs having CSSA in the "gray area" between 174.9 μm^2 and 347.7 um^2 were classified as macrovesicular steatotic by the tree if above a LD-nucleus adjacency cutoff of 0.9, indicating that a nucleus was likely displaced as confirmed by trained pathologist.

The utilization of a decision tree based assessment, which essentially mimics the thinking process used by pathologists by taking into account both the size and nucleus adjacency of LDs, afforded the high sensitivity of the low 176μm^2 cutoff criteria ($P<0.02$), together with the high specificity of the high 350μm^2 cutoff criteria (Figure 4). Importantly, the decision tree based assessment resulted in optimal correlation with the pathologists' macrovesicular steatotic percentage assessment (Log_2-fold difference=0.19, Fractional deviation=0.12 and R^2= 0.97) (Figure 3).

E. Discussion:

In total, our data indicates that separation of macrovesicular steatotic LD from the microvesicular steatotic ones is crucial when assessing macrovesicular steatosis percentage in human H&E stained liver slides images and leads to improved correlation with the gold standard macrovesicular steatosis assessment by trained pathologists.

While the current algorithms utilize only the LD size (CSSA) to separate between micro and macrovesicular steatotic LDs, we have demonstrated that combining the LD size together with the ability of macrovesicular steatotic LDs to dislocate the cell's nucleus to its periphery, improves separation between micro and macrovesicular steatosis droplets compared with algorithms using LDs' size alone or any other published algorithm. This improved separation led to optimal automated image analysis detection and quantification of macrovesicular steatosis in human liver H&E stained histology images comparable to pathologists' assessment. Importantly, the algorithm described here enables on per LD assessment utilizing a flexible range of CSSAs which does not require utilization of a pre-determined value as in other methods [15, 17, 56] and enable a fully automated macrovesicular diagnostic.

While assessment of macrovesicular steatosis percentage plays a key role in the process of determining liver graft eligibility for orthotopic transplantation, liver graft with macrovesicular steatosis percentage at or marginally below the center acceptable cutoff for transplantation may be still discarded due to additional factors, such as the health of the donor and the recipient, the time of warm and cold ischemia, age and other factors [2, 8] . Nevertheless, this method for automated determination of macrovesicular steatosis level can play a key role in liver transplantability assessment by assisting the pathologist in determining the macrovesicular steatosis state of the liver graft in real time as well as by creating a uniform non-biased macrovesicular steatosis assessment index that can bridge any discrepancies among pathologists and centers [7, 9, 12]. Currently, many transplantation centers use a pathologists' macrovesicular steatosis percentage cutoff of ~30% as steatotic liver graft transplantability criterion. This cutoff may potentially be overly conservative to account for human variability in the assessment, and as a result, some livers that would have been suitable otherwise are discarded. An objective method like the one presented here may provide a more reliable cutoff, which could help refine the steatotic liver graft transplantability criterion, and possibly reduce the number of discarded livers.

It is important to note that variability in macrovesicular steatosis can be generated from the preparation method of the H&E stained liver slide. Heller et al; has demonstrated that assessment of macrovesicular steatosis percentage using frozen sections have led to an overestimation compared with permanent sections, which brought 7% of the livers examined (96 livers in the study) to be considered ineligible for transplantation based on the center macrovesicular steatosis cutoff of 30% [9]. While such discrepancies may be caused by the varying appearance of the LDs size depending on the preparation method, our image analysis method incorporates nucleus displacement as a very robust additional criterion for macrovesicular steatosis LDs, which was shown herein to improve the specificity of macrovesicular steatotic LD classification.

Currently, the only biomarker used to assess liver graft macrovesicular steatosis and transplantability is based on scoring H&E stained liver tissue sections either by a pathologist or image analysis methods as discussed here. Recent studies in animal and in-vitro models of steatosis indicate that in addition to steatosis assessment based on histology alone, an array of biochemical biomarkers could also be used to refine the transplantability assessment of macrovesicular steatotic liver grafts. Some of these methods require tissue biopsies, such as intracellular TG [4, 23] or ATP [4, 66] levels, but may be performed well within the timeframe needed for histopathology slide preparation. Other less invasive methods utilize blood biomarkers such as the levels of released intrahepatic enzymes (aspartate aminotransferase, AST and alanine transaminase, ALT) to the blood stream as an indicator of hepatic injury [4], which can also be done very quickly. In recent years, perfusion methods are being developed to replace the static cold storage approach for graft preservation; in such cases, data collected during perfusion can be also be included in transplantability assessment [4, 43, 67]. A quantitative macrovesicular steatotic percentage could be easily combined with these other quantitative markers to develop

more comprehensive transplantability scores in the future that can be first explored in animal models.

While our automated software can assess macrovesicular steatosis in H&E stained liver slides with high specificity and sensitivity to closely match pathologists' assessment, it is not intended to replace the pathologist during the transplantation process mainly since additional pathological features, such as necrosis, fibrosis, malignancies, bile duct damage etc. need to be assessed prior to transplantation [8, 56, 68]. This novel algorithm enables a fully automated macrovesicular steatosis percentage assessment that can be utilized in real-time and post-diagnosis of human liver grafts to ensure their transplantability and monitor the steatotic state of livers.

CHAPTER 3:

In-Vitro Macrosteatosis Primary Rat Hepatocytes system

The materials, images and text used in this chapter have been previously published, at least in part, in the Journal of Hepatology as an original manuscript as can be found in the appendix (Nir I. Nativ, Gabriel Yarmush, Alvin Chen, David Dong, Scot D. Henry, James V. Guarrera, Kenneth M. Klein,Tim Maguire, Rene Schloss, Francois Berthiaume and Martin L. Yarmush."Rat Hepatocyte Culture Model of Macrosteatosis: Effect of Macrosteatosis Induction and Reversal on Viability and Liver-specific Function", Journal of Hepatology, 59: 1307-14. December 2013). This publication represent the original work of Nir Israel Nativ as a first author as part of collaborative effort with several co-authors as customary to this field of research. Nir Israel Nativ has significantly contributed the following to this publication: Literature search, understanding the current state of art in steatotic in-vitro systems, performing all experimental work and data analysis, writing and/ or editing the text in all sections of the review, creating the relevant figures and tables, addressing reviewers' comments and submission of the original manuscript.

A. Abstract:

A common cause of liver donor ineligibility is macrosteatosis. Recovery of such livers could enhance donor availability. Living donor studies have shown diet-induced reduction of macrosteatosis enables transplantation. However, cadaveric liver macrosteatotic reduction must be performed ex-vivo within hours. Towards this goal, we investigated the effect of accelerated macrosteatosis reduction on hepatocyte viability and function using a novel system of macrosteatotic hepatocytes. Hepatocytes isolated from lean Zucker rats were cultured in a

collagen sandwich, incubated for 6 days in fatty acid-supplemented medium to induce steatosis, and then switched for 2 days to medium supplemented with lipid metabolism promoting agents. Intracellular lipid droplet size distribution and triglyceride, viability, albumin and urea secretion and bile canalicular function were measured.

Fatty acid-supplemented medium induced microsteatosis in 3 days and macrosteatosis in 6 days, the latter evidenced by large lipid droplets dislocating the nucleus to the cell periphery. Macrosteatosis significantly impaired all functions tested. Macrosteatosis decreased upon returning hepatocytes to standard medium, and the rate of decrease was 4-fold faster with supplemented agents, yielding 80% reduction in 2 days. Viability of macrosteatosis reduced hepatocytes was similar to control lean cells. Accelerated macrosteatotic reduction led to faster recovery of urea secretion and bile canalicular function, but not of albumin secretion.

Macrosteatosis reversibly decreases hepatocyte function and supplementary agents accelerate macrosteatosis reduction and some functional restoration with no effect on viability. This in-vitro model may be useful to screen agents for macrosteatotic reduction in livers before transplantation.

B. Introduction:

Orthotopic liver transplantation is limited by donor scarcity [2, 8, 53]. This has motivated the development of strategies to recover livers from deceased donors currently not considered suitable for transplantation [53, 69]. Macrosteatosis, defined as the accumulation of TG in the form of large lipid droplets that displace the nucleus to the cell periphery, when found in more than 30% of the hepatocytes, is a common cause of donor ineligibility [2, 8]. Macrosteatotic livers are more sensitive to I/R injury inherent to liver transplantation, and more prone to primary non-function, as well as increased morbidity and mortality post-transplantation [2, 8]. The incidence of hepatic macrosteatosis is likely to surge due to the obesity epidemic. Thus,

techniques to salvage macrosteatotic livers could significantly enhance donor supply in both the short and long terms [69].

Various approaches targeting the downstream effects of macrosteatosis during I/R have shown promise in pre-clinical and clinical settings [21, 27, 39, 41, 69]. However, several studies suggest that excessive hepatic lipid storage is a primary cause of the exuberant I/R response, especially when in the macrosteatotic form [21-23]. Therefore, an alternative approach could be to eliminate the intracellular lipid droplets, thus decreasing the frequency of macrosteatotic hepatocytes below acceptable levels [69]. Dieting, exercise, and fibrate drugs over several weeks have been shown to decrease macrosteatosis and enable living donor liver transplantation [31, 32]. In a rat liver model of macrosteatosis (induced by CMDD), switching to a normal diet 3 days prior to transplantation reduced intrahepatic TG content by 35% and increased recipient viability from 0% to >75% post-transplantation [23].

Diet/drug-induced macrosteatosis reduction occurs over days to weeks, a timescale that is not applicable to deceased human donors, which would require macrosteatotic reduction ex-vivo within a few hours [43, 69]. Animal studies have demonstrated the feasibility of macrosteatosis reduction via machine perfusion of explanted steatotic livers. This process was accelerated by introducing agents that promote lipid metabolism [14, 38, 70]. However, a thorough exploration of such agents, and combinations thereof, has yet to be performed. Furthermore, there has been little investigation of the impact of accelerated macrosteatosis reduction on the viability and function of hepatocytes, parameters that are critical for the successful outcome of liver transplantation [22, 23, 25, 31, 43, 70].

A suitable cell culture model would facilitate the evaluation of these agents with the ultimate goal of developing protocols to promote accelerated macrosteatosis reduction and functional recovery of transplanted steatotic livers. Microsteatotic hepatocyte culture systems

have been described in this context in the literature [23, 69, 70]; however, their relevance is unclear given that clinical evidence suggests that macrosteatotic – and not microsteatotic – livers are hypersensitive to I/R [69]. Herein, we describe a novel macrosteatotic hepatocyte culture system to investigate the effect of macrosteatosis on viability and liver-specific functions in hepatocytes, and use this system to explore the impact of accelerated macrosteatosis reduction on viability and the recovery of such functions.

C. Methods:

Hepatocyte Isolation and Culture

Male lean Zucker rats, (Charles River, Wilmington, MA) (310±20g) were housed in a 12h light-dark cycle and temperature-controlled environment (25°C) with water and standard chow ad libitum. All experimental procedures followed National Research Council guidelines and were approved by the Rutgers University Animal Care and Facilities Committee. Hepatocytes were isolated using a two-step in situ collagenase perfusion technique [23, 70]. Viability was 90±4% as determined by trypan-blue exclusion [70]. Six-well culture plates (Beckton-Dickinson, Franklin Lakes, NJ) were pretreated with 50ug/ml rat type 1 collagen solution (Beckton-Dickinson) in 0.02M acetic acid (Sigma-Aldrich, St. Louis, MO) overnight at 4°C and washed with phosphate buffered saline (PBS, Invitrogen, Grand Island, NY). Freshly isolated hepatocytes were suspended (10^6 cells/ml) in standard hepatocyte medium and seeded (10^6 cells/well) as previously described [70]. After incubating the cells at 37^0C in a 90% air/10% CO_2 atmosphere for 24h, medium was removed and a collagen gelling solution (0.5ml/well) was added to form a gel overlay [70]. Cultures were maintained in standard hepatocyte medium for 4 days with a fresh medium change every other day. Spent medium was collected (Figure 1A, experimental days 1-5) for analysis.

Steatosis Induction and Reversal

Five-day hepatocyte cultures were switched to steatosis-inducing medium. Standard hepatocyte medium was supplemented with 2,000µM oleic acid, 2,000µM linoleic acid, and 4% (weight to volume) bovine serum albumin (Sigma-Aldrich) for 3 days as previously described [23, 70]. Medium was replaced with fresh steatosis-inducing medium for another 3 days of steatosis induction and the spent medium was collected (Figure 1A, experimental days 5-11). These concentrations of FFAs were chosen based on a dose response study to determine the FFA dose required to induce macrosteatosis, as indicated in Supplementary Figure 1. Following 6-day steatosis induction (11 days post-seeding), the medium was replaced with fresh hepatocyte medium with no steatosis reduction supplements (NSRS), or with a combination of the following steatosis reduction supplements (SRS): 10uM forskolin, 1uM GW7647, 10uM scoparone (Sigma-Aldrich), 1uM GW501516, 10uM hypericin (Enzo, Farmingdale, NY), 0.4ng/ml visfatin (Biovision, Mountain view, CA) and amino acids (Invitrogen) at final concentrations described in supplementary table 1. This cocktail promoted in-vitro microsteatosis reduction by activating hepatocellular TG metabolism [70]. SRS medium pH was adjusted to match that of NSRS. Cells were incubated in SRS or NSRS medium for 48h, after which (13 days post-seeding) the spent medium from all cultures was collected and replaced with NSRS medium for another 48h. On post-seeding day 15, the spent medium from all experimental conditions was collected (Figure 1A).

Hepatocyte Steatosis Assessment

A nondestructive quantitative image analysis method was used to quantify lipid droplet size distribution. Hepatocyte cultures were fixed in 4% paraformaldehyde, stained with the lipid-specific Nile red stain (Adipored™, Lonza, Walkersville, MD), and counterstained with 1ug/ml nuclei-specific Hoechst-33342 stain (Invitrogen), following the manufacturer recommendations. Confocal fluorescence images were obtained with an Olympus IX-80 microscope and analyzed using an in-house algorithm for edge detection, yielding unbiased measurements of size (cross

sectional surface area) and lipid droplet distribution/cell. In addition, hepatocytes were scraped and sonicated in NSRS medium and using a lipase assay kit (Sigma-Aldrich), the TG content measured by quantification of liberated glycerol [23]. Time lapse bright-field images of hepatocytes undergoing macrosteatotic reduction were acquired every 15min for 36h using a temperature and gas controlled (37°C and 10% CO_2 balanced with air) Olympus IX-80 microscope stage. The size of individual lipid droplets was monitored using SLIDEBOOK™ software (Intelligent Imaging Innovations, Denver, CO) to calculate a rate of change in cross sectional surface area.

Hepatocyte Viability Assessment

Cells were washed with PBS, and dead cells quantified following incubation with 4.29ug/ml Ethidium Homodimer-1 (EthD-1, Invitrogen) , and 1ug/ml Hoechst-33342 (Invitrogen) to stain all cells, for 20 min at 37°C [71]. Five 20X epifluorescence images were obtained in 5 separate wells/experimental condition. Cells containing EthD-1 labeled nuclei were counted as dead, while those with Hoechst-stained nuclei were counted as live (Supplementary Figure 2). Percentage of viable cells was determined in each well and averaged for 5 wells/condition [71].

Hepatocyte Function Assessment

Rat albumin was measured by enzyme-linked immunosorbent assay (Bethyl laboratories, Montgomery, TX) and urea nitrogen using a biochemical assay (Stanbio), both using spent media samples and following the manufacturer's recommendations. Concentrations were normalized to the time period between medium changes and the number of viable hepatocytes to convert into specific secretion rates. Bile canaliculi function was assessed by visualization of excreted fluorescent products after incubation with 5-(and-6)-carboxy-2',7'-dichlorofluorescein diacetate (carboxy-DCFDA) (Sigma-Aldrich) at a final concentration of 2uM. This molecule passively enters the cytoplasm of normal hepatocytes, where esterases metabolize it to a fluorescent product

excreted into bile canaliculi [72]. The nuclei were counterstained using Hochest-33342 as described above. Images were captured with an Olympus IX-80 microscope. General intracellular esterase activity was assessed using calcein-acetoxymethylester (calcein-AM, Invitrogen) at 5 ug/ml. Five epifluorescence images were captured using a 20X objective on an Olympus IX-80 microscope in 5 separate wells/experimental condition. The fluorescence levels obtained in each image were quantified using SLIDEBOOK™ software (Intelligent Imaging Innovations) and averaged for the 5 wells/condition. we assessed inducible cytochrome P450 activity as measured by breakdown of resorufin derivatives per established method [72] and found positive activity in all groups (data not shown).

Human Liver Histology

Human liver tissue samples were obtained, stained with hematoxylin and eosin (H&E) and imaged as described elsewhere [43].

Statistical Analysis

Results shown in text and figures are means ±1 standard error. One-way ANOVA followed by Fisher's LSD post-hoc test was performed using KaleidaGraph (Synergy Software, Reading, PA). Values of $p<0.05$ indicate statistical significance.

D. Results:

Macrosteatosis Induction in Primary Hepatocytes

Incubation of collagen sandwiched hepatocytes with steatosis-inducing medium for 3 days (corresponding to 8 days post-seeding) induced a microsteatotic appearance and increased the TG content ~2.7-fold; consistent with prior studies [23, 70](Figure 1B-C). Incubation with steatosis-inducing medium for an additional 3 days increased the TG content even further, reaching ~5 fold the level in lean controls (Figure 1B-C). This level is consistent with two in-vivo models of liver

macrosteatosis (ob/ob mouse and obese Zucker rat) where the intraheptic TG level is also ~5 fold the corresponding lean controls [21, 73]. The additional 3 days of steatosis induction also led to a dramatic increase in the lipid droplet size distribution (Figure 1C). The number of lipid macrodroplets (cross-sectional surface area >350 um^2, defining a macrosteatotic lipid droplet (Supplementary Figure 3)) increased 20-fold compared to the 3-day fatted cells (Figure 1D). The 6-day fatted cells exhibited morphological characteristics found in macrosteatotic human livers, notably large intracellular lipid droplets displacing the nucleus to the cell periphery, as shown in Figure 1 B, E [2]. In addition, lipid droplet cross sectional surface area was comparable to that in macrosteatotic human livers (Figure 1B, E). Hepatocyte viability was 85-90% after the 3-day and 6-day fattening protocols and was not significantly different from lean controls (Table 1A).

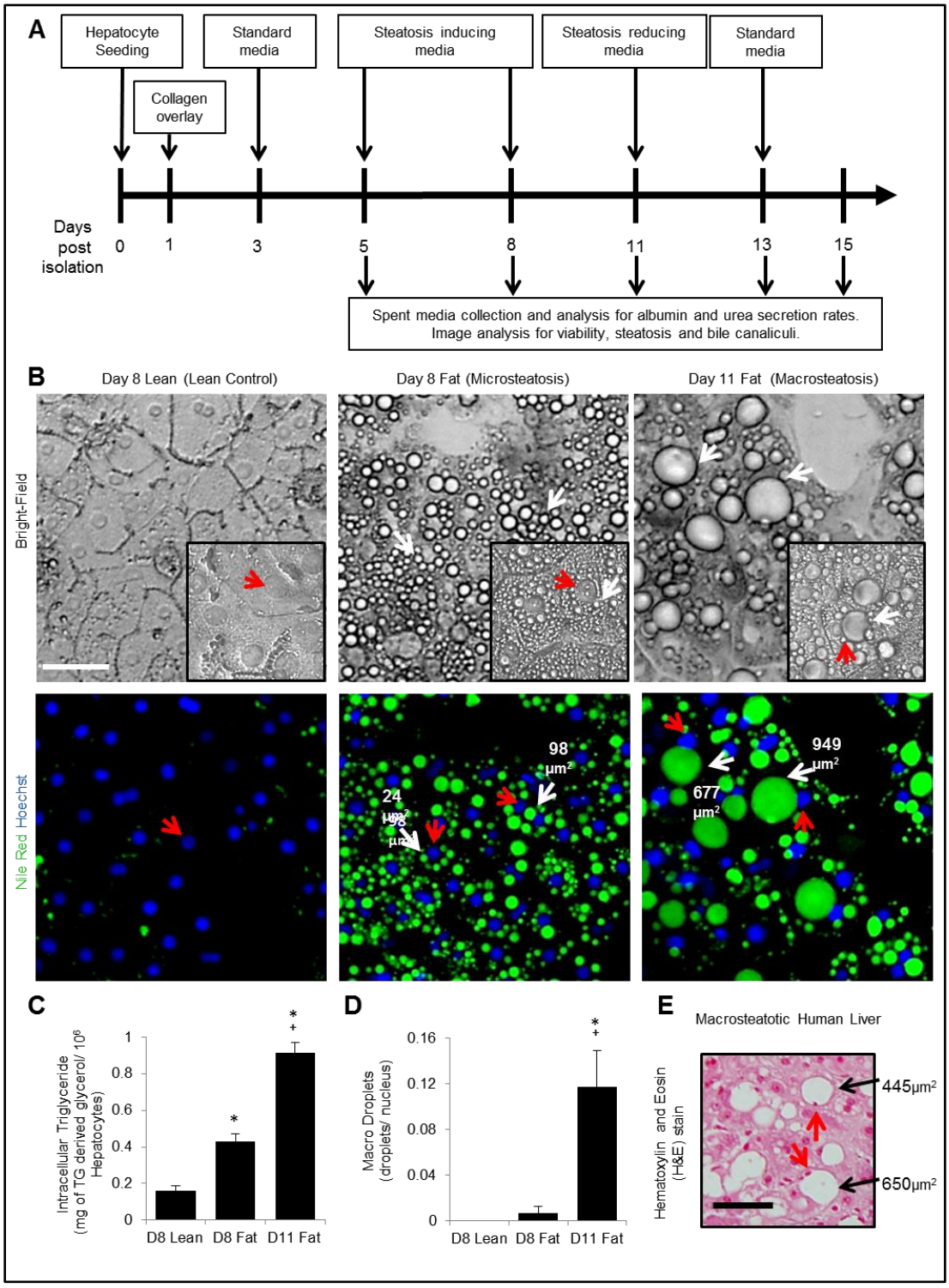
A
Hepatocyte Seeding
Collagen overlay
Standard media
Steatosis inducing media
Steatosis reducing media
Standard media
Days post isolation
0
1
3
5
8
11
13
15
Spent media collection and analysis for albumin and urea secretion rates.
Image analysis for viability, steatosis and bile canaliculi.
B
Day 8 Lean (Lean Control)
Day 8 Fat (Microsteatosis)
Day 11 Fat (Macrosteatosis)
Bright-Field
Nile Red Hoechst
98 µm²
24 µm²
949 µm²
677 µm²
C
Intracellular Triglyceride (mg of TG derived glycerol/ 10⁶ Hepatocytes)
D8 Lean
D8 Fat
D11 Fat
D
Macro Droplets (droplets/ nucleus)
D8 Lean
D8 Fat
D11 Fat
E
Macrosteatotic Human Liver
Hematoxylin and Eosin (H&E) stain
445µm²
650µm²

Chapter 3, Figure 1: Macrosteatosis induction in primary rat hepatocytes.

A. Experimental timeline. B. Hepatocyte morphology post-FFA-supplemented culture. Bright-field (top) and fluorescent images of Nile red and Hoechst stained hepatocytes (bottom) for lean (day 8), microsteatotic (day 8), and macrosteatotic hepatocytes (day 11). White arrows=lipid droplets and cross-sectional areas. Red arrows=hepatocyte nuclei. C, D. Intracellular TG content and macrosteatotic (>350 μm^2) droplet number as a function of steatosis. Means±S.E. N = 6. *p<0.002 vs. D8 Lean, $^+$p<0.007 vs. D8 Fat. E. H&E-stained human steatotic liver. Arrows=macrovesicular lipid droplets and cross-sectional surface areas. Bars=50μm.

A	Day 8	Day 11
Lean Hepatocytes (NSRS)	89.308% ±0.982	88.494% ±0.818
Steatosis induced Hepatocytes	85.414% ±1.833	86.387% ±2.028
B	Day 13	Day 15
Lean Hepatocytes (NSRS)	88.558% ±1.232	85.631% ±2.911
Macrosteatosis Hepatocytes defatted using NSRS	81.994%±2.085	76.195%±2.461
Macrosteatosis Hepatocytes defatted using SRS	83.544%±1.862	74.013%±3.828

Chapter 3, Table 1: Hepatocyte Viability

Percent viable hepatocytes in various experimental groups at the relevant time points (based on images obtained from the EtHD-1 viability assay; sample viability staining is shown in Supplementary Figure 2). Means±S.E. N=5. There are no statistically significant differences between treated hepatocytes and corresponding lean controls on the same experimental day.

Reduction of Macrosteatosis in Primary Hepatocytes

Using the 6-day macrosteatotic hepatocytes, the effect of macrosteatosis reduction on viability and liver-specific function was assessed. To accelerate macrosteatosis reduction, SRS previously shown to accelerate steatosis reduction in microsteatotic cultured hepatocytes, were utilized [70]. NSRS or SRS-containing medium was added to the macrosteatotic hepatocytes for 2 days. When SRS medium was used, macrosteatosis reduction was accelerated ~4-fold compared to NSRS medium to yield ~80% reduction within 2 days (Figure 2A-B). Interestingly, both media compositions were equally effective in reducing TG content by ~30% during that time frame (Figure 2C). The size of individual lipid droplets in macrosteatotic hepatocyte cultures during the first 36h macrosteatosis reduction period decreased linearly as a function of time, while the nucleus returned towards the center of the hepatocyte (Supplementary Figure 4A-B).

After 2 days in NSRS or SRS medium, all cells were switched to NSRS medium for an additional 2 days (days 13-15 post-seeding). At the end of this observation period, regardless of the medium used to reduce macrosteatosis for the first 2 days, the hepatocytes exhibited steatosis levels comparable to control lean hepatocyte cultures (Figure 2D). Thus, while macrosteatotic hepatocytes can eventually exhibit lean-like lipid droplet distribution, SRS medium provides accelerated steatosis reduction during the first few hours.

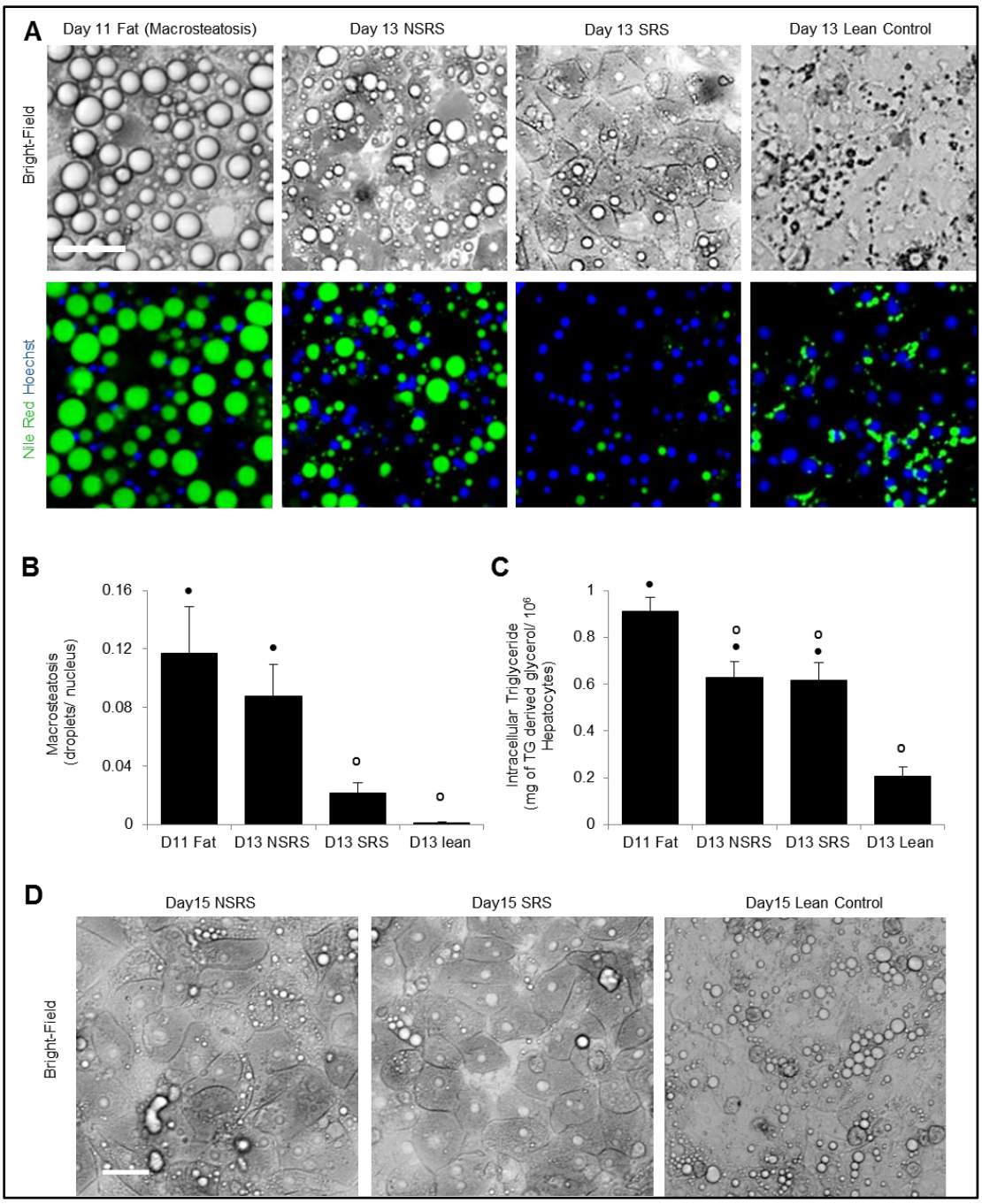
A
Day 11 Fat (Macrosteatosis)
Day 13 NSRS
Day 13 SRS
Day 13 Lean Control
Bright-Field
Nile Red Hoechst
B
Macrosteatosis (droplets/ nucleus)
0.16
0.12
0.08
0.04
0
D11 Fat
D13 NSRS
D13 SRS
D13 lean
C
Intracellular Triglyceride (mg of TG derived glycerol/ 10^6 Hepatocytes)
1
0.8
0.6
0.4
0.2
0
D11 Fat
D13 NSRS
D13 SRS
D13 Lean
D
Day15 NSRS
Day15 SRS
Day15 Lean Control
Bright-Field

Chapter 3, Figure 2: Hepatocyte morphology and lipid content during macrosteatosis reduction.

Macrosteatotic hepatocytes cultures were supplemented (SRS) or not (NSRS) with steatosis reducing agents for 2 days. A. Bright-field (top) and fluorescent images of Nile red and Hoechst stained macrosteatotic hepatocytes (bottom) after 2 days of culture. B, C. Macrosteatotic (>350μm^2) droplet number and intracellular TG content for different steatosis reduction media. Means±S.E. N= 6. •p<0.01 vs. D13 Lean. ^{0}p<0.03 vs. D11 Fat. D. Bright-field images of initially SRS or NSRS treated macrosteatotic hepatocytes after 2 additional days of culture in NSRS medium compared to lean controls. Bar=50μm.

Viability and Function Assessment

As indicated in Figure 3A, macrosteatosis reduction was uneven among the hepatocytes. Viability assessment revealed that reduction occurred only in the viable population (EtHD-1 negative), suggesting that active metabolism was critical. Nevertheless, during the first 2 macrosteatosis reduction days and the subsequent 2 days in NSRS medium, both SRS and NSRS medium treatments maintained hepatocyte viability similar to lean controls on the same experimental day (Table 1B).

Next, cell function was assessed with liver-specific hepatocyte markers used to assess the function of hepatocyte cultures and livers in transplantation settings including albumin and urea secretion rates (Figure 3B-D), as well as bile canalicular morphology and function (Figure 4) [14, 22, 25, 31, 43, 72, 74]. Microsteatotic hepatocytes maintained the albumin secretion rate and exhibited only a 1.7-fold decrease in urea secretion rates compared to lean hepatocyte cultures. On the other hand, macrosteatotic hepatocytes exhibited ~1.5 fold lower albumin secretion levels and a 5-fold reduction in urea secretion levels compared to lean hepatocyte cultures (Figure 3B-C). Thus, macrosteatosis induction for 6 days had a more deleterious effect on hepatocyte function than microsteatosis induction for 3 days.

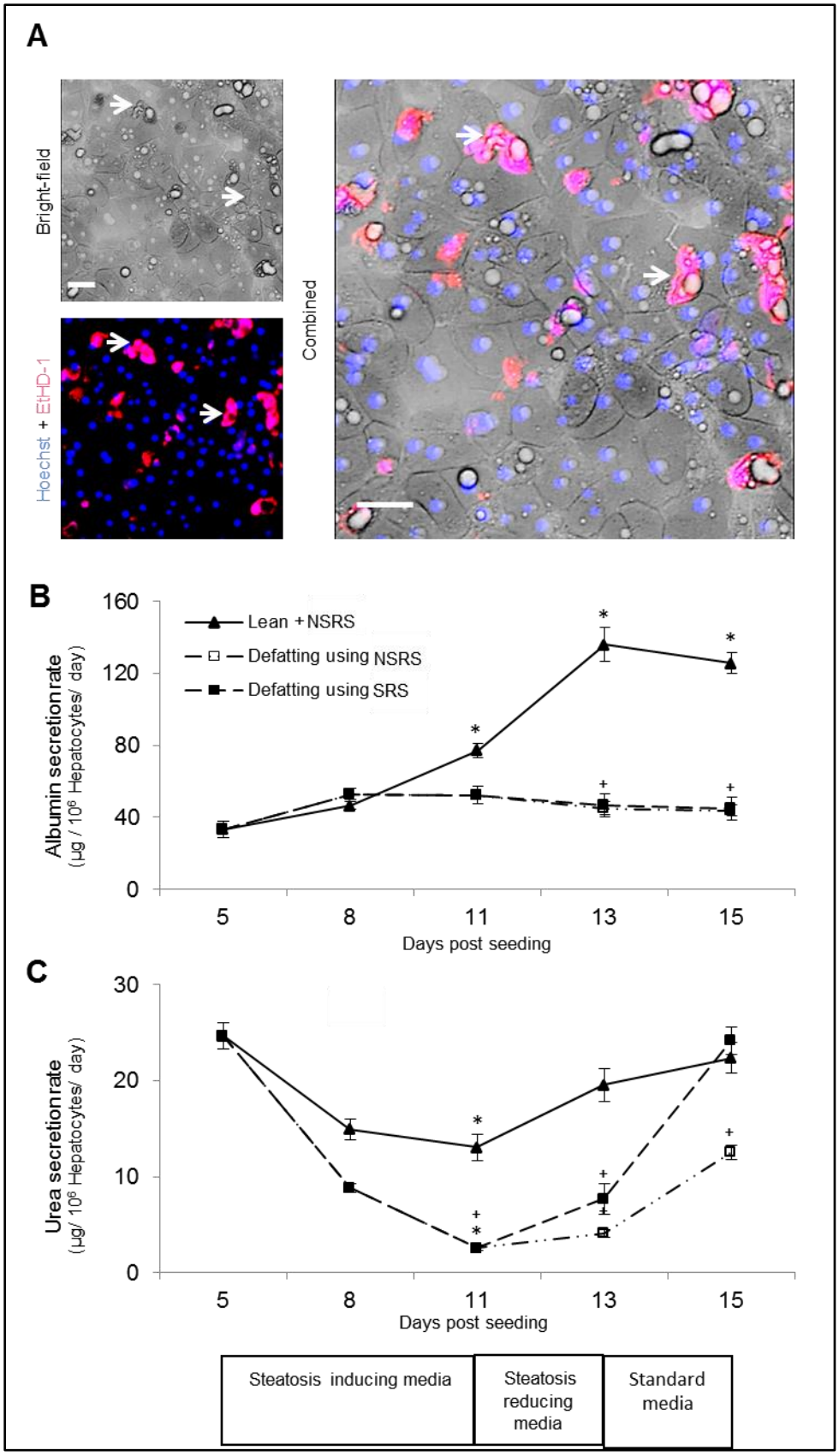
A
Bright-field
Hoechst + EthD-1
Combined
B
Albumin secretion rate
(µg / 10⁶ Hepatocytes/ day)
Lean + NSRS
Defatting using NSRS
Defatting using SRS
Days post seeding
C
Urea secretion rate
(µg/ 10⁶ Hepatocytes/ day)
Days post seeding
Steatosis inducing media
Steatosis reducing media
Standard media

Chapter 3, Figure 3: Effect of steatosis induction and reversal on hepatocyte viability, albumin and urea secretion.

Macrosteatotic hepatocytes were cultured in steatosis reducing medium until day 13 and then standard medium until day 15. A. Hepatocyte viability at the end of the steatosis reduction period (15 days post-seeding). Note that nonviable hepatocytes (EtHD-1^{+}) did not reduce steatosis. White arrows=EtHD-1^{+} cells. Bar=50µm. B, C. Albumin and urea secretion rates normalized to viable cell number. Means±S.E. N=6. *p<0.0001 vs. day 5 lean and $^{+}$p<0.01 vs. lean at the same time point.

In macrosteatosis induction and reversal cycled hepatocytes, albumin secretion remained flat until the end of the observation time (day 15 post-seeding) below lean hepatocyte control levels and did not recover. In this respect, macrosteatotic reduced hepatocytes, treated with SRS or NSRS, behaved similarly (Figure 3B). On the other hand, the urea secretion rate at the end of the observation period returned to ~50% of the lean hepatocyte culture levels in hepatocytes initially treated with NSRS and to ~100% in hepatocytes initially treated with SRS medium (Figure 3C). During the last 2 days, all the cultures received NSRS medium. Therefore, the improved urea secretion recovery rate in hepatocytes initially treated with SRS medium at 15 days post-seeding can be attributed to the long-term effects of SRS treatment, such as the improved macrosteatosis reduction (Figure 3C).

In lean hepatocyte cultures, bile canaliculi and the accumulation of fluorescent carboxy-DCFDA were easily visualized, suggesting a functional bile canalicular network (Figure 4A-B), consistent with similar studies [72]. In macrosteatotic hepatocytes, neither fluorescent carboxy-DCFDA nor the bile canalicular structure was observed (Figure 4A-B). Because carboxy-DCFDA requires cleavage by intracellular esterases to fluoresce and eventually be transported into the bile, we investigated whether esterase activity was affected by macrosteatosis. Similar cultures were incubated with calcein-AM, which requires the same esterases to fluorescently label the cytoplasm. Calcein staining was similar in lean and macrosteatotic hepatocytes, suggesting no

impairment in esterase activity (Figure 4C). Thus, the lack of carboxy-DCFDA accumulation in macrosteatotic hepatocytes most likely reflects a disruption of the bile canalicular function.

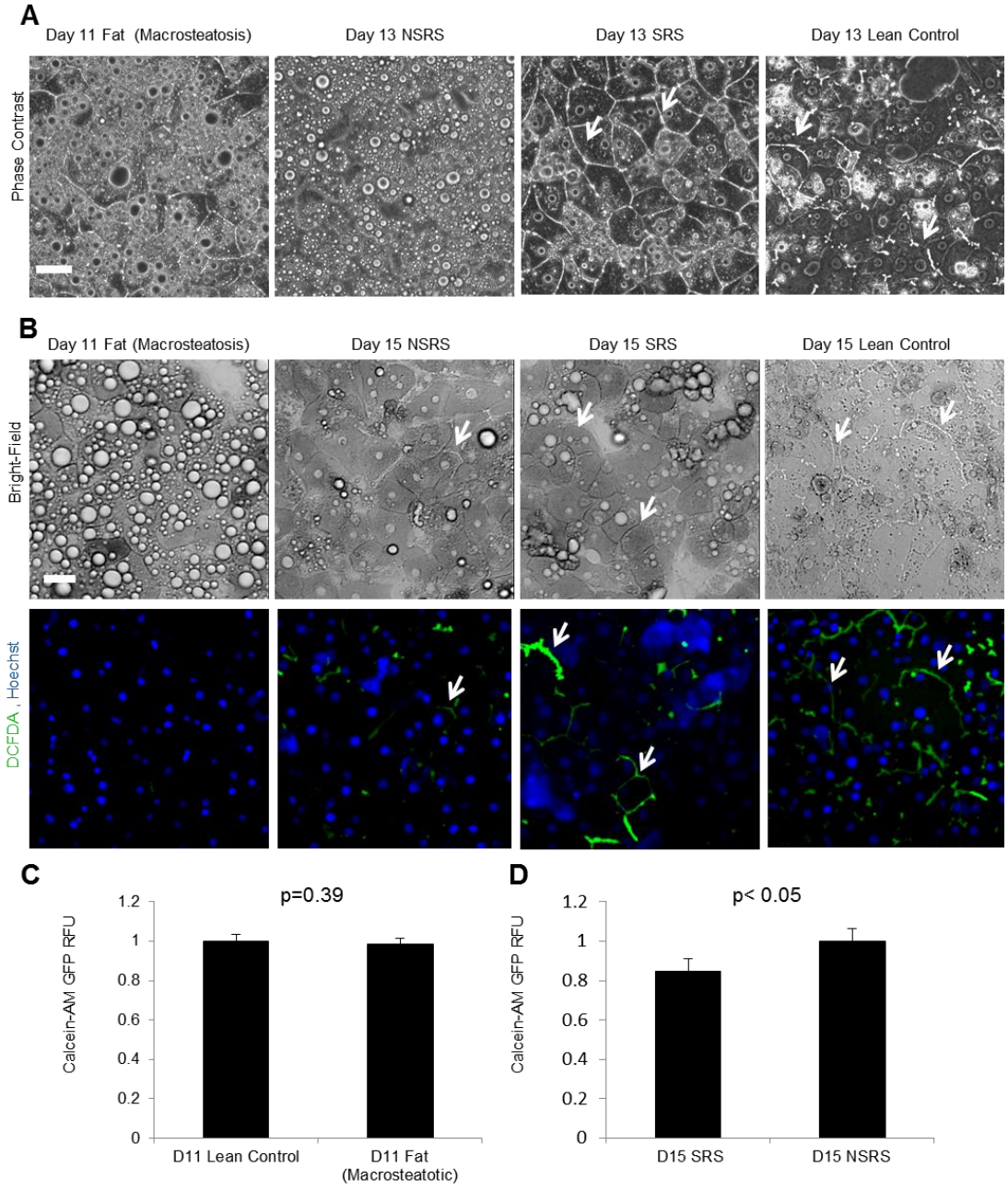

Chapter 3, Figure 4: Effect of steatosis induction and reversal on bile canaliculi morphology and function.

A. Bile canalicular structures visualized by phase contrast appear as bright white hepatocyte borders (white arrows). B. Bright-field (top) and fluorescent images (bottom) of hepatocytes stained with green carboxy-DCFDA, which accumulates in functional bile canaliculi, and blue Hoechst, which stains nuclei. Bar= 50μm. C, D. Esterase activity, assessed by the accumulation of calcein in calcein–AM-incubated cells, is not significantly different between lean and macrosteatotic hepatocytes. Data shown are means±S.E. N=5

Immediately following macrosteatosis reduction (13 days post-seeding), the bile canalicular morphology recovered completely to levels similar to lean controls, but only in hepatocytes treated with SRS medium (Figure 4A). Bile canalicular function partially recovered after macrosteatosis reduction using NSRS medium, while it appeared nearly complete and comparable to lean controls after using the SRS medium (15 days post-seeding) (Figure 4B). Similarly, the recovery in bile canalicular function was not attributed to levels of esterase activity (Figure 4D).

E. Discussion:

We characterized a novel in-vitro primary rat macrosteatotic hepatocyte system whereby intracellular TG accumulation and macrosteatotic lipid droplet formation were induced by incubation in FFA-rich medium. Macrosteatosis induction did not decrease hepatocyte viability, but significantly decreased urea secretion, disrupted the bile canalicular network, and maintained albumin secretion rates below lean controls. Macrosteatosis was morphologically reversed by switching hepatocytes back to NSRS medium within 4 days. Comparable macrosteatosis reduction was achieved in only 2 days with SRS medium. Hepatocyte viability remained high and did not depend on the macrosteatosis reduction rate. Macrosteatosis reduction led to the recovery of liver-specific functions at different rates. Using the SRS medium, urea secretion and the bile canalicular network fully recovered, while albumin secretion rate remained flat and below control

lean hepatocyte levels during the macrosteatosis reduction experimental 4-day timeframe. Since some aspects of hepatocyte functional recovery were improved by accelerated macrosteatosis reduction, this recovery may be dependent upon macosteatosis reduction time and/or may be sensitive to the composition of the supplements and their target pathways. We also found that albumin secretion does not fully recover even if we extend culture time (data not shown). It is possible that the extent of defatting is not sufficiently complete to recover this particular function (since the data show that triglyceride content was still ~68% of macrosteatotic levels, thus remaining well above the "lean" baseline).

Our data show that hepatocytes induced for macrosteatosis after 6 days exhibited lower albumin and urea secretion rates than those induced for microsteatosis after 3 days. This may be due to the direct effect of the increased lipid storage on these functions or to the difference in exposure times to FFA-rich medium. It is worth noting that in the clinic, albumin and urea blood data suggest that macrosteatotic patients are asymptomatic, although they exhibit elevated liver enzymes [10]. These tests, however, do not equate the hepatocyte production rates, as in our system, since blood levels are also affected by clearance mechanisms.

Our study indicates that macrosteatosis significantly decreased bile canalicular function, consistent with observations made post 70% partial hepatectomy in a CMDD rat macrosteatotic liver model, where the recovery of the bile canalicular network was significantly delayed [25]. During recovery, the animals were given a normal diet, which is expected to reduce the steatosis level to that of lean animals [23, 25]. In addition, steatotic rat liver perfusion studies indicate an increased bile secretion rate post-steatosis reduction [38, 70]. Therefore, the steatosis reduction process could have contributed to some aspects of functional recovery of macrosteatotic hepatocytes.

Interestingly, the addition of SRS significantly reduced lipid droplet size compared to NSRS, but TG content was reduced to the same level using either media composition. This contrasts with prior studies using microsteatotic hepatocyte cultures, where SRS promoted a higher degree of TG reduction compared to NSRS medium [70]. The macrosteatotic culture system, which contains 2-fold higher TG levels compared to the microsteatotic system, may have impaired ability to eliminate lipolysis products from the cytoplasm, allowing their re-esterification to TG stored in small lipid droplets, which may not be detectable using the Nile red stain method [70, 75]. If this is the case, further improvement in TG removal may be possible by preventing TG re-esterification, which would also help elucidate whether the redistribution of TG from macro- to micro-droplets, or its removal from the cell altogether, is required [69].

Our study suggests that accelerated macrosteatosis reduction strategies may be used and consequently recover some liver-specific function. The macrosteatosis reduction time scale was ~48h to reduce the number of macrodroplets by ~80%. In order to clinically translate this approach to liver grafts, this would need to be accomplished in a few hours [13, 53, 69]. Interestingly, one study showed that ex-vivo perfusion of obese Zucker rat steatotic liver with a similar cocktail could achieve a significant reduction in lipid droplet size as well as 50% TG reduction within 3h [70]. Thus, it is possible that faster dynamics occur in perfused livers, possibly due to the flow conditions, which likely enhance nutrient and waste transport between cells and the bathing medium [69]. Further improvements to the macrosteatotic hepatocyte culture model could include introducing flow, thus enabling a more rigorous analysis of the combined effects of lipid reduction agents and flow parameters on the macrosteatosis reduction process [69].

In summary, we have established a model system in which macrosteatosis can be induced by culturing hepatocytes in FFA-rich medium. This model is suitable to explore the effect of macrosteatosis reduction approaches on lipid droplet size as well as hepatocyte viability and

liver-specific function. Macrosteatotic hepatocyte cultures maintain high viability but decreased function. Accelerated macrosteatosis reduction does not adversely affect viability and accelerates some functional restoration. This system may be useful to improve our understanding of the effect of macrosteatosis on lipid metabolism and storage, liver-specific functions and hepatocellular response to stresses, such as I/R. This model may also serve as platform to screen and test various lipid metabolism promoting agents that could be eventually used to reduce macrosteatosis in human livers, possibly in conjunction with other methods, such as I/R preconditioning and/or anti-oxidant-based methods to expand the liver donor pool [27, 38, 41, 69].

CHAPTER 4:

Defatting of Macrosteatotic Hepatocytes In-Vitro to Reverse Their Hypersensitivity to Hypoxia/ Reoxygenation Stress

The materials, images and text used in this chapter are in the process of been published, at least in part, in Liver transplantation as an original manuscript as can be found in the appendix (Nir I. Nativ, Gabriel Yarmush, Ashley So, Jeffery Barminko, Timothy J. Maguire, Rene Schloss, Francois Berthiaume and Martin L. Yarmush. "Macrosteatotic Rat Hepatocyte Hypersensitivity to Hypoxia-Reoxygenation Stress Is Reversed by Defatting with Agents That Promote Fatty Acid β-Oxidation", Liver Transplantation, under review). This publication represent the original work of Nir Israel Nativ as a first author as part of collaborative effort with several co-authors as customary to this field of research. Nir Israel Nativ has significantly contributed the following to this publication: Literature search, understanding the current state of art of macrosteatotic H/R hypersensitivity and its reversal using in-vitro systems, performing all experimental work and data analysis, writing and/ or editing the text in all sections of the review, creating the relevant figures and tables, addressing reviewers' comments and submission of the original manuscript.

A. Abstract:

Macrosteatotic liver grafts exhibit elevated intrahepatic TG in the form of large lipid droplets LDs, reduced ATP, and elevated ROS, contributing to their hypersensitivity to I/R injury during transplantation. Decreasing macrosteatosis in living donors through dieting has been shown to improve transplantation outcome. Accomplishing the same feat in deceased donor grafts would require ex-vivo exposure to potent defatting agents. Herein, we used a rat hepatocyte culture

system, which exhibits macrosteatotic LD morphology, elevated TG levels, and hypersensitivity to hypoxia and reoxygenation (H/R), to test for agents that promote defatting and ameliorate H/R hypersensitivity. Preconditioning of macrosteatotic cultures for 48h with a defatting cocktail, previously developed to promote TG catabolism, reduced the number of macrosteatotic LDs by 82% and reduced intracellular TG levels by 27%, but did not ameliorate hypersensitivity to H/R. L-carnitine supplementation to this cocktail, together with hyperoxic exposure, yielded a similar reduction in macrosteatotic LD numbers, and to a 57% reduction in intrahepatic TG storage, likely by promoting FFA β-oxidation, as indicated by a 70% increase in ketone body secretion. Furthermore, this treatment reduced ROS levels by 32%, increased ATP levels by 27%, nearing ATP levels of lean cultures, and completely abolished H/R hypersensitivity as indicated by ~85% viability post H/R and cytosolic LDH release levels similar to lean cultures. Cultures maintained for an additional 48h post hypoxia induction were ~83% viable and exhibited superior urea secretion and bile canalicular transport compared to untreated macrosteatotic cultures. These findings show that macrosteatotic hepatocyte H/R hypersensitivity can be overcome using defatting preconditioning, suggesting a possible route for the recovery of discarded macrosteatotic liver grafts.

B. Introduction:

Orthotopic liver transplantation is the only therapeutic option for end-stage liver disease, but is limited by the scarcity of suitable grafts [2, 8, 43, 53]. Macrosteatotic livers contain excessive intrahepatic TG, which is stored in the form of large LDs, and exhibit hypersensitivity to I/R stress associated with graft preservation injury. Such livers are known to exhibit increased rates of primary non-function post transplantation and are therefore excluded from the donor pool [2, 8, 23, 43, 53]. The extent of preservation injury in both whole livers and hepatocyte cultures, as demonstrated by elevated hepatocellular death, is likely mediated by reduced baseline ATP levels and elevated ROS-related stress, and can be correlated to intrahepatic TG content and the number

of macrosteatotic LDs [4, 21, 23, 29, 38, 66, 76]. Reduction of liver intrahepatic macrosteatosis and TG content while in the donor's body by dieting for several days to weeks has been shown to ameliorate I/R hypersensitivity and enable successful liver transplantation in both humans and animal models [4, 23, 31]. The donor shortage could be significantly alleviated by implementing methods to recondition macrosteatotic livers explanted from deceased donors. Such methods may require ex-vivo exposure of macrosteatotic grafts to agents that decrease LD size and the removal of stored TG, which would in turn reduce hepatocyte hypersensitivity to I/R stress [4].

For efficient evaluation of such agents, we have recently described a macrosteatotic primary rat hepatocyte culture system, which exhibits clinically relevant features observed in human macrosteatotic livers [77]. Using this system, macrosteatotic cultures were preconditioned for 48h with a defatting cocktail previously developed using a microsteatotic hepatocyte culture system. The cocktail contained steatosis reduction supplements, SRS, shown to promote various TG catabolism pathways including LDs breakdown and FFAs oxidation [35]. This preconditioning method was shown to decrease the number of macrosteatotic LDs to levels similar to that in control lean cultures; however, the hepatocytes maintained a relatively high content of intrahepatic TG, possibly due to re-esterification of FFAs released during LD breakdown [77, 78]. It is unclear whether the decrease in LD size alone, or more complete removal of TG, is required to ameliorate hepatocyte hypersensitivity to H/R induced stress, which simulates I/R injury in a static culture system.

Herein, we hypothesized that L-carnitine, which is involved in the shuttling of FFAs from the cytosol into the mitochondria [79, 80], may promote FFA β-oxidation and decrease re-esterification to TG, thus leading to decreased TG storage. Administration of L-carnitine as a nutritional supplement to dieting patients with nonalcoholic steatohepatitis or to rats with steatotic

livers has been shown to effectively reduce hepatic steatosis and TG levels [81, 82]. In addition, L-carnitine addition to a cold preservation solution for 24h was reported to increase ATP levels in steatotic rat livers [83]. Furthermore, the use of hyperoxic conditions, either by oxygenation of isolated perfused livers, or by hyperbaric treatment of whole animals, effectively prevented rat liver graft preservation injury, including in steatotic livers [84-86]. While the mechanism of action was not fully elucidated, it is noteworthy that increased ATP and reduced ROS levels were observed in several of these studies while oxygen consumption was elevated during hepatocyte defatting [35].

Therefore, we investigated the combination of L-carnitine supplementation to the defatting cocktail containing the previously explored SRS and hyperoxia to achieve more complete defatting of the hepatocytes. Furthermore, we investigated the impact of the various defatting strategies on the sensitivity of hepatocytes to H/R induced stress in terms of viability and functional preservation using urea secretion and bile canaliculi transport as biomarkers [77, 87].

C. Methods:

Hepatocyte Isolation and Culture

Male lean Zucker rats, (Charles River, Wilmington, MA) (310±20g) were housed in a 12h light-dark cycle and temperature-controlled environment (25°C) with water and standard chow ad libitum. All experimental procedures followed National Research Council guidelines and were approved by the Rutgers University Animal Care and Facilities Committee. Hepatocytes were isolated using a two-step in-situ collagenase perfusion technique. Hepatocytes with viability of 92±3%, as determined by trypan-blue exclusion, were seeded in 6-well plates in a collagen sandwich configuration at a concentration of 10^6 cells/well [23, 70]. Cultures were maintained in

standard hepatocyte medium for 4 days with a fresh medium change every other day [77] (Figure 1A).

Steatosis Induction

Five-day hepatocyte cultures were switched to steatosis-inducing medium. Standard hepatocyte medium was supplemented with 2,000µM oleic acid, 2,000µM linoleic acid and 4% (weight to volume) bovine serum albumin (Sigma-Aldrich) for 3 days. Medium was replaced with fresh steatosis-inducing medium for another 3 days of steatosis induction to induce macrosteatosis and the spent medium was collected as previously described [77] (Figure 1A, experimental days 5-11).

Steatosis Reversal

Following 6-day steatosis induction, the macrosteatotic cultures were incubated for 48h in a 90% air/10% CO_2 gas mixture at 37^0C in a standard incubator with fresh hepatocyte medium supplemented with a combination of SRS or with SRS media supplemented with 0.8mM L-carnitine (3-hydroxy-4-N, N, N-trimethylaminobutyric acid, Sigma-Aldrich) (SRS+ L-car) (Figure 1A). SRS media was previously shown to accelerate macrosteatosis reduction in-vitro by activating hepatocellular TG metabolism [70, 77], and its component concentrations are described in supplementary table 1. L-carnitine concentration was determined based on cytotoxicity titration experiments (data not shown) and is in agreement with concentrations used in in-vitro studies using steatotic human hepatocyte cell line, HepG2 [80], which were used in an ex-vivo perfusion experiments exploring L-carnitine effect on ketogenesis in perfused steatotic livers from juvenile visceral steatosis mice [88]. In parallel, macrosteatotic cultures were incubated in fresh SRS+L-car medium for 48h under 90% oxygen at atmospheric pressure (SRS+ L-car+ 90% O_2) using a hyperoxia induction chamber consisting of a hermetically closed plastic box (8x12x10 inches)

with drilled ports for gassing and an oxygen probe [23]. The tissue culture plates were placed in the humidified chamber, the chamber closed tightly, and purged for 5 minutes with 90% O_2/10% CO_2 gas mixture and the ports were closed. The chamber was inserted to a 37^0C incubator for 48h, where the oxygen level was maintained ~90% in the chamber. Then, spent medium from all cultures was collected (Figure 1A). L-carnitine uptake during 48h was only ~20% as measured using a commercially available kit (Abcam, Cambridge, MA), and therefore, it was available to the cultures in excess (Supplementary Figure 1).

Exposure of Hepatocytes to Hypoxia-Reoxygenation

The tissue culture plates were placed in the chamber described above. The humidified chamber was purged for 5 minutes with 90% N2/10% CO_2 gas mixture and the ports were closed. The chamber was inserted in a 37^0C incubator for 8h, where the oxygen level was maintained ~0% in the chamber. This hypoxia induction duration was determined based on its ability to display significant macrosteatotic culture hypersensitivity to H/R stress while keeping lean cultures unaffected (Supplementary figure 2A). After the prescribed hypoxia time, the plates were retrieved from the chamber, the culture medium collected for further analysis, and the cells fed with fresh hepatocyte medium pre-equilibrated at normoxic conditions. The plates were then placed back in a standard 37^0C and 90% air/10% CO_2 atmosphere incubator for 6h of reoxygenation (Figure 3A). Then, the cultures were tested for viability using the ethidium homodimer-1 (EhD-1) assay (Supplementary figure 2) and the collected media during hypoxia and reoxygenation was tested for enzymatic release using a commercially available LDH release assay (Roche, Indianapolis, IN) [23, 77, 87] as described below. The media was changed again at 12, 24, 36 and 48h post hypoxia or normoxia induction and tested for urea secretion as a marker for liver specific detoxification ability [77, 87]. At the end of the 48h, relevant cultures were assayed for viability (EhD-1 assay) as well as for bile canalicular transport as an indicator of their

ability to metabolize and excrete compounds using the 5-(and-6)-carboxy-2',7'-dichlorofluorescein diacetate (DCFDA) assay as described elsewhere [77, 87]. The same treatment to the cultures that underwent 8h of exposure to normoxic was used as control.

Hepatocyte Steatosis Assessment

Hepatocyte cultures were fixed in 4% paraformaldehyde, stained with the lipid-specific Nile red stain (Adipored^{TM}, Lonza, Walkersville, MD), counterstained with 1ug/ml nuclei-specific Hoechst-33342 stain (Invitrogen) and confocal fluorescence images were obtained with an Olympus IX-80 microscope [77]. In addition, hepatocytes were scraped and sonicated in standard hepatocyte medium and using a lipase-based assay kit (Sigma-Aldrich), where the TG content is measured by quantification of liberated glycerol [23, 77].

Hepatocyte Viability Assessment

Cultures were washed with PBS, and dead cells quantified following incubation with 4.29ug/ml EthD-1, 5ug/ml Calcein-AM and 1ug/ml Hoechst-33342 (Invitrogen) to stain all cells, for 20 min at 37°C [77]. Five 20X epifluorescence images were obtained in 5 separate wells/experimental condition. Cells containing EthD-1 labeled nuclei were counted as dead, while those with Hoechst-stained nuclei were counted as live. Dead cells were confirmed to be negative for Calcein-AM (Invitrogen) esterase dependent metabolic assay (Supplementary figure 2B). Percentage of viable cells was determined in each well and averaged for 5wells/condition [77]. Hepatocyte injury was assessed by measuring LDH released in the culture medium using a commercial kit (Roche).

Hepatocyte Function Assessment

Urea nitrogen secretion was measured using a biochemical assay (Stanbio), ketone body secretion using a biochemical assay (Bioassay systems, Hayward, CA) and VLDL secretion using a lipase assay kit (Sigma-Aldrich). All assays used spent media samples following the manufacturer's recommendations. Concentrations were normalized to the time period between medium changes and to the number of viable hepatocytes to convert into specific secretion rates. Intracellular ATP content was measured in deproteinized cultures using a colorimetric assay (Biovision, Milpitas, CA). ROS stress was assessed by the ratio of glutathione oxidized to non-oxidized forms (GSSG/GSH) as well as the sum of the two in deproteinized cultures using a colorimetric assay (Biovision) [85].

Statistical Analysis

Results shown in text and figures are means ±1 standard error. One way ANOVA followed by Fisher's Least Significant Difference post-hoc test was performed using KaleidaGraph (Synergy Software, Reading, PA). Values of $p<0.05$ indicate statistical significance.

D. Results:

The primary rat macrosteatotic hepatocyte system previously developed in our laboratory exhibits morphological characteristics of large LDs displacing the hepatocyte nucleus to the periphery and elevated intrahepatic TG, as seen in humans and animal models of macrosteatotic livers (Figure 1) [77]. Preconditioning of these cultures for 48h with the SRS cocktail (steatosis reduction supplements, SRS) or L-carnitine supplemented SRS cocktail under normoxic (SRS+ L-car) or hyperoxic (SRS+ L-car+ 90% O_2) conditions led to a similar reduction of ~82% in the number of macrosteatotic LDs to levels of control lean cultures (Figure 1B, C). However, while the SRS cocktail reduced the intrahepatic TG levels by only 27%, SRS+ L-car reduced it by 41%, and

SRS+ L-car+ 90%O_2 by 57% ($p<0.05$),to levels slightly below that of microsteatotic cultures (Figure 1C).

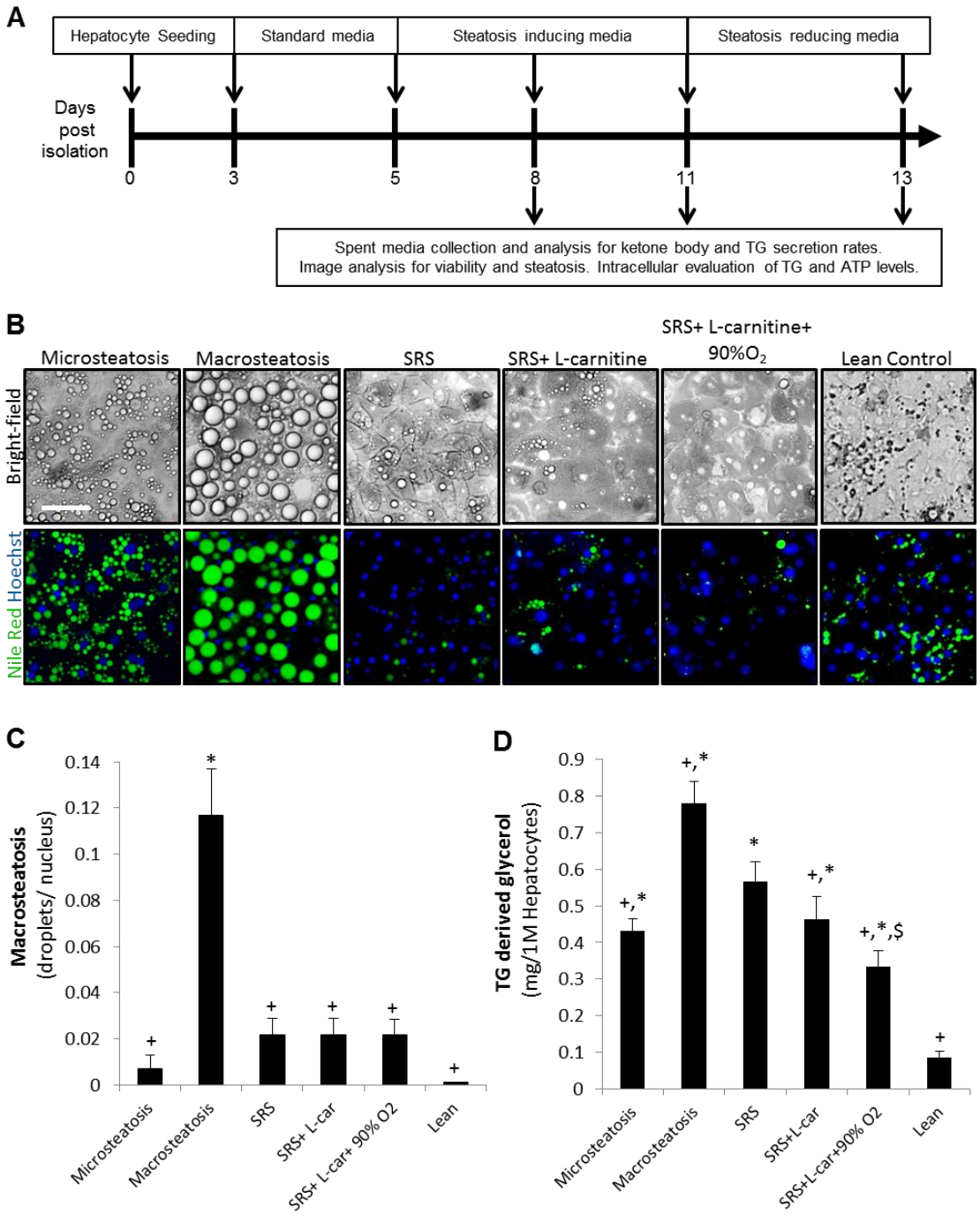

Chapter 4, Figure 1: Hepatocyte morphology and lipid content during macrosteatosis reversal

Macrosteatotic hepatocyte cultures were preconditioned for 48h with SRS, SRS+L-car, or SRS+L-car+ 90% O_2. (A) Experimental timeline. (B) Hepatocyte morphology post-FFA-supplementation (microsteatosis and macrosteatosis), and macrosteatotic cultures after 48h of preconditioning with the 3 treatments. Bright-field (top) and fluorescent images of Nile red (showing LDs) and Hoechst (showing nuclei) stained hepatocytes (bottom). Bar= 50µm^2. (B and C) Macrosteatotic (>350 um2) droplet number and intracellular TG content for different preconditioning treatments. Means ± S.E. N = 6. *p<0.001 vs. lean, +p<0.01 vs. macrosteatosis, #p<0.05 vs microsteatosis and $p< 0.05 vs SRS.

To test the hypothesis that L-carnitine supplementation to SRS media reduces intrahepatic TG levels by promoting the transport of FFAs from the cytoplasm to the mitochondria for β-oxidation, total ketone body secretion rates (a surrogate marker of β-oxidation) and intrahepatic ATP levels were determined. L-carnitine supplementation increased the ketone body secretion rate by 35% and 70% under normoxic and hyperoxic conditions, respectively, compared with the SRS cocktail alone (Figure 2A). The intrahepatic ATP levels in macrosteatotic hepatocytes were reduced by 30% compared to control lean cultures (Figure 2B). While preconditioning with the SRS cocktail increased this value by 11%, L-carnitine supplemented SRS increased it by 22% under normoxia, and by 27% under hyperoxia, up to levels similar to control lean cultures (Figure 2B). The uptake rate of L-carnitine was similar under normoxic and hyperoxic conditions (Supplementary Figure 1). To assess whether the change in intracellular TG levels was affected by TG secretion rates, the latter were measured and found to be the same for all 3 treatments (Figure 2C), thus suggesting that altered TG secretion is not the mechanism of action. A hallmark of macrosteatotic livers is their increased ROS stress as measured by the ratio of oxidized to reduced glutathione (GSSG/GSH) [85]. While the total glutathione levels in all cultures were similar (p=0.3, Figure 2E), the GSSG/GSH in the macrosteatotic cultures was 4.6 fold higher compared with control lean cultures. This ratio was reduced by ~33% (p<0.05) following 48h of preconditioning with any of the 3 treatments, although it remained significantly above that of lean control cultures (Figure 2F).

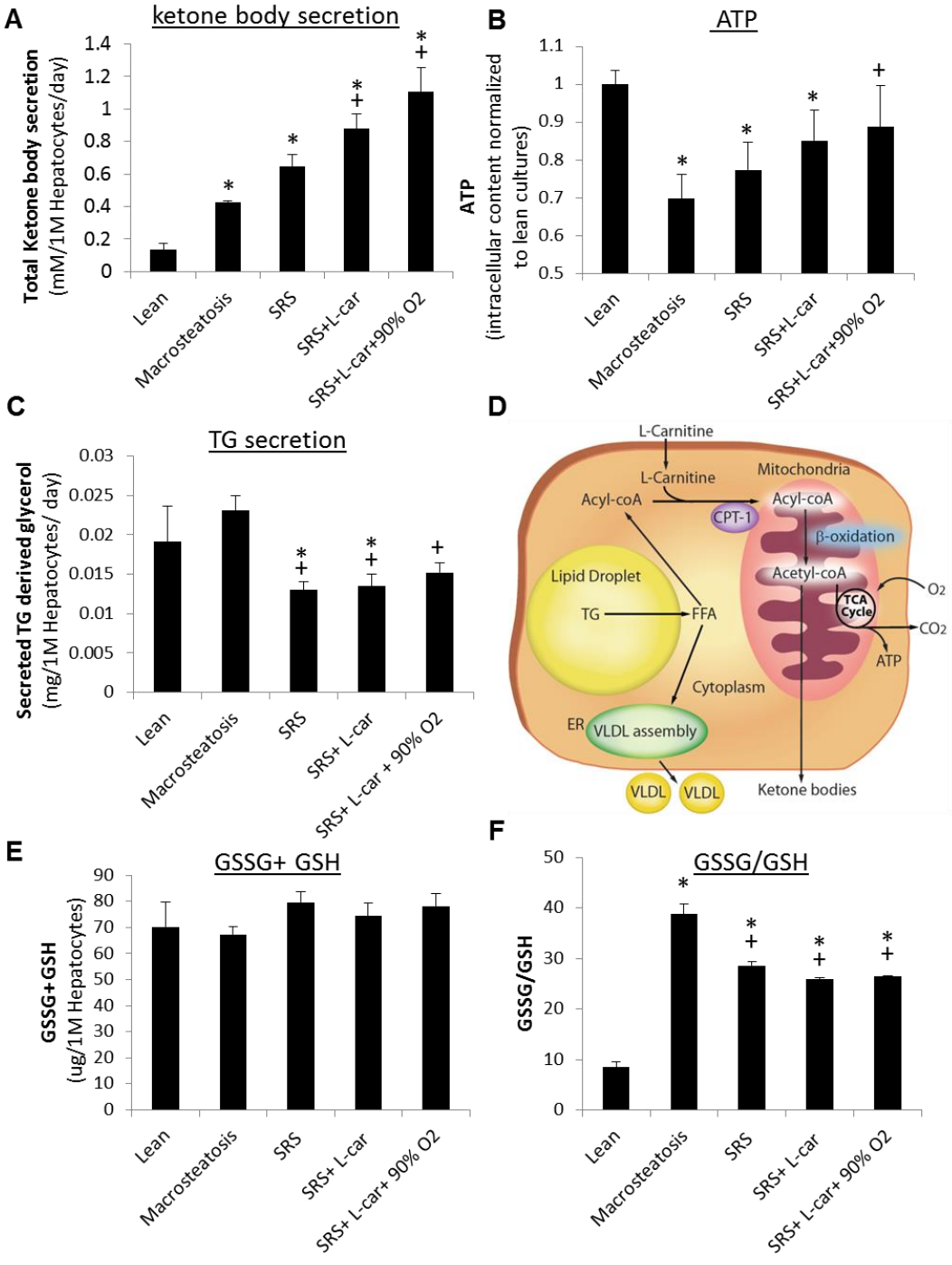

Chapter 4, Figure 2: Hepatocyte macrosteatosis reversal mechanism of action

Macrosteatotic cultures preconditioned for 48h with SRS, SRS+L-car, or SRS+L-car+ 90% O_2 were assayed for total ketone body secretion during treatment (A), intrahepatic ATP content post treatment (B) and TG secretion during treatment (C) to elucidate the possible illustrated defatting mechanisms (D). In addition, the total intracellular glutathione (E, p=0.3) and the ratio between the oxidized (GSSG) to non-oxidized (GSH) forms of glutathione were determined as indicators of ROS stress in the cultures. Means ± S.E. N = 6. *p<0.05 vs. lean, +p<0.05 vs. macrosteatosis.

The viability of lean, microsteatotic, and macrosteatotic hepatocytes that underwent 8h of normoxia followed by 6h of reoxygenation remained >87% (Figure 3A, B, C). However, following 8h of hypoxia followed by 6h of reoxygenation, macrosteatotic cultures exhibited hypersensitivity to the H/R induced stress as indicated by a reduction in viability down to 41% compared to only 78% in the microsteatotic group and 90% in the lean control group (Figure 3A, B, C). Macrosteatotic H/R hypersensitivity was also demonstrated by the ~17 fold increased LDH release after 8h of hypoxia and 6h of reoxygenation compared to the lean controls. Microsteatotic cultures also exhibited hypersensitivity to H/R, although the LDH increase was only ~5.9 times that of the lean controls (Figure 3D).

Preconditioning of macrosteatotic cultures with the SRS cocktail alone for 48h prior to exposure to 8h of hypoxia and 6h of reoxygenation did not reduce H/R hypersensitivity and even showed a trend towards further reduced viability (~10%) and increased LDH release (~25%) compared to macrosteatotic cultures (Figure 3). L-carnitine supplementation to the SRS media during preconditioning under normoxia led to a 10% increase in viability and 60% reduction in LDH release compared to macrosteatotic cultures (Figure 3C, D). However, preconditioning of macrosteatotic cultures with L-carnitine supplemented SRS cocktail under hyperoxia led to a 44% increase in viability over macrosteatotic cultures to reach 85% viability overall, which was comparable to that of control lean cultures (Figure 3B, C). In the same experiment, LDH release

post H/R stress was reduced by 97% compared to macrosteatotic cultures, reaching a level comparable to control lean cultures undergoing the same H/R protocol (Figure 3D).

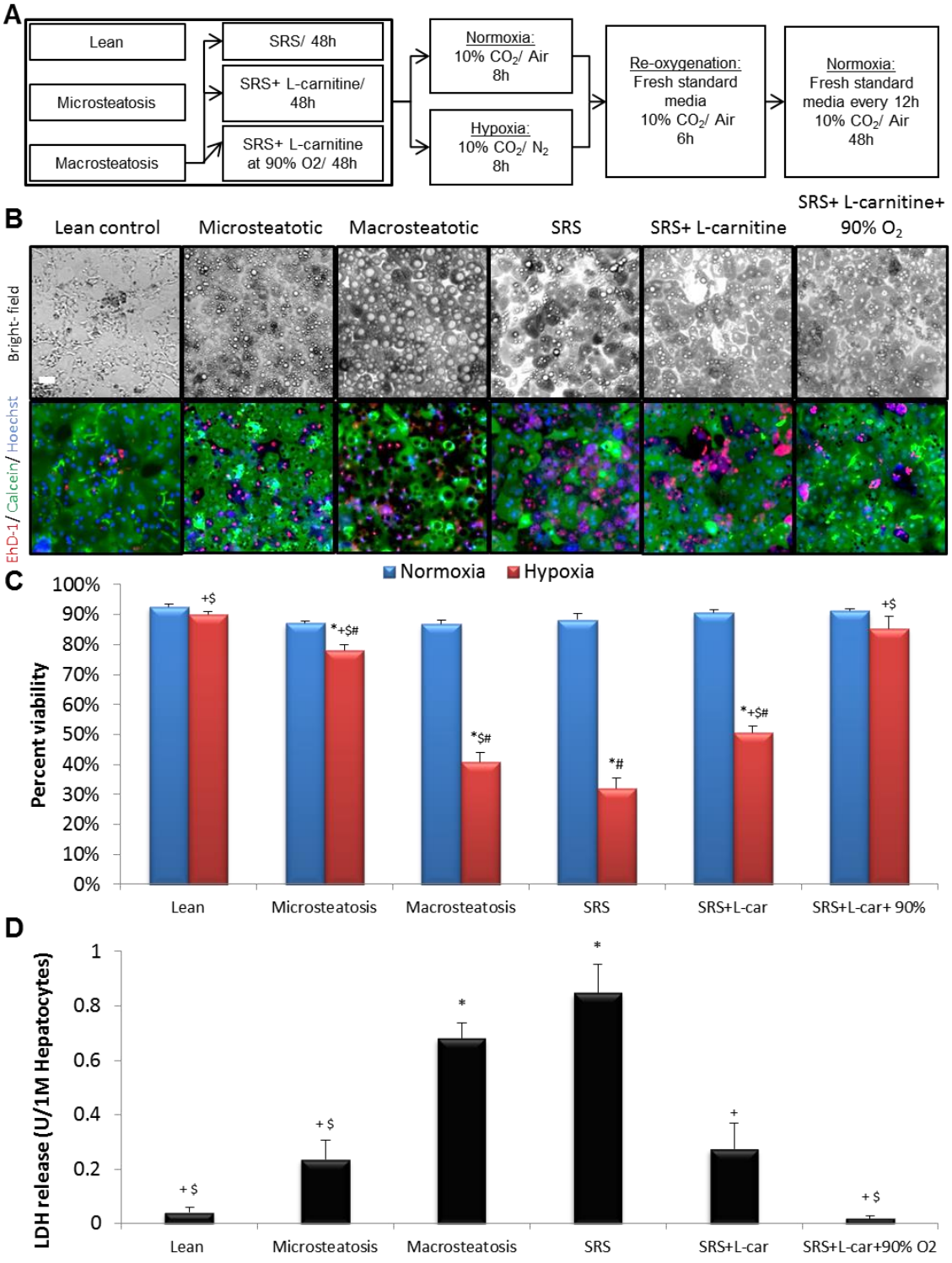

Chapter 4, Figure 3: Hepatocyte sensitivity to in-vitro hypoxia and reoxygenation stress

Lean, microsteatotic and macrosteatotic cultures as well as macrosteatotic hepatocytes preconditioned with SRS, SRS+L-car, or SRS+L-car+ 90% O_2 were exposed to 8h of hypoxia or normoxia followed by 6h of reoxygenation under normoxic conditions as indicated in the flow diagram (A). (B) Bright-field (top) and EhD-1 (red)/ Calcein-AM (green)/ Hoechst (blue) stained epi-fluorescent images of the culture following 8h of hypoxia and 6h of reoxygenation. Bar=50um. (C) EhD-1^+ hepatocytes were considered dead, as confirmed by being Calcein-AM $^-$, to quantify the cultures' % viability post 8h of hypoxia (red bars) or normoxia (blue bars) induction followed by 6h of reoxygenation. (D) Intrahepatic LDH release during 8h of hypoxia and 6 hours of re- oxygenation. Means ± S.E. N = 6. *p<0.05 vs. lean, +p<0.05 vs. macrosteatosis, $p<0.03 vs. SRS and #<0.05 vs. same condition following 8h of normoxia.

Since the L-carnitine supplemented SRS cocktail combined with hyperoxia abolished H/R associated hepatocyte death at 6h post hypoxia induction, we extended the observation period for 48h post hypoxia in standard hepatocyte culture media under normoxia to determine whether viability is maintained and to analyze functional parameters. Macrosteatotic, lean and SRS+ L-car+ 90%O_2 pretreated macrosteatotic cultures that underwent 8h of normoxia exhibited ~90% viability 48h post induction (figure 4A, B), consistent with the data in Figure 3. The viability of macrosteatotic cultures 48h post 8h of hypoxia induction was further reduced to 28%, whereas macrosteatotic cultures preconditioned with SRS+ L-car+ 90%O_2 maintained an elevated viability at about 83%, which was similar to that of control lean cultures that underwent the same H/R protocol (Figure 4A, B).

Urea secretion levels during 48h following 8 hours of hypoxia was higher in the control lean hepatocytes compared with either macrosteatotic or macrosteatotic cultures preconditioned with SRS+ L-car+ 90%O_2 ($p<0.001$) (Figure 4C). However, the accumulated urea in macrosteatotic cultures preconditioned with SRS+ L-car+ 90%O_2 was 95% higher than in macrosteatotic cultures at 48h following 8h of hypoxia ($p<0.001$) (Figure 4C). The accumulation

of the fluorescent DCFDA molecule in the bile canaliculi 48h post 8h of hypoxia induction was used as indicator of the hepatocyte cultures' ability to utilize this transport mechanism for excretion of bile and other metabolized compounds [77, 87]. Macrosteatotic cultures exhibited compromised bile canalicular transport of DCFDA compared with control lean cultures. Preconditioning macrosteatotic cultures with SRS+ L-car+ 90%O_2 for 48h prior to H/R enabled full recovery of bile canalicular transport to levels comparable to those in control lean hepatocytes (Figure 4D).

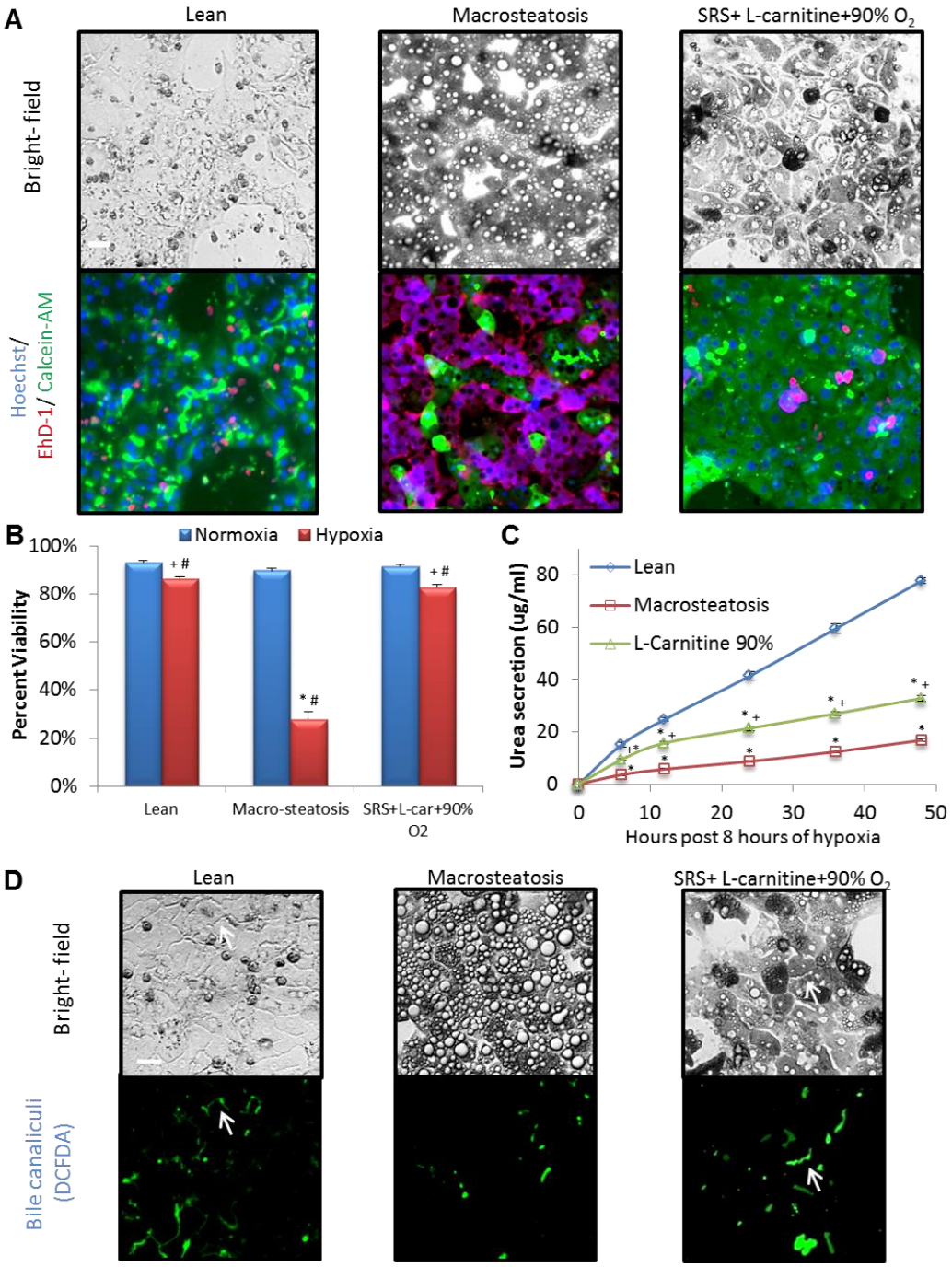
A
Lean
Macrosteatosis
SRS+ L-carnitine+90% O2
Bright-field
Hoechst/
EhD-1/ Calcein-AM
B
Normoxia
Hypoxia
Percent Viability
100%
80%
60%
40%
20%
0%
Lean
Macro-steatosis
SRS+L-car+90% O2
C
Urea secretion (ug/ml)
Lean
Macrosteatosis
L-Carnitine 90%
Hours post 8 hours of hypoxia
D
Lean
Macrosteatosis
SRS+ L-carnitine+90% O2
Bright-field
Bile canaliculi (DCFDA)

Chapter 4, Figure 4: Hepatocyte viability and function 48h following in-vitro hypoxic induction

Lean, macrosteatotic and macrosteatotic cultures preconditioned with SRS+L-car+ 90% O_2 treatment were evaluated for viability and hepatocyte specific functions 48h post hypoxic induction. (A) Bright-field (top) and EhD-1 (red)/ Calcein-AM (green)/ Hoechst (blue) stained epi-fluorescent images of the culture 48h post 8h of hypoxia. Bar=50um. (B) EhD-1^+ hepatocytes were scored dead, as confirmed by being Calcein-AM $^-$ to quantify the percentage viability post 8h of hypoxia (red bars) or normoxia (blue bars) followed by 48h of reoxygenation. Means ± S.E. N = 6. *p<0.001 vs. lean or SRS+L-car+ 90% O_2, +p<0.001 vs. macrosteatosis and #<0.05 vs. same condition following 8h of normoxia. (C) Urea secretion for 48h following 8h of hypoxia stress. Means ± S.E. N = 6. *p<0.001 vs. lean, +p<0.001 vs. macrosteatosis. (D) Bright-field (top) and DCFDA (green) accumulation in the bile canaliculi epi-fluorescent images as an indicator of bile canalicular transport function, as demonstrated by the white arrows. Bar=50um.

E. Discussion:

Herein, we show that macrovesicular steatotic hepatocyte cultures are significantly more sensitive to H/R injury than control lean and microvesicular steatotic hepatocytes. Furthermore, macrosteatotic hepatocytes exhibit lower levels of ATP and increased levels of ROS-related stress (as evidenced by the increased GSSG/GSH ratio) compared to control lean cultures. Therefore, this in-vitro system exhibits many clinically relevant with human macrosteatotic livers in terms of LD content and morphology, as well as with respect to elevated sensitivity to preservation-related stress such as H/R (albeit requiring a longer ischemic period than that typically seen in actual whole livers). The combination of these features makes this system suitable to characterize the hepatocellular responses and biochemical pathways that differentiate macrosteatotic, microsteatotic, and lean hepatocytes, as well as the lipid lowering effects of individual "defatting" agents and combinations thereof. Thus, this system could also potentially be used as a screen for such agents that could be used to decrease hepatic macrosteatosis and H/R sensitivity in actual whole livers.

The data also indicate that preconditioning macrosteatotic hepatocytes for 48h using the SRS cocktail, which reduces macrosteatotic LDs numbers while keeping relatively high TG and low intrahepatic ATP levels, does not ameliorate hypersensitivity to H/R stress. However, pretreatment with L-carnitine supplemented SRS cocktail under hyperoxic conditions led to a complete resolution of H/R stress hypersensitivity, which was correlated with a reduction in intrahepatic TG towards a level slightly lower that seen in microsteatotic hepatocytes and an increase in ATP levels matching that of control lean cultures. Therefore, the intracellular TG did not need to be decreased to the control lean baseline to recover the typical H/R responses of lean hepatocytes. Based on the increased ketone body production, used as a surrogate marker of β-oxidation, it is likely that the reduction of intracellular TG levels was achieved by directing cytoplasmic FFA liberated from the LDs towards β-oxidation before it underwent re-esterification to TG, as summarized in figure 2D [4, 78, 89]. In addition, the fact that we observed similar TG secretion rates for all explored treatments indicates that the different outcomes in terms of intrahepatic TG levels were likely due to other metabolic routes, of which catabolism of TG followed by FFA β-oxidation is likely the main one. Additional studies involving FFA labeling and organelle fractionation will further elucidate this mechanism of action [78].

Preconditioning methods, such as defatting of microsteatotic hepatocyte cultures [23] or perfusion of macrosteatotic livers with high oxygen tension [86] lead to reduction in ROS stress, among others alterations, and lower levels of hepatic injury markers following preservation stress. Here we found that all 3 preconditioning methods led to similar reduction in ROS stress (GSSG/GSH), independent of the oxygen tension or the final TG levels. Therefore, reduction in GSSG/GSH was not a single cause for abolishing H/R hypersensitivity of macrosteatotic cultures preconditioned with L-carnitine supplemented SRS cocktail under hyperoxia. However, it is

likely that the combination of (1) ROS stress reduction; (2) increased ATP levels, possibly arising from the stimulated TG metabolism towards β-oxidation; and (3) reduced TG levels, improved the hepatocyte resistance to H/R stress.

The main effect of hypoxic stress at the cell level is the depletion of intracellular ATP. Therefore, cells containing relatively low ATP levels, such as macrosteatotic hepatocytes, exhibit increased tendencies to die under hypoxic stress. The reason for reduced ATP content in macrosteatotic hepatocytes is not fully elucidated. One possibility is that it may result from increased ROS levels that together with elevated intrahepatic FFA levels generate elevated levels of harmful lipid peroxidation products. These products may damage the mitochondrial respiratory chain complex and impede ATP production as illustrated in Figure 5 [90]. In our studies, exposing macrosteatotic hepatocytes to FFA- free media during defatting, led to a reduction in ROS stress to similar levels in all defatting conditions. It is reasonable to hypothesize that the reduced ROS and FFA levels lowered the lipid peroxidation product levels and enabled the recovery of the mitochondrial respiratory chain complex. Our data indicate that following this hypothesized mitochondrial recovery, ATP was generated proportionally to the flux of FFA into the mitochondria. In order to prove or disprove this hypothesis, however, additional studies will be required. Such studies would involve measurements of lipid peroxidation products and damage markers to the mitochondrial respiratory chain complex.

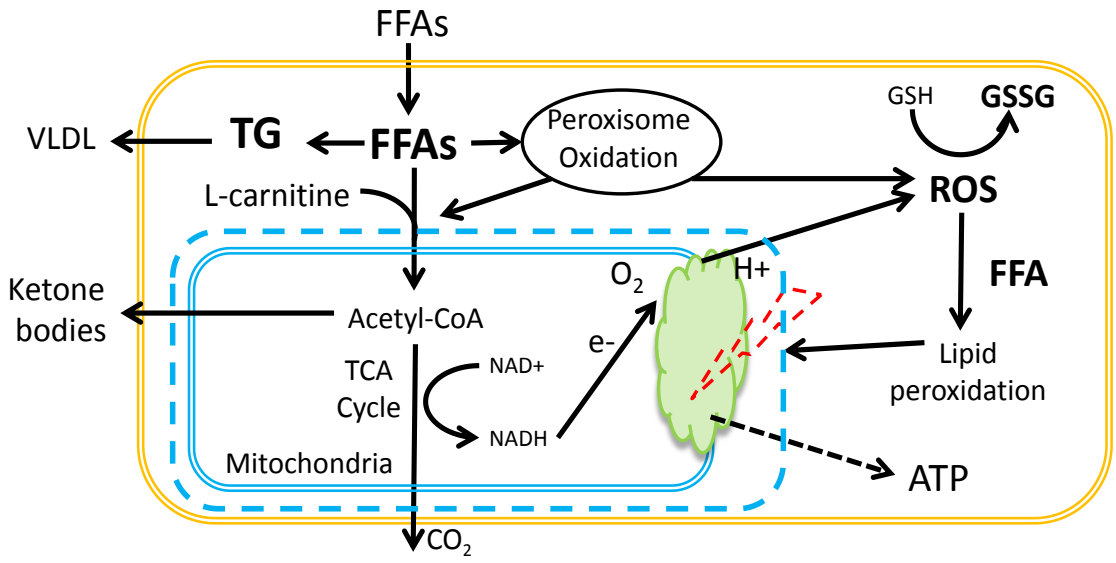

Chapter 4, Figure 5: Postulated intrahepatic mechanisms of sensitivity to hypoxia and reoxygenation stress

The illustration presents relevant intracellular molecules and pathways involved in the development and reversal of sensitivity of hepatocytes to hypoxia and reoxygenation stress. The green shape represents the mitochondrial respiratory chain complex.

A limitation of the hepatocyte culture model is that it does not reproduce the tissue scale abnormalities associated with macrosteatosis, such as sinusoid narrowing, which causes poor microcirculation. On the other hand, the narrowing is largely due to the increased size of the macrosteatotic hepatocytes; thus, hepatocyte defatting would likely resolve this issue, in addition to promoting intracellular ATP production via FFA β-oxidation and reducing ROS stress [4, 23, 35, 77]. Thus, the defatting approach may be advantageous compared to other methods aimed at increasing the ATP levels or reducing ROS stress without addressing other consequences of macrosteatosis [4]. Nevertheless, this in-vitro system may facilitate the exploration of combination therapies that would include defatting together with other agents that promote liver metabolism as well as stress preconditioning methods such as heat-shock [4, 91] or ischemic

preconditioning [4, 21], all of which have individually shown some ability to reduce I/R related damage in steatotic livers.

We have previously shown that urea secretion is significantly reduced in macrosteatotic hepatocytes induced with oleic and linoleic acids and that defatting of these cultures improves urea secretion [77]. Oleic acid has been reported to suppress urea cycle enzyme gene induction in livers of a juvenile visceral steatosis animal model, which was reversed by L-carnitine administration [92]. Herein, we observed that macrosteatotic cultures treated with SRS+ L-car+ 90% O_2 exhibited ~2 fold increase in urea secretion 48h following hypoxia induction compared with macrosteatotic cultures. This significant difference may be explained in part by a combination of higher viability of pretreated macrosteatotic cultures as well as functional improvement in these cultures. The bile canalicular impairment observed in macrosteatotic hepatocytes was consistent with impaired hepatobiliary transport in steatotic livers previously reported in several animal models [25, 93]. We have also shown that defatting of macrosteatotic hepatocytes completely reverses the fat-induced impairment in bile canalicular excretion of DCFDA [77]. Here, we also show that this recovery is maintained for at least 48h post H/R induced stress.

In summary, we describe a preconditioning method which is effective in salvaging macrosteatotic hepatocytes from in-vitro H/R induced death and promotes high viability and functionality for at least 48h post H/R stress. Scaling up this approach to actual livers will most likely need to be performed in an organ perfusion system. Recent ex-vivo perfusion studies using obese Zucker rat livers have indicated that normothermic but not subnormothermic perfusion reduced the defatting timescale from days to hours compared to static culture systems, as reported herein [35, 94]. This time scale would make the defatting approach clinically feasible;

interestingly, there is a recent report of the successful transplantation of two livers that were normothermally perfused for 10h using an OrganOx® perfusion device [34]. While these perfused and transplanted livers were lean, studies involving normothermic perfusion of discarded macrosteatotic human livers with a perfusate containing a defatting cocktail such as the one developed here may be a promising avenue to recover macrosteatotic livers and alleviate the persistent shortage of suitable livers for transplantation.

DISSERTATION DISCUSSION

The shortage of suitable whole liver grafts from deceased donors leads to the deaths of up to 4,000 patients awaiting liver transplantation annually in the U.S alone. To alleviate the shortage in such grafts this dissertation focused on two novel approaches to enable transplantation of currently discarded macrosteatotic grafts: 1. non-biased quantification of macrosteatosis to ensure optimal utilization of marginal macrosteatotic grafts and 2. macrosteatosis reversal prior to the graft transplantation to enable transplantation of currently sub-optimal grafts.

The first approach involves the development of an automated and non-biased image analysis method to quantify a graft's macrosteatotic percentage from H&E stained liver histology slides. The developed method (chapter 2) does not require user intervention or predetermined values such as in previous methods where a predetermined LD CSSA cut-off value was the only determining criterion used to distinguish micro and macrosteatotic LDs. For the first time, the developed method quantifies the ability of LDs to displace the hepatocyte nucleus. Herein, this feature is utilized in conjunction with LD size as part of a decision tree algorithm that mimics the thinking process of pathologists. The performed studies demonstrate that above or below specific size cut-offs, a LD can be accurately considered macro or microsteatotic, respectively. However, in the "gray area" between these two size cut-offs, the LD-nucleus displacement feature enables correct separation between micro and macrosteatotic LDs as confirmed by trained pathologists (specificity=94% and sensitivity= 99%, chapter 2). Furthermore, "off-line" analysis of paraffin embedded and H&E stained liver sections revealed that this method is superior to other methods in predicting the pathologists' assessment of macrosteatotic percentage (R^2=0.97, chapter 2).

In addition, this image analysis based method can be applied to frozen liver sections and therefore can assist clinicians determining in "real-time" if a graft is below the 30%

macrosteatotic cut-off value. It is worth noting that the final decision for graft transplantability is based on macrosteatosis percentage together with other parameters such as donor and recipient age and BMI, graft ischemia time etc. Retroactive analysis of macrosteatotic graft previous transplantation outcomes together with grafts' macrosteatotic percentage and other transplantation related parameters may lead to an improved transplantation cut-off criterion that may be particularly relevant for marginal macrosteatotic grafts. This may improve "real-time" assessment of a graft's suitability for transplantation and ensure optimal use of the macrosteatotic graft pool by not discarding marginally macrosteatotic livers that would otherwise succeed. This novel algorithm is in the process of being patented by Rutgers University at the U.S patent office (U.S. patent published on December 2013, US20130331293 A1).

The second approach developed in this dissertation deals with expanding the liver graft pool by preconditioning currently discarded macrosteatotic livers by means of reversing their macrosteatosis and abolishing their hypersensitivity to I/R stress. To advance this method, a novel in-vitro system of macrosteatotic primary rat hepatocytes was developed by culturing lean hepatocytes for several days with FFAs rich media while maintaining high viability, as described in chapter 3. This system exhibited several features observed in whole macrosteatotic livers of human and animal models such as large macrosteatotic LDs that are able to displace the hepatocyte nucleus, elevated TG levels comparable to those of whole liver animal models, reduced ATP levels, elevated ROS stress and the important hypersensitivity to H/R induced stress, simulating I/R stress induction in static in-vitro cultures (chapters 3 and 4). This is the first system to exhibit all these clinically relevant features and was submitted for patent evaluation at the U.S patent office (United States Application No.: 14/169,605 on January 31, 2014). Furthermore, these clinically relevant features exhibited in an in-vitro system enable the performance of defatting studies in a more manageable manner that when performed using whole livers. In our experience, a single rat liver yields ~70-90 experimental wells of hepatocytes when

used in a 6-well format to test numerous conditions. This in-vitro system enables exploration of hepatocyte macrosteatosis reversal and its effect on hepatocyte viability, function, intrahepatic processes, and reversal of H/R hypersensitivity in a pure hepatocyte population. Following several studies performed using this in-vitro system, questions in the field of macrosteatotic liver preconditioning that were raised in the introduction of this dissertation received appropriate answers as follows.

What agents can be used to reverse macrosteatosis? Can this process be accelerated? What are the suggested intrahepatic pathways governing defatting?

Herein, it was demonstrated that LD macrosteatosis can be fully reversed to levels comparable to un-fatted lean cultures. This process can be accelerated 2 fold by incubation of macrosteatotic hepatocyte cultures with a defatting cocktail previously used to defat microsteatotic cultures, SRS media [35]. The cocktail agents are described in the methods section of chapter 2 as well as in chapter 4 appendix and target several intracellular metabolism pathways as described before [35]. It is suggested that the mechanism of action during accelerated macrosteatotic reversal relates to the breakdown of LDs via lipolysis as the rate of LD CSSA reduction was accelerated. However, due to low levels TG secretion and insufficient oxidation of FFAs released from LDs, the intrahepatic TG levels remained relatively high within hepatocytes defatted with SRS (chapter 3). The suggested mechanism for that is reesterification of FFA released from the LD into small LDs that remain in the cytoplasm. Interestingly, the intrahepatic TG levels were further reduced when L-carnitine was supplemented to the defatting cocktail under a hyperoxic environment during the 48h defatting preconditioning period (chapter 4). This treatment enables the same acceleration in macrosteatosis reversal while reducing intrahepatic TG levels by half compared to macrosteatotic hepatocytes to levels slightly below that of microsteatotic hepatocytes. These outcomes were accompanied by increase in ketone body secretion and elevated ATP levels likely due to increase FFAs transfer to the mitochondria for β-

oxidation followed by TCA cycle metabolism. Therefore, eliminating the FFA pool in the cytoplasm is critical in reducing intrahepatic TG levels. This suggested mechanism can be explored in more details by following the metabolism of TG using radioactive labeled FFAs.

What is the effect of accelerated macrosteatotic reversal on hepatocyte viability and function?

Acceleration of macrosteatotic reversal did not reduce the hepatocyte viability and maintained it comparably to lean cultures. Accelerated macrosteatotic reversal using SRS media led to recovery in urea secretion and bile canalicular transport. These two functions serve as indicators for hepatocyte ability to perform metabolism and clearance of molecules. However, albumin secretion rate in defatted cultures remained similar to that of macrosteatotic cultures which was lower than lean un-fatted cultures. The intracellular albumin levels among conditions were similar, indicating that the difference in secretion rate may be due to alteration in albumin synthesis mechanisms or internal degradation of albumin. Further studies are required to fully elucidate the relevant mechanisms, which may also lead to methods that enable albumin secretion normalization. Previous in-vitro studies which explored albumin secretion in freshly isolated lean primary rat hepatocytes have indicated a dramatic reduction in albumin secretion due to compromised hepatic cytoskeletal structure that leads to loss of hepatic polarity [95, 96]. Hepatic polarity is critical to hepatocyte function [97] and may have been lost in our macrosteatotic system due to disturbances of cytoskeletal structures by large LDs [98]. This hypothesis requires additional studies exploring cytoskeletal organization in macrosteatotic hepatocytes, and how it affects both protein synthesis and secretion.

Increasing the concentration of the defatting cocktails (by 2 fold or more) or changing the culture media more often during defatting with fresh defatting cocktail media led to significantly decreased viability while no changes in defatting were observed (data not shown). Therefore, it is likely that the concentrations used represent the upper-bound concentrations. Nevertheless, as

discussed below, altered defatting dynamics may exist in an ex-vivo perfusion system and may affect the defatting time frames as well as agents' concentrations.

What is the time scale for such a process in a static in-vitro culture system?

Although the time scale of macrosteatotic reversal was reduced by 2 fold to 48h, it is still not within the clinically relevant time frame of several hours. In the static in-vitro system the concentrations of defatting agents decrease over time and the levels of waste products increase over time and remain in the cells' environment. This may lead to a defatting dynamics slower than can be obtained in an ex-vivo perfusion system where the system parameters can remain constant over the perfusion duration and the waste products are being constantly removed from the cell's environment. In previous studies, the defatting levels obtained in microsteatotic primary rat cultures during 48h of static culture were achieved in a whole steatotic rat liver perfusion after 3h [35]. Therefore, it is likely that the results obtained using the macrosteatotic in-vitro system described here following 48h of preconditioning can be achieved in whole livers in several hours to be within the clinically relevant time frame.

In case that the defatting cocktail discovered here does not yield sufficient defatting within a clinical relevant time under flow conditions or when applied to whole livers, additional defatting agents may be added to the cocktail. These agents can be selected using the developed macrosteatotic in-vitro system based on both hypothesis driven studies and high throughput screens. The image analysis based method to quantify macrosteatotic LD size distribution together with TG metabolism relevant biomarkers can be used in such a screening system.

How much defatting is required? Is breaking macrosteatotic LDs alone is sufficient to abolish H/R hypersensitivity? Is further catabolism of TG and FFA is required to abolish H/R hypersensitivity? What is the effect of such defatting on hepatocyte viability and function post H/R induced stress?

Herein, it was demonstrated that complete breakdown of the LDs alone while maintaining the intrahepatic TG levels at ~70% was not sufficient to reduce macrosteatotic hepatocytes hypersensitivity to H/R stress. An additional 20% reduction in the TG levels to levels slightly below that of microsteatotic cultures in parallel to promotion of FFA β-oxidation and increase in ATP levels were required to reduce H/R hypersensitivity and to maintain hepatocyte viability ~85% even 48h after H/R induced stress. The functionality of these hepatocytes, as assessed by urea secretion and bile canalicular transport, was superior to that of macrosteatotic hepatocytes that were not preconditioned prior to H/R stress. Therefore, intrahepatic TG level reduction is a significant factor in ameliorating H/R hypersensitivity, but it is not required to fully reduce TG levels to that of lean hepatocyte cultures levels to fully abolish H/R stress associated hepatic death.

Future directions

In our studies, we developed a method to fully reverse H/R associated death of macrosteatotic hepatocytes which does not require a full reversal of TG content. In future studies, it might be desirable to explore complete defatting of macrosteatotic hepatocytes by reducing the TG levels to that of lean un-fatted hepatocytes. This additional defatting may further reduce ROS stress and enable an increase in albumin secretion. Based on the knowledge generated in our studies the two major pathways to target in order to promote TG reduction are FFA oxidation and VLDL secretion. In regards to promoting FFA oxidation, it is not clear if we already "maximized" the flux through that pathway. Additional exploration under fatting and defatting conditions may reveal additional critical steps in the oxidation pathways that could be optimized to promote FFA oxidation. Such pathways may include the release of FFA from the LDs TG, FFA transport into the mitochondria, β-oxidation, and the TCA cycle. In regards to promoting VLDL secretion, our data suggest that there is room for improvement by at least 2 fold. However, in our system only ~5% of the reduced intracellular TG is mediated by VLDL secretion while the

rest is mediated by fat oxidation. Therefore, increasing VLDL secretion by 2 fold may not be sufficient. Nevertheless, to improve VLDL assembly and secretion, exploration of limiting steps in that process will be required. These limiting steps may be related to the synthesis of VLDL proteins, such as the Apo-B, and the VLDL transport and release mechanism.

Currently, only a few biomarkers are available to determine eligibility of liver grafts for transplantation, such as macrosteatotic percentage. Exploring intrahepatic metabolism, energy balance, protein expression, gene expression and secreted products in macrosteatotic hepatocytes using the in-vitro system developed here may reveal additional biomarkers to indicate the health and translatability of macrosteatotic livers. These biomarkers can complement the macrosteatotic assessment of grafts and can be incorporated into a multifactorial transplantability criterion. Such a biomarker based scoring system has been previously developed to successfully predict transplantability of lean rat livers that underwent ischemia injury followed by normothermic ex-vivo perfusion, using analysis of soluble metabolites present in the perfusate [99, 100]. Therefore, analysis of metabolites during in-vitro defatting of macrosteatotic hepatocytes using methods such as metabolic flux analysis [51] may promote discovery of biomarkers that can be later represent the transplantability of whole livers during ex-vivo perfusion.

Several methods to precondition macrosteatotic liver prior to their transplantation was previously explored as described in chapter 1, such as I/R or heat-shock preconditioning. With increasing knowledge of macrosteatosis H/R hypersensitivity underlying mechanisms a hypothesis driven combinational therapy composed of selected methods superimposed on macrosteatotic reversal may be performed using the developed in-vitro macrosteatotic system. Furthermore, temporal analysis of such studies can elucidate the dynamics of processes governing macrosteatosis reversal and H/R hypersensitivity. This can improve macrosteatotic liver preconditioning since required agents and/ or treatments can be introduced at their optimal stage during the ex-vivo perfusion preconditioning. Also, real-time monitoring of such defatting and its

related biomarkers may enable gauging the graft responsiveness to preconditioning and adjusting the treatment accordingly so that the graft reaches its optimal condition prior to transplantation. For example, as a non-invasive biomarker, ketone body secretion level, correlates with increased FFA oxidation and ATP content, and may be used in the future to assess the extent of defatting in whole livers during perfusion.

The next steps in the research of developing preconditioning methods to reverse I/R hypersensitivity in macrosteatotic livers may include development of additional in-vitro systems that are more relevant to human whole livers. For example, a human hepatocyte based static in-vitro system or an in-vitro system containing rat or human hepatocytes that exhibits flow and the ability to induce I/R stress instead of H/R may be superior to static culture system. Such systems involve increased costs and reduced high throughput for screenings agents. However, since primary rat hepatocyte in-vitro static systems based study results have been widely translated to predict metabolism in human livers, the development of flow systems may be excessive. Therefore, it might be advantageous to use whole macrosteatotic animals or discarded human liver ex-vivo perfusion studies as the next step towards a clinical therapeutic.

Furthermore, the studies described in chapter 4 demonstrate the importance of macrosteatotic hepatocyte preconditioning under elevated oxygen tension. While elevated oxygen tension can be achieved in an in-vitro system of mono-layered hepatocytes by insertion of a culture plate into a hyperoxic chamber, obtaining high oxygen in the tissue of whole microsteatotic livers is more challenging and may require perfusion under hyperbaric conditions [85] or supplementation of the perfusate with oxygen carriers such as red blood cells [34, 101]. Both methods have been successfully performed using lean livers; however, neither preconditioning of macrosteatotic livers under hyperbaric environments nor using red blood cells as an oxygen carrier have yet to be tested on macrosteatotic livers.

In summary, the developed in-vitro system of macrosteatotic primary rat hepatocytes together with the preconditioning methods introduced here for reversing macrosteatosis and abolishing hepatocytes hypersensitivity to H/R stress may promote the development of clinically effective preconditioning methods to enable preconditioning of macrosteatotic livers. If successful, such a method could be implemented in the short term to save the lives of 1,000 people awaiting liver transplantation annually in the U.S alone.

References

1. Cohen, J.C., J.D. Horton, and H.H. Hobbs, *Human fatty liver disease: old questions and new insights.* Science, 2011. **332**(6037): p. 1519-23.
2. de Graaf, E.L., et al., *Grade of deceased donor liver macrovesicular steatosis impacts graft and recipient outcomes more than the Donor Risk Index.* J Gastroenterol Hepatol, 2012. **27**(3): p. 540-6.
3. Guarrera, J.V. and N.A. Karim, *Liver preservation: is there anything new yet?* Current Opinion in Organ Transplantation, 2008. **13**(2): p. 148-154 10.1097/MOT.0b013e3282f63930.
4. Nativ, N.I., et al., *Liver Defatting: An Alternative Approach to Enable Steatotic Liver Transplantation.* American Journal of Transplantation, 2012. **12**(12): p. 3176-3183.
5. Perez-Daga, J.A., et al., *Influence of Degree of Hepatic Steatosis on Graft Function and Postoperative Complications of Liver Transplantation.* Transplantation Proceedings, 2006. **38**(8): p. 2468-2470.
6. Selzner, M. and P.-A. Clavien, *Fatty Liver in Liver Transplantation and Surgery.* Semin Liver Dis, 2001. **21**(01): p. 105,114.
7. El-Badry, A.M., et al., *Assessment of Hepatic Steatosis by Expert Pathologists: The End of a Gold Standard.* Annals of Surgery, 2009. **250**(5): p. 691-697 10.1097/SLA.0b013e3181bcd6dd.
8. Spitzer, A.L., et al., *The biopsied donor liver: incorporating macrosteatosis into high-risk donor assessment.* Liver Transpl, 2010. **16**(7): p. 874-84.
9. Benjamin Heller, S.P., *Assessment of Liver Transplant Donor Biopsies for Steatosis Using Frozen Section: Accuracy and Possible Impact on Transplantation.* Journal of clinical medicine research, 2011. **3**(4): p. 191-194.
10. Angulo, P., *Nonalcoholic Fatty Liver Disease.* New England Journal of Medicine, 2002. **346**(16): p. 1221-1231.
11. Fabbrini, E., S. Sullivan, and S. Klein, *Obesity and nonalcoholic fatty liver disease: Biochemical, metabolic, and clinical implications.* Hepatology, 2010. **51**(2): p. 679-689.
12. D'Alessandro, E., et al., *Frozen-Section Diagnosis in Donor Livers: Error Rate Estimation of Steatosis Degree.* Transplantation Proceedings, 2010. **42**(6): p. 2226-2228.
13. Guarrera, J.V.M.D., et al., *Digital imaging of extended criteria donor livers to facilitate placement and utilization.* Progress in Transplantation, 2010. **20**(1): p. 14-7.
14. Jamieson, R.W., et al., *Hepatic Steatosis and Normothermic Perfusion—Preliminary Experiments in a Porcine Model.* Transplantation, 2011. **92**(3): p. 289-295 10.1097/TP.0b013e318223d817.
15. TH, B., *A validated method for quantifying macrovesicular hepatic steatosis in chronic hepatitis C*

Analytical & Quantitative Cytology & Histology, 2007. **29**(4): p. 244-50.

16. Li, M., et al., *Comparing morphometric, biochemical, and visual measurements of macrovesicular steatosis of liver.* Human Pathology, 2011. **42**(3): p. 356-360.
17. Marsman, H., et al., *Assessment of donor liver steatosis: pathologist or automated software?* Human Pathology, 2004. **35**(4): p. 430-435.
18. Bessems, M., et al., *Preservation of steatotic livers: A comparison between cold storage and machine perfusion preservation.* Liver Transplantation, 2007. **13**(4): p. 497-504.

19. Ben Mosbah, I., et al., *Addition of carvedilol to University Wisconsin solution improves rat steatotic and nonsteatotic liver preservation.* Liver Transplantation, 2010. **16**(2): p. 163-171.
20. Guarrera, J.V., et al., *Hypothermic Machine Preservation in Human Liver Transplantation: The First Clinical Series.* American Journal of Transplantation, 2010. **10**(2): p. 372-381.
21. Selzner, N., et al., *Mouse livers with macrosteatosis are more susceptible to normothermic ischemic injury than those with microsteatosis.* Journal of Hepatology, 2006. **44**(4): p. 694-701.
22. Taneja, C., L. Prescott, and B. Koneru, *Critical Preservation Injury in Rat Fatty Liver Is to Hepatocytes, Not Sinusoidal Lining Cells 1.* Transplantation, 1998. **65**(2): p. 167-172.
23. Berthiaume, F., et al., *Steatosis Reversibly Increases Hepatocyte Sensitivity to Hypoxia-Reoxygenation Injury.* Journal of Surgical Research, 2009. **152**(1): p. 54-60.
24. Dutta, A., et al., *Impairment of mitochondrial β-oxidation in rats under cold-hypoxic environment.* International Journal of Biometeorology, 2009. **53**(5): p. 397-407.
25. Ninomiya, M., et al., *Sustained spatial disturbance of bile canalicular networks during regeneration of the steatotic rat liver.* Transplantation, 2004. **77**(3): p. 373-379.
26. Selzner, M., et al., *Mechanisms of ischemic injury are different in the steatotic and normal rat liver.* Hepatology, 2000. **32**(6): p. 1280-1288.
27. Serafín, A., et al., *Ischemic Preconditioning Increases the Tolerance of Fatty Liver to Hepatic Ischemia-Reperfusion Injury in the Rat.* The American journal of pathology, 2002. **161**(2): p. 587-601.
28. Sun, C.-K., et al., *Effect of Ischemia-Reperfusion Injury on the Microcirculation of the Steatotic Liver of the Zucker Rat1.* Transplantation, 2001. **72**(10): p. 1625-1631.
29. Laurens, M., et al., *Warm ischemia-reperfusion injury is decreased by tacrolimus in steatotic rat liver.* Liver Transplantation, 2006. **12**(2): p. 217-225.
30. Yamagami, K., et al., *Heat-shock preconditioning protects fatty livers in genetically obese Zucker rats from microvascular perfusion failure after ischemia reperfusion.* Transpl Int, 2003. **16**(8): p. 456-63.
31. Nakamuta, M., et al., *Short-term intensive treatment for donors with hepatic steatosis in living-donor liver transplantation.* Transplantation, 2005. **80**(5): p. 608-12.
32. Clavien, P.A., et al., *What is critical for liver surgery and partial liver transplantation: size or quality?* Hepatology, 2010. **52**(2): p. 715-29.
33. Vogel, T., et al., *The role of normothermic extracorporeal perfusion in minimizing ischemia reperfusion injury.* Transplant Rev (Orlando), 2012. **26**(2): p. 156-62.
34. http://www.ox.ac.uk/media/news_stories/2013/130315.html, U.o.O. *World first: device keeps human liver alive outside body*. 2013 [cited 2013 12/21/13].
35. Nagrath, D., et al., *Metabolic preconditioning of donor organs: defatting fatty livers by normothermic perfusion ex vivo.* Metab Eng, 2009. **11**(4-5): p. 274-83.
36. Chavez-Tapia, N., N. Rosso, and C. Tiribelli, *Effect of intracellular lipid accumulation in a new model of non-alcoholic fatty liver disease.* BMC Gastroenterology, 2012. **12**(1): p. 20.
37. Ogden, C.L. and M.D. Carroll, *Prevalence of Overweight, Obesity, and Extreme Obesity Among Adults: United States, Trends 1960–1962 Through 2007–2008.* 2010.
38. Vairetti, M., et al., *Subnormothermic machine perfusion protects steatotic livers against preservation injury: A potential for donor pool increase?* Liver Transplantation, 2009. **15**(1): p. 20-29.

39. Nakano, H., et al., *The effects of N-acetylcysteine and anti-intercellular adhesion molecule-1 monoclonal antibody against ischemia-reperfusion injury of the rat steatotic liver produced by a choline-methionine-deficient diet.* Hepatology, 1997. **26**(3): p. 670-678.
40. Pierre-Alain Clavien, S.Y., David Sindram, and Rex C. Bentley, *Protective Effects of Ischemic Preconditioning for Liver Resection Performed Under Inflow Occlusion in Humans.* Annals of Surgery, 2000. **232**(2).
41. Mokuno, Y., et al., *Technique for expanding the donor liver pool: heat shock preconditioning in a rat fatty liver model.* Liver Transpl, 2004. **10**(2): p. 264-72.
42. Chavin, K.D., et al., *Fatty Acid Synthase Blockade Protects Steatotic Livers from Warm Ischemia Reperfusion Injury and Transplantation.* American Journal of Transplantation, 2004. **4**(9): p. 1440-1447.
43. Guarrera, J.V., et al., *Hypothermic Machine Preservation Attenuates Ischemia/Reperfusion Markers After Liver Transplantation: Preliminary Results.* Journal of Surgical Research, 2011. **167**(2): p. e365-e373.
44. Tolboom, H., et al., *Subnormothermic Machine Perfusion at Both 20°C and 30°C Recovers Ischemic Rat Livers for Successful Transplantation.* Journal of Surgical Research, 2012. **175**(1): p. 149-156.
45. Moers, C., et al., *Machine perfusion or cold storage in deceased-donor kidney transplantation.* N Engl J Med, 2009. **360**(1): p. 7-19.
46. Lankester, D.L., A.M. Brown, and V.A. Zammit, *Use of cytosolic triacylglycerol hydrolysis products and of exogenous fatty acid for the synthesis of triacylglycerol secreted by cultured rat hepatocytes.* J Lipid Res, 1998. **39**(9): p. 1889-95.
47. Karlsson, M., et al., *cDNA cloning, tissue distribution, and identification of the catalytic triad of monoglyceride lipase. Evolutionary relationship to esterases, lysophospholipases, and haloperoxidases.* J Biol Chem, 1997. **272**(43): p. 27218-23.
48. Wang, H., et al., *Unique Regulation of Adipose Triglyceride Lipase (ATGL) by Perilipin 5, a Lipid Droplet-associated Protein.* Journal of Biological Chemistry, 2011. **286**(18): p. 15707-15715.
49. Wolins, N.E., et al., *OXPAT/PAT-1 Is a PPAR-Induced Lipid Droplet Protein That Promotes Fatty Acid Utilization.* Diabetes, 2006. **55**(12): p. 3418-3428.
50. Raubenheimer, P.J., M.J. Nyirenda, and B.R. Walker, *A choline-deficient diet exacerbates fatty liver but attenuates insulin resistance and glucose intolerance in mice fed a high-fat diet.* Diabetes, 2006. **55**(7): p. 2015-20.
51. Chan, C., et al., *Metabolic flux analysis of hepatocyte function in hormone- and amino acid-supplemented plasma.* Metabolic Engineering, 2003. **5**(1): p. 1-15.
52. Murosaki, S., et al., *A combination of caffeine, arginine, soy isoflavones, and L-carnitine enhances both lipolysis and fatty acid oxidation in 3T3-L1 and HepG2 cells in vitro and in KK mice in vivo.* J Nutr, 2007. **137**(10): p. 2252-7.
53. Henry, S.D., et al., *Hypothermic Machine Preservation Reduces Molecular Markers of Ischemia/Reperfusion Injury in Human Liver Transplantation.* American Journal of Transplantation, 2012: p. no-no.
54. Hatta, T., et al., *Accurate and simple method for quantification of hepatic fat content using magnetic resonance imaging: a prospective study in biopsy-proven nonalcoholic fatty liver disease.* Journal of Gastroenterology, 2010. **45**(12): p. 1263-1271.
55. Noworolski, S.M., et al., *Liver Steatosis: Concordance of MR Imaging and MR Spectroscopic Data with Histologic Grade.* Radiology, 2012. **264**(1): p. 88-96.

56. Zaitoun, A.M., et al., *Quantitative assessment of fibrosis and steatosis in liver biopsies from patients with chronic hepatitis C.* Journal of Clinical Pathology, 2001. **54**(6): p. 461-465.
57. Caselles, V., R. Kimmel, and G. Sapiro, *Geodesic Active Contours.* Int. J. Comput. Vision, 1997. **22**(1): p. 61-79.
58. Gunn, S.R. and M.S. Nixon, *A Robust Snake Implementation; A Dual Active Contour.* IEEE Trans. Pattern Anal. Mach. Intell., 1997. **19**(1): p. 63-68.
59. Kass, M., A. Witkin, and D. Terzopoulos, *Snakes: Active contour models.* Int J Comp Vision, 1988. **1**(4): p. 321-331.
60. Fatakdawala, H., et al., *Expectation-maximization-driven geodesic active contour with overlap resolution (EMaGACOR): application to lymphocyte segmentation on breast cancer histopathology.* IEEE Trans Biomed Eng, 2010. **57**(7): p. 1676-89.
61. Cumani, A., *Edge detection in multispectral images.* Graphical Models and Image Processing, 1991. **53**(1): p. 40-51.
62. Sapiro, G., *Color snakes.* Comput. Vis. Image Underst., 1997. **68**(2): p. 247-253.
63. Yang, L., P. Meer, and D.J. Foran, *Unsupervised segmentation based on robust estimation and color active contour models.* IEEE Trans Inf Technol Biomed, 2005. **9**(3): p. 475-86.
64. Rousseeuw, P., *Silhouettes: a graphical aid to the interpretation and validation of cluster analysis.* J. Comput. Appl. Math., 1987. **20**(1): p. 53-65.
65. Kohavi, R., *A study of cross-validation and bootstrap for accuracy estimation and model selection*, in *Proceedings of the 14th international joint conference on Artificial intelligence - Volume 2*1995, Morgan Kaufmann Publishers Inc.: Montreal, Quebec, Canada. p. 1137-1143.
66. Berendsen, T.A., et al., *Hepatocyte Viability and Adenosine Triphosphate Content Decrease Linearly Over Time During Conventional Cold Storage of Rat Liver Grafts.* Transplantation Proceedings, 2011. **43**(5): p. 1484-1488.
67. Vogel, T., et al., *The role of normothermic extracorporeal perfusion in minimizing ischemia reperfusion injury.* Transplantation Reviews, 2012. **26**(2): p. 156-162.
68. Kleiner, D.E., et al., *Design and validation of a histological scoring system for nonalcoholic fatty liver disease.* Hepatology, 2005. **41**(6): p. 1313-1321.
69. Nir I. Nativ, T.J.M., Gabriel Yarmush, Dawn L. Brasaemle, Scot D. Henry, James V. Guarrera, François Berthiaume, Martin L. Yarmush, *Liver Defatting: An Alternative Approach to Enable Steatotic Liver Transplantation.* American Journal of Transplantation, 2012. **12**(12): p. 3176-3183.
70. Nagrath, D., et al., *Metabolic preconditioning of donor organs: Defatting fatty livers by normothermic perfusion ex vivo.* Metabolic Engineering. **11**(4-5): p. 274-283.
71. Maguire, T., et al., *Alginate-PLL microencapsulation: Effect on the differentiation of embryonic stem cells into hepatocytes.* Biotechnology and Bioengineering, 2006. **93**(3): p. 581-591.
72. Tuschl, G., et al., *Serum-free collagen sandwich cultures of adult rat hepatocytes maintain liver-like properties long term: A valuable model for in vitro toxicity and drug–drug interaction studies.* Chemico-Biological Interactions, 2009. **181**(1): p. 124-137.
73. Wang, C.S., N. Fukuda, and J.A. Ontko, *Studies on the mechanism of hypertriglyceridemia in the genetically obese Zucker rat.* Journal of Lipid Research, 1984. **25**(6): p. 571-9.
74. Washizu, J., et al., *Amino Acid Supplementation Improves Cell-Specific Functions of the Rat Hepatocytes Exposed to Human Plasma.* Tissue Engineering, 2000. **6**(5): p. 497-504.

75. Gibbons, D.W.a.G.F., *The lipolysis/esterification cycle of hepatic triacylglycerol. Its role in the secretion of very-low-density lipoprotein and its response to hormones and sulphonylureas.* Biochem J, 1992. **284**(Pt 2): p. 457–462.
76. Fukumori, T., et al., *Why is fatty liver unsuitable for transplantation? Deterioration of mitochondrial ATP synthesis and sinusoidal structure during cold preservation of a liver with steatosis.* Transplantation Proceedings, 1997. **29**(1–2): p. 412-415.
77. Nativ, N.I., et al., *Rat hepatocyte culture model of macrosteatosis: Effect of macrosteatosis induction and reversal on viability and liver-specific function.* Journal of hepatology, 2013.
78. Lankester, D.L., A.M. Brown, and V.A. Zammit, *Use of cytosolic triacylglycerol hydrolysis products and of exogenous fatty acid for the synthesis of triacylglycerol secreted by cultured rat hepatocytes.* Journal of Lipid Research, 1998. **39**(9): p. 1889-1895.
79. Janine Keller, R.R., Steffen Priebe, Reinhard Guthke, Holger Kluge and Klaus Eder *Effect of L-carnitine on the hepatic transcript profile in piglets as animal model.* Nutrition & Metabolism, 2011. **8**(76): p. 1-10.
80. Murosaki, S., et al., *A Combination of Caffeine, Arginine, Soy Isoflavones, and l-Carnitine Enhances Both Lipolysis and Fatty Acid Oxidation in 3T3-L1 and HepG2 Cells in Vitro and in KK Mice in Vivo.* The Journal of Nutrition, 2007. **137**(10): p. 2252-2257.
81. Malaguarnera, M., et al., *l-Carnitine Supplementation to Diet: A New Tool in Treatment of Nonalcoholic Steatohepatitis[mdash]A Randomized and Controlled Clinical Trial.* Am J Gastroenterol, 2010. **105**(6): p. 1338-1345.
82. Li-Jian Liang, X.-Y.Y., Shi-Min Luo, Jin-Fang Zheng, Ming-De Lu, Jie-Fu Huang, *A study of the ameliorating effects of carnitine on hepatic steatosis induced by total parenteral nutrition in rats.* World J Gastroenterol, 1999. **5**(4): p. 312-315.
83. Tolba, R.H., et al., *L-carnitine ameliorates abnormal vulnerability of steatotic rat livers to cold ischemic preservation.* Transplantation, 2003. **76**(12): p. 1681-1686.
84. Minor, T., et al., *Cold preservation of fatty liver grafts: prevention of functional and ultrastructural impairments by venous oxygen persufflation.* Journal of hepatology, 2000. **32**(1): p. 105-111.
85. Giannone, F.A., et al., *An Innovative Hyperbaric Hypothermic Machine Perfusion Protects the Liver from Experimental Preservation Injury.* The Scientific World Journal, 2012. **2012**: p. 9.
86. Chen, M.-F., et al., *Hyperbaric oxygen pretreatment attenuates hepatic reperfusion injury.* Liver, 1998. **18**(2): p. 110-116.
87. Ramaiah, S.K., *A toxicologist guide to the diagnostic interpretation of hepatic biochemical parameters.* Food and Chemical Toxicology, 2007. **45**(9): p. 1551-1557.
88. Nakajima, T., et al., *The Effect of Carnitine on Ketogenesis in Perfused Livers from Juvenile Visceral Steatosis Mice with Systemic Carnitine Deficiency.* Pediatr Res, 1997. **42**(1): p. 108-113.
89. Fromenty, B. and D. Pessayre, *Impaired mitochondrial function in microvesicular steatosis effects of drugs, ethanol, hormones and cytokines.* Journal of hepatology, 1997. **26, Supplement 2**(0): p. 43-53.
90. Pessayre, D., A. Mansouri, and B. Fromenty, *V. Mitochondrial dysfunction in steatohepatitis.* American Journal of Physiology - Gastrointestinal and Liver Physiology, 2002. **282**(2): p. G193-G199.
91. Mokuno, Y., et al., *Technique for expanding the donor liver pool: Heat shock preconditioning in a rat fatty liver model.* Liver Transplantation, 2004. **10**(2): p. 264-272.

92. Tomomura, M., et al., *Long-chain fatty acids suppress the induction of urea cycle enzyme genes by glucocorticoid action.* FEBS Letters, 1996. **399**(3): p. 310-312.
93. Pizarro, M., et al., *Bile secretory function in the obese Zucker rat: evidence of cholestasis and altered canalicular transport function.* Gut, 2004. **53**(12): p. 1837-1843.
94. Liu, Q., et al., *Perfusion Defatting at Subnormothermic Temperatures in Steatotic Rat Livers.* Transplantation Proceedings, 2013. **45**(9): p. 3209-3213.
95. Dunn, J.C.Y., R.G. Tompkins, and M.L. Yarmush, *Long-Term in Vitro Function of Adult Hepatocytes in a Collagen Sandwich Configuration.* Biotechnology Progress, 1991. **7**(3): p. 237-245.
96. Ezzell, R.M., et al., *Effect of Collagen Gel Configuration on the Cytoskeleton in Cultured Rat Hepatocytes.* Experimental Cell Research, 1993. **208**(2): p. 442-452.
97. Decaens, C., et al., *Which in vitro models could be best used to study hepatocyte polarity?* Biology of the Cell, 2008. **100**(7): p. 387-398.
98. Franke, W.W., M. Hergt, and C. Grund, *Rearrangement of the vimentin cytoskeleton during adipose conversion: Formation of an intermediate filament cage around lipid globules.* Cell, 1987. **49**(1): p. 131-141.
99. Izamis M-L, T.H., Uygun B, Berthiaume F, Yarmush ML, et al, *Resuscitation of Ischemic Donor Livers with Normothermic Machine Perfusion: A Metabolic Flux Analysis of Treatment in Rats.* PLoS ONE, 2013. **8**(7).
100. Perk S, I.M.-L., Tolboom H, Uygun B, Berthiaume F, *A Metabolic Index of Ischemic Injury for Perfusion-Recovery of Cadaveric Rat Livers.* PLoS ONE, 2011. **6**(12).
101. Orman MA, I.M., Androulakis IP, Berthiaume F, *Effect of Fasting on the Metabolic Response of Liver to Experimental Burn Injury.* PLoS ONE, 2013. **8**(2): p. e54825.

Appendix 1: Supplementary Figures and Tables

1. Supplementary figures for chapter 2

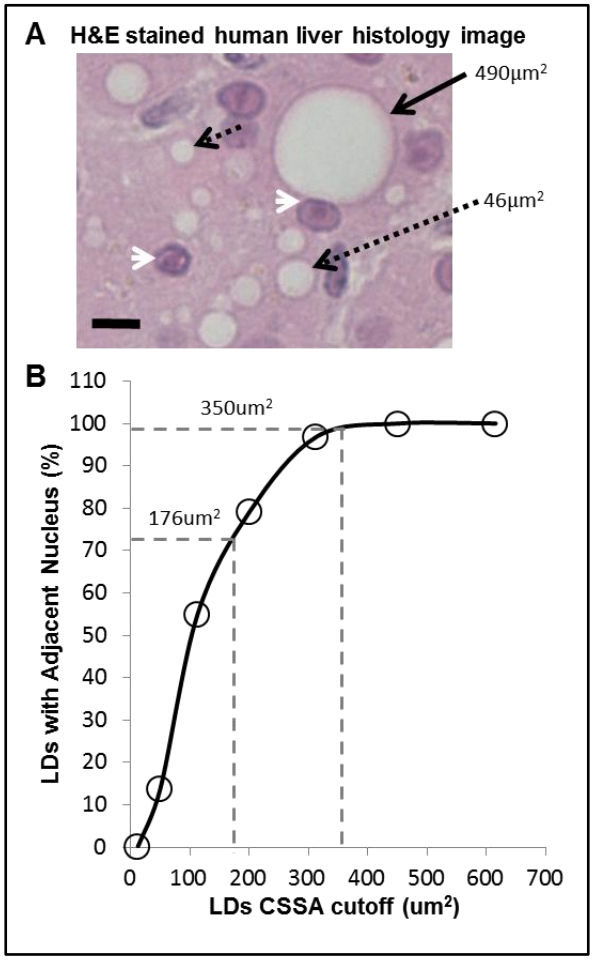

Chapter 2, Supplementary Figure 1: Distinguishing macrovesicular steatotic from microvesicular steatotic LDs based on LD size and ability to displace the nucleus.

A. H&E stained human liver histology image containing macrovesicular steatotic (black arrow) as well as microvesicular steatotic (dashed arrow) LDs. The CSSA of LDs is indicated. The macrovesicular steatotic LD, but not microvesicular steatotic one, is observed to be large enough to displace the nucleus, which requires the LDs to be adjacent to the nucleus (white arrow). Bar= 10µm^2

B. LD-nuclei adjacency (illustrated in Supplementary Figure 2) was determined in micro- and macrovesicular LDs based on a fixed CSSA cutoff for macrovesicular steatosis. 52,000 LDs were clustered into 7 groups based on their CSSA and the fraction of LDs with LD-nuclei adjacency ≥

0.9 (criterion defining adjacent LD-nucleus) in each group was determined. Specific CSSA cutoffs and their corresponding fraction of adjacent LD-nuclei are indicated.

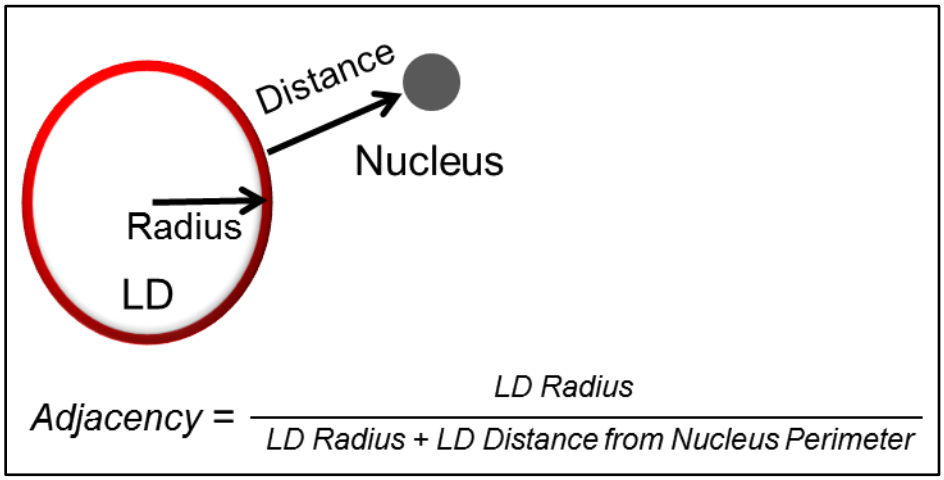

Chapter 2, Supplementary Figure 2: LD-nucleus adjacency parameter.

The shortest distance between each LD's perimeter and the perimeter of its nearest nucleus was quantified and LD-nucleus adjacency was calculated as follows: LD-nucleus adjacency = Radius of LD/ Radius of LD+ Distance between LD and nucleus perimeters. Adjacency values ≥ 0.9 up to the theoretical limit of 1 were used to define LDs adjacent to the nucleus.

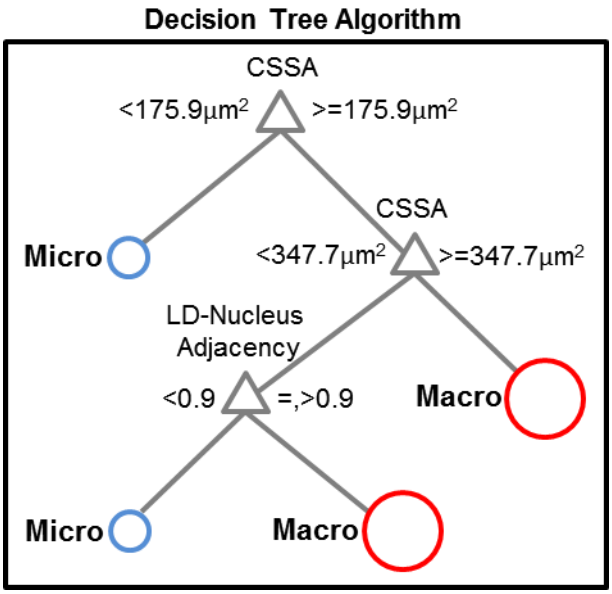

Chapter 2, Supplementary Figure 3: Decision tree structure.

A decision tree algorithm was generated to distinguish between macrovesicular steatotic and microvesicular steatotic LDs. The decision tree was trained and optimized from the raw data using N-fold cross-validation (N=10) to yield two levels of decision making: The first level assigns micro- and macrovesicular -steatotic labels to LDs that have CSSA values below a low threshold or above a high threshold, respectively. The second level deals with the LDs that have CSSAs that fall between the low and high threshold, and uses LD-nucleus adjacency as a criteria to micro- and macrovesicular steatotic labels.

2. Supplementary figures for chapter 3

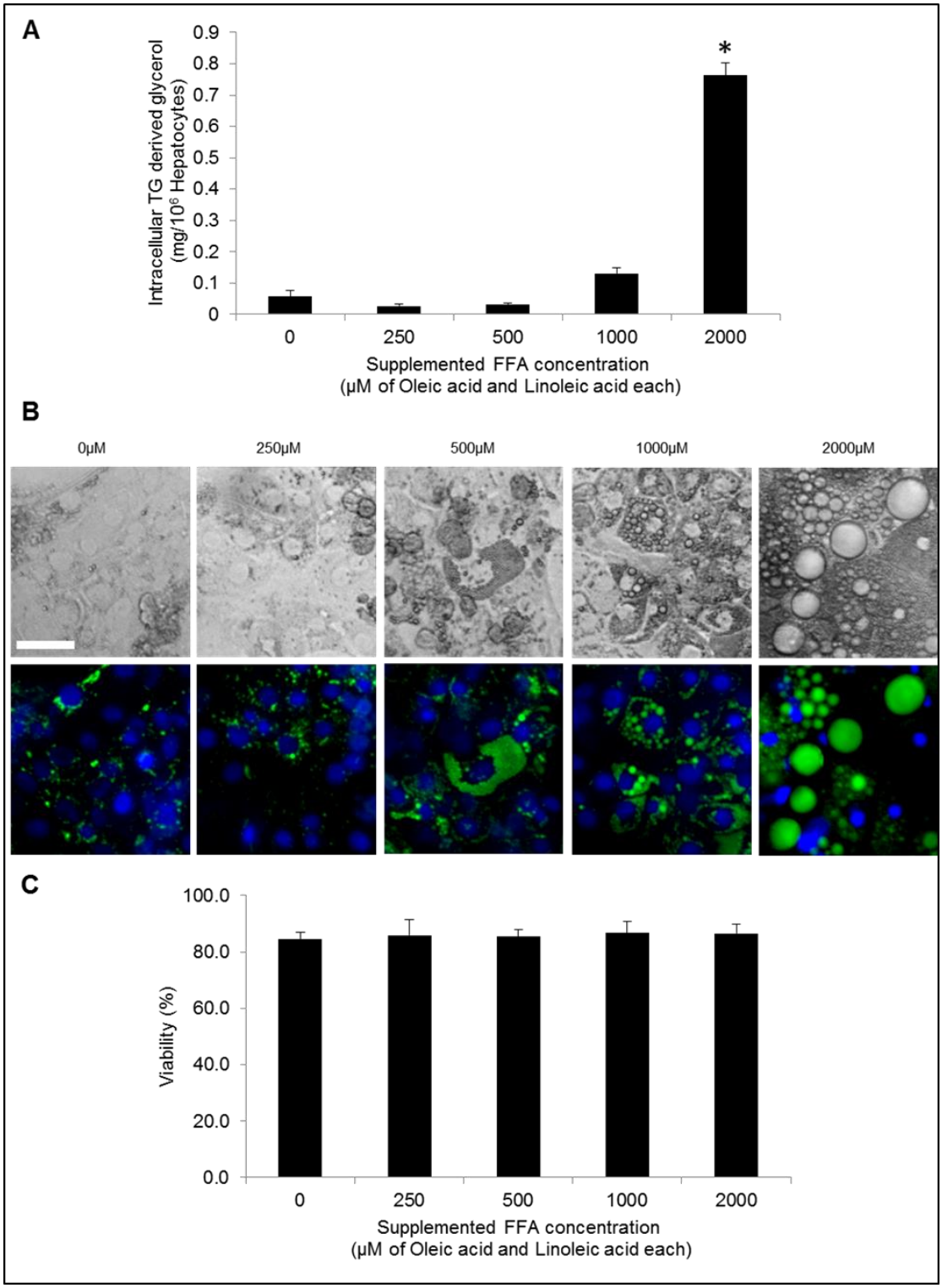

Chapter 3, Supplementary Figure 1: Effect of FFA concentration on steatotic induction.

Hepatocyte cultures were incubated for 6 days (Days 5-11 post-seeding with one media change at day 8 post-seeding) in standard hepatocyte culture medium supplemented with 0, 250, 500, 1000 or 2000μM of oleic acid and the same concentration of linoleic acid. A. Intrahepatic TG for these cultures on day 11 post-seeding. *p<0.05 vs. 0μM. B. Representative bright-field images (top), Nile red (green), and Hoechst (blue) stained cultures (bottom). Bar=50um. C. Hepatocyte percent viability in each of the cultures as assessed by EHD-1 assay. p=0.99 indicating no significant difference among the conditions. Means±S.E. N=5

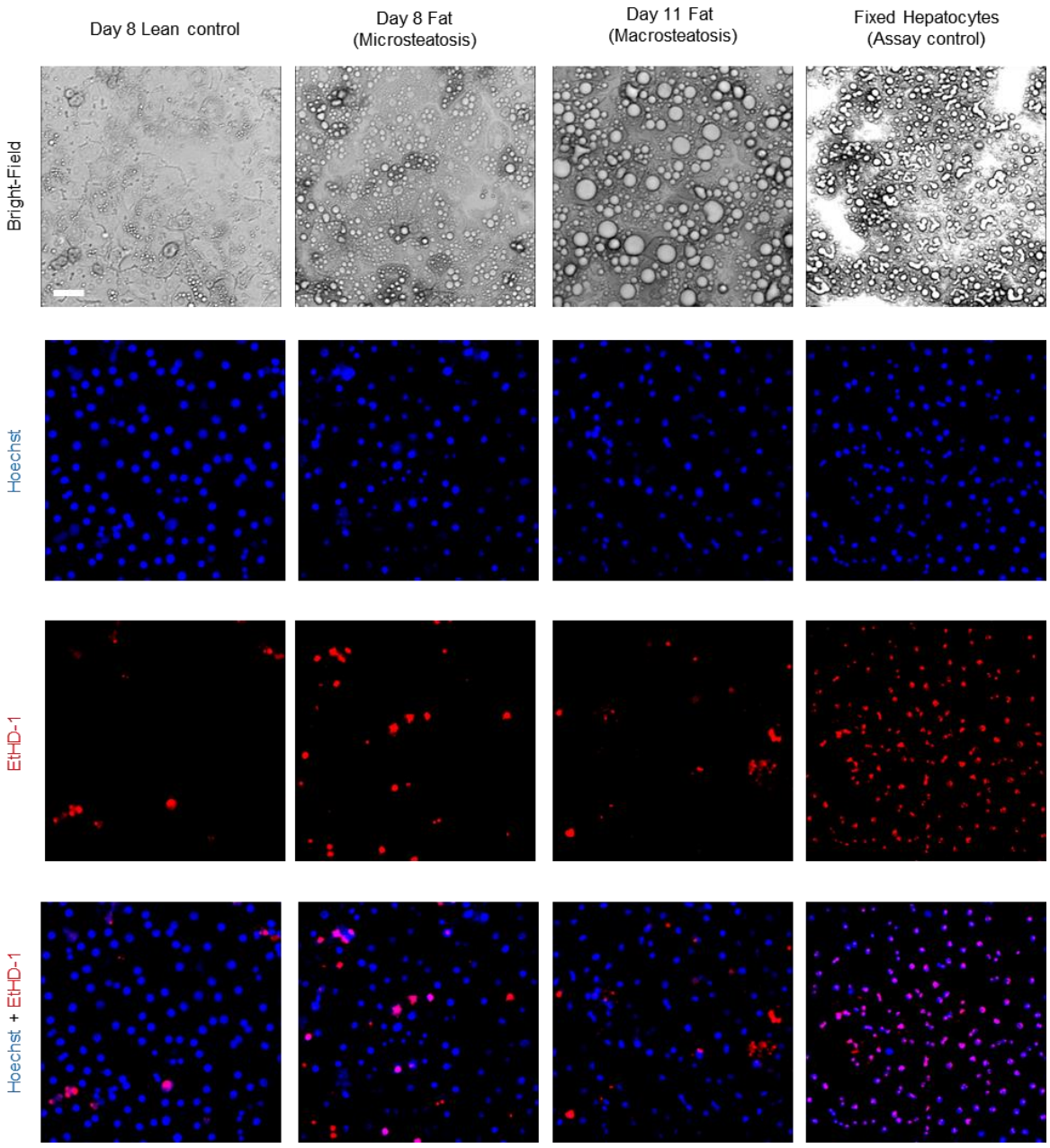

Chapter 3, Supplementary Figure 2: Viability distribution in hepatocyte cultures after microsteatosis and macrosteatosis induction.

Viable cell nuclei are stained with Hoechst (blue) but not EtHD-1 (red). Lean controls and methanol fixed cultures (which are all dead) are also shown for comparison. Bar=50µm.

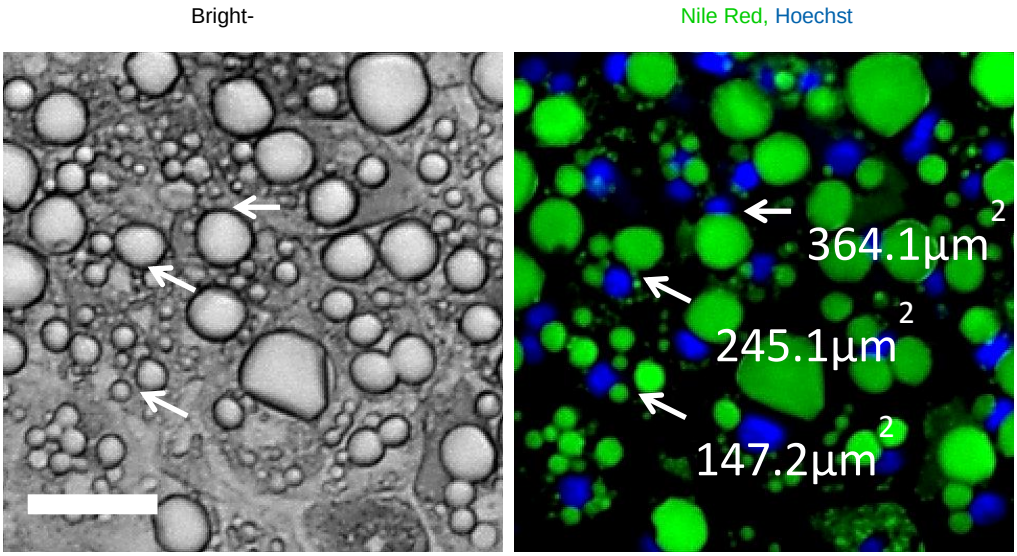

Chapter 3, Supplementary Figure 3: Lipid droplet minimal cross-sectional surface area defining macrosteatosis.

Lipid droplet sizes were measured within hepatocyte cultures exposed to steatosis inducing medium for 6 days. A survey of individual cells revealed that nuclear dislocation to the cell periphery occurred when the cross-sectional surface area of lipid droplets reached 350µm^2. Shown is a representative image of hepatocyte cultures showing lipid droplet sizes and nuclear location. Bar= 50µm.

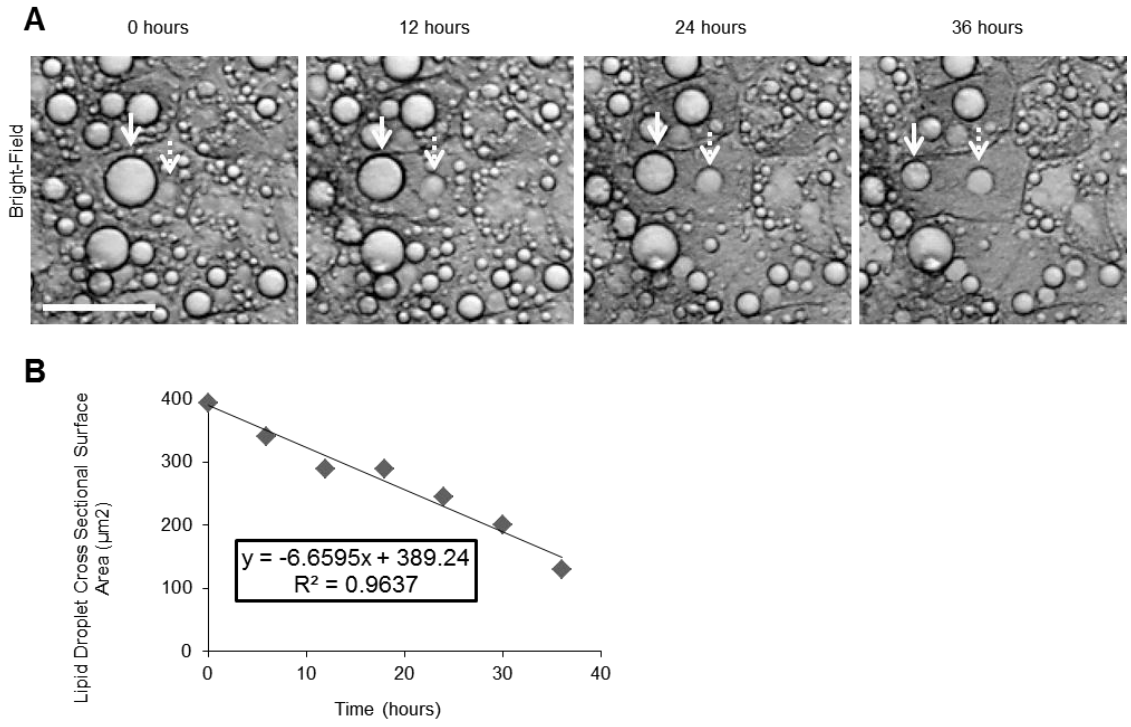

Chapter 3, Supplementary Figure 4: Morphological changes of representative lipid droplets during macrosteatosis reduction.

A. Bright-field time lapse images of macrosteatotic hepatocytes during the first 36h in SRS medium. Solid arrows=a single macrovesicular droplet; dashed arrows= nucleus in the same cell. The image sequence shows shrinking of the lipid droplet and return of the nucleus to the center. Bar=50µm. B. Cross sectional surface area of the lipid droplet visualized in panel A decreases linearly with time.

3. Supplementary figures and table for chapter 4

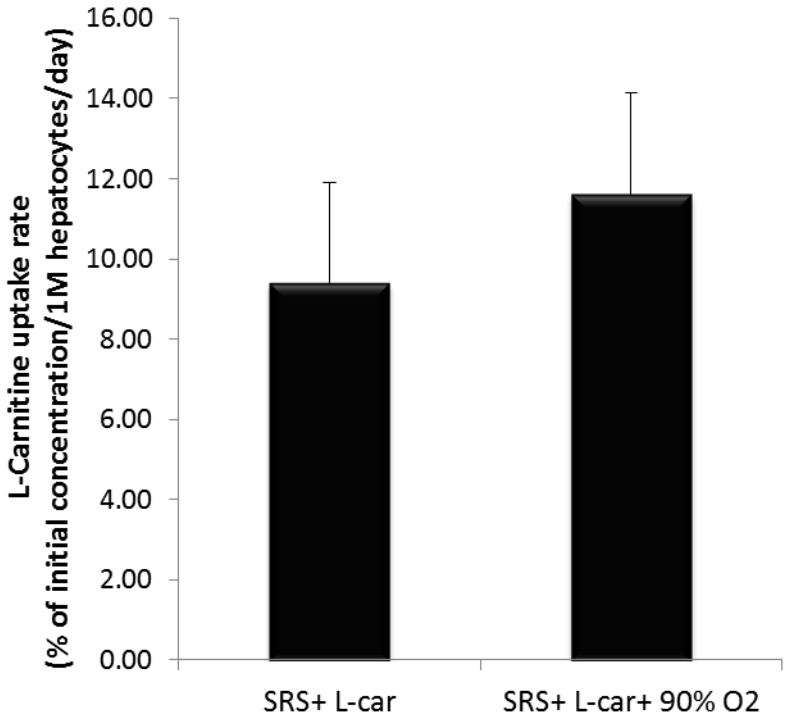

Chapter 4, Supplementary Figure 1: L-carnitine uptake rate of macrosteatotic hepatocytes under normoxic and hyperoxic conditions

L-carnitine uptake rates were calculated based on the remaining amounts of L-carnitine at the end of 48h preconditioning of macrosteatotic cultures with SRS cocktail supplemented with 0.8mM of L-carnitine under normoxia or hyperoxia. Means ± S.E. N = 6. p=0.577 indicates similar uptake rate of ~20% of the supplemented L-carnitine over the 48h preconditioning, which suggests that L-carnitine was present in excess.

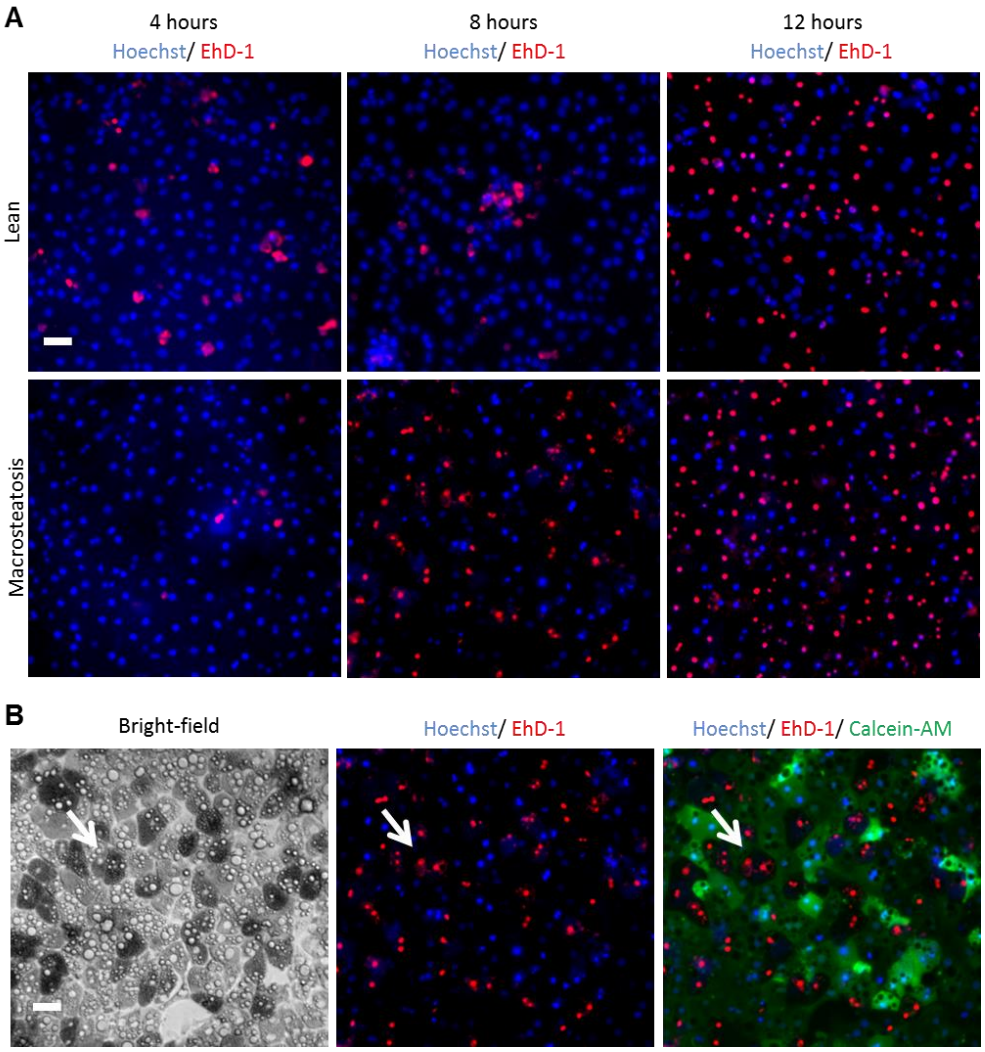

Chapter 4, Supplementary Figure 2: Effect of hypoxia induction time on viability of macrosteatotic hepatocytes

To determine the optimal hypoxia induction duration effective in displaying macrosteatotic hypersensitivity to H/R stress, lean and macrosteatotic hepatocyte cultures were exposed to 4, 8 or 12h of hypoxic environment (oxygen tension ~0%) at 37^{o}C followed by 6h of reoxygenation under normoxic environment. Then, the cultures were stained with EthD-1 for dead cells nuclei (red), Calcein-AM for live cells cytoplasm (green) and Hoechst for all cells nuclei (blue). (A) Epi-fluorescent images of lean (top panel) and macrosteatotic (bottom panel) hepatocyte culture stained for EthD-1and Hoechst indicates that 8h of hypoxia induction display macrosteatotic hepatocytes hypersensitivity to H/R stress while maintaining lean hepatocyte cultures unaffected. Bar=50um. (B) Macrosteatosis hepatocytes stained with EthD-1, Calcein-AM and Hoechst following 8h of hypoxia and 6h of reoxygenation. EthD-1^{+} hepatocytes are considered dead as confirmed by being Calcein-AM^{-}, as indicated by the white arrows. Bar=50um.

Cocktail	Supplemented Agent	Concentration
SRS	L-Arginine hydrochloride	252.8 mg/L
	L-Cystine	48 mg/L
	L-Histidine hydrochloride-H2O	84 mg/L
	L-Isoleucine	104.8 mg/L
	L-Leucine	104.8 mg/L
	L-Lysine hydrochloride	145 mg/L
	L-Methionine	30.2 mg/L
	L-Phenylalanine	66 mg/L
	L-Threonine	95.2 mg/L
	L-Tryptophan	20.4 mg/L
	L-Tyrosine	72 mg/L
	L-Valine	93.6 mg/L
	Glycine	30 mg/L
	L-Alanine	35.6 mg/L
	L-Asparagine	52.8 mg/L
	L-Aspartic acid	53.2 mg/L
	L-Glutamic Acid	58.8 mg/L
	L-Proline	46 mg/L
	L-Serine	42 mg/L
	L-Glutamine	584 mg/L
	Forskolin	10 uM
	GW7647	1 uM
	Scoparone	10 uM
	GW501516	1 uM
	Hypericin	10 uM
	Visfatin	0.4 ug/L
SRS+ L-car	SRS	As described above
	L-carnitine	0.8uM

Chapter 4, Supplementary Table 2: Defatting cocktail agent concentrations

The following agents were supplemented to fresh standard hepatocyte culture medium to formulate the SRS and SRS+ L-car defatting cocktails.